Himalayan earthquakes: a review of historical seismicity and early 21st century slip potential

ROGER BILHAM

CIRES and Geological Sciences, University of Colorado Boulder, 216 UCB, Boulder, CO 80309, USA

0000-0002-5547-4102

roger.bilham@colorado.edu

Abstract: This article summarizes recent advances in our knowledge of the past 1000 years of earthquakes in the Himalaya using geodetic, historical and seismological data, and identifies segments of the Himalaya that remain unruptured. The width of the Main Himalayan Thrust is quantified along the arc, together with estimates for the bounding coordinates of historical rupture zones, convergence rates, rupture propagation directions as constrained by felt intensities. The 2018 slip potential for fifteen segments of the Himalaya are evaluated and potential magnitudes assessed for future earthquakes should these segments fail in isolation or as contiguous ruptures. Ten of these fifteen segments are sufficiently mature currently to host a great earthquake ($M_w \geq 8$). Fatal Himalayan earthquakes have in the past occurred mostly in the daylight hours. The death toll from a future nocturnal earthquake in the Himalaya could possibly exceed 100 000 due to increased populations and the vulnerability of present-day construction methods.

This chapter discusses the large damaging earthquakes that have occurred in the Himalaya in the past several centuries. Their study is important because historical earthquakes hold clues about future seismicity that threatens populated regions of the Himalaya. Populations have increased by an order of magnitude in the past 200 years, and this has been accompanied by an increase in the vulnerability of dwellings subjected to seismic shaking.

Prior to the occurrence of the 2015 Gorkha earthquake, our understanding of Himalayan seismicity was based on pre-twentieth century felt-intensity data reports, relative modest constraints from recent instrumental seismic data and palaeoseismic evidence for great earthquakes recorded as offsets of the frontal thrust faults of the Himalaya. The $M_w = 7.8$ Gorkha earthquake provided a template on which to base our interpretation of several aspects of major Himalayan earthquakes, but tantalizingly fell short of bridging the gap in our knowledge between major earthquakes and the great $8 < M_w < 9$ earthquakes that are essential to accommodate most of the convergence between the Indian Plate and southern Tibet.

This review attempts to synthesize current knowledge of Himalayan earthquakes, and the intensity of shaking they impart to engineered structures, cities and villages in the Himalaya. Several excellent accounts of recent findings concerning Himalayan seismicity are now available, many that review the works of others and others that build upon these former contributions (Avouac 2015*a*, *b*; Mugnier *et al.* 1998; Rajendran *et al.* 2017, 2018*b*; Mohadjer *et al.* 2017). I have avoided mention of some summaries that have unnecessarily repeated findings that can now be abandoned in the light of recent knowledge. The purpose of this article is to demonstrate improved insights into seismic processes, and to admit that although we can describe several general principles governing the location or lateral reach of future Himalayan earthquakes, we remain ignorant of the most important parameters of the next damaging earthquake – its location, magnitude and timing.

The account will start with an overview of convergence in the Himalaya made possible by significant advances in geodesy starting around 1987 (Bilham *et al.* 1997). It then discusses the setting of Himalayan earthquakes and such information as we have for earthquakes from 1500 to 2015, including details of the slip geometry and bounds of the 2015 Gorkha earthquake. This is followed by an outline of results from palaeoseismic trench studies that have incompletely and somewhat unevenly extended the seismic record to past millennia. It will conclude with an attempt to distinguish between uncertain seismic futures for the Himalaya.

Himalayan geodesy

The rate of convergence of India relative to EuroAsia is fundamental to quantifying the anticipated

From: Treloar, P. J. & Searle, M. P. (eds) 2019. *Himalayan Tectonics: A Modern Synthesis*. Geological Society, London, Special Publications, **483**, 423–482.
First published online February 5, 2019, https://doi.org/10.1144/SP483.16

recurrence interval of earthquakes in the Himalaya, but although India is effectively rigid to within a few millimetres (Paul *et al.* 1995; Banerjee *et al.* 2008; Jade *et al.* 2017), the collisional velocity along the Himalaya is reduced by the absorption of more than half of this convergence as internal deformation within Asia. Prior to the availability of GPS geodesy, this relative velocity was known only indirectly through global plate-closure summations (Molnar & Stock 2009), there being no spreading centre between the two plates. Recent studies reveal that rapid northwards motion of the Indian Plate exceeded 14 cm a^{-1} at 70–50 Ma BP as a result of convergence across two approximately parallel, east–west subduction zones (Van der Voo *et al.* 1999; Jagoutz *et al.* 2015) but rapidly slowed to 6 cm a^{-1} following the closure of the Tethys ocean at *c.* 50 Ma BP and the onset of continent–continent collision. The pole of rotation between the India Plate and the EuroAsian Plate is currently considered to lie at 51.70° ± 0.3° N, 11.85 ± 1.8° E (roughly 100 km SW of Berlin), with convergence specified by an angular velocity of 0.553 ± 0.006°/Ma (Jade *et al.* 2017). Previous determinations with fewer high-accuracy GPS data yielded a pole position between Ireland and London, and its east–west position remains the largest uncertainty. The pole defines a clockwise rotation of the Indian Plate relative to Asia with *c.* 44 mm a^{-1} of convergence at the longitude of Pakistan and 65 mm a^{-1} of convergence at the longitude of Bangladesh. Since most of the convergence dispersed in Tibet and in the mountains to the north, the convergence across the Himalaya, which is responsible for its seismic productivity, is reduced to less than 18 mm a^{-1}. Near Kashmir in the westernmost Himalaya, the convergence rate is ≤12 mm a^{-1}, in the central Himalaya the rate attains 17 mm a^{-1} and in Assam in the east, instead of increasing, which would be anticipated from Indian's counterclockwise rotation, it reduces as a result of the clockwise rotation of the Brahmaputra Valley. The valley is the surface manifestation of a 300 km-long segment of northeasternmost India that fragmented from the India Plate at *c.* 5 Ma BP (Vernant *et al.* 2014).

Historical triangulation and GPS geodesy

Although precise geodetic measurements of India were initiated in the 1830s, few measurements extended into the Himalaya because of an 1815 treaty forbidding surveyors or others from entering Nepal territory. Measurements with inferior accuracy were extended into Kashmir and Ladakh (to 35° N, 75.5° E) to establish the international boundary in 1855–79 (Montgomerie 1860), but no trans-Himalayan surveys existed until 1911–13, when a survey line connecting the Indian and Russian triangulation surveys was measured (Mason 1914). In 1980, this triangulation network was remeasured to search for evidence of Indo-Asian convergence. Typical Survey of India accuracy of 10 mm km^{-1} in scale (3 mm km^{-1} in angle) offered a 1 m accuracy for a 100 km north–south line. However, the results of the survey were impaired by weak survey geometry, by the incomplete recovery of triangulation points and by typological errors in the printed 1914 report, the original notes for which had been lost in the intervening years (Chen *et al.* 1984). No signal was detected above the triangulation uncertainties of ±1 m (Chen *et al.* 1984), consistent with our current knowledge of the convergence here of <0.3 m in 67 years.

GPS geodesy became available just 4 years after the 1980 measurements, but its application was delayed due to the unjustified suspicion that GPS position information with millimetre precision was of military value. Although this suspicion continues to thwart scientific applications of precise geodesy in the region, GPS measurements in 1989 were undertaken in Pakistan and Nepal following public interest in the resolution of a height controversy between K2 and Everest. The measurements demonstrated that Everest exceeds the height of K2 but it opened the door for the precise measurement of points in the Himalaya. The present density of measurements in the Himalaya is remarkable (Figs 1 & 2) given the difficulties of access to many mountainous tracks, and the political difficulties in undertaking scientific measurements near sensitive international borders.

Because the Indian Plate is essentially rigid to within a few millimetres per year (Paul *et al.* 2001; Banerjee *et al.* 2008; Jade *et al.* 2017), whereas the Tibetan Plateau to its north is both converging in a north–south sense and extending east–west by approximately 2 cm a^{-1} (Wang *et al.* 2001), it is convenient to refer tectonic movements in the region relative to the Indian Plate. Figure 2 shows a map view of southwards velocities relative to India, and the projections of along-arc (Fig. 2b) and across-arc (Fig. 2c) displacement vectors onto the Himalayan arc fit to a small circle at 42.1° N and 90.72° E with a radius of 1642 km. The parameters of the small-circle projection correspond to a least-squares fit to the 3.5 km elevation contour along the Himalaya, which is empirically equated to the locking line between India's aseismic slip descent beneath Tibet and the locked Indian Plate to its south (Bendick & Bilham 2001; Avouac 2003, 2015*a*, *b*). This small circle also follows the locus of microseismicity along the Himalaya and approximates to the northern nucleation zone of major Himalayan earthquakes (Fig. 3).

The 'arc normal' velocity field can be fit to elastic dislocation models that constrain convergence rates. Two synthetic curves are shown in Figure 2c corresponding to locking at 18 km depth and convergence velocities of 16 and 18 mm a^{-1}. The calculation

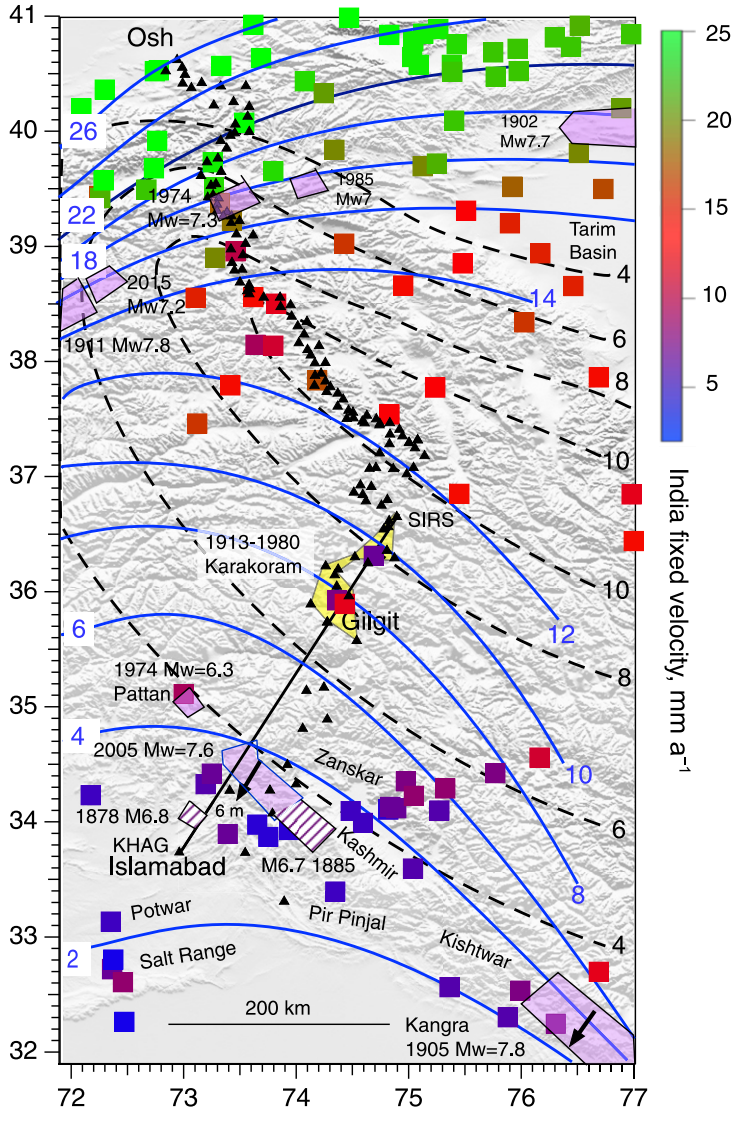

Fig. 1. Historical geodesy. Small black triangles indicate trigonometrical points linking the nineteenth century Great Trigonometrical Survey of India to the Russian Survey network measured in 1913 (Mason 1914). A small part of the 1913 Indo-Russian network connecting Osh to Islamabad was remeasured in 1980 (yellow: Chen *et al.* 1984). The *c.* 300 km-long trigonometrical distance between Sirsar (SIRS) and Khagriani (KHAG) was measured directly with GPS methods in 2001 and 2005. Colour-coded squares indicate GPS velocities relative to India obtained in the past 30 years. Smoothed blue solid contours indicate southwards velocity; dashed black contours indicate westwards velocity. Earthquake ruptures are indicated by violet shading with the magnitudes indicated. Hatched areas indicate pre-instrumental earthquakes in the late nineteenth century.

of convergence rate at any longitude depends somewhat on the inclusion of observations more than 50 km north of the Himalaya, because of the north–south convergence of Tibet. The appropriate truncation distance is also dependent on the assumed or calculated depth of the transition zone (between fully locked and freely creeping décollement) on the upper surface of the Indian Plate. For example, in central Nepal, convergence estimates vary from 15 mm a^{-1} (Zheng *et al.* 2017; Lindsey *et al.* 2015) to 18 mm a^{-1} (Ader *et al.* 2012). Convergence velocities are low (12 mm a^{-1}) and 30° oblique to the Himalaya in the west near 75° E, are arc-normal and approach *c.* 18 mm at 90° E, and decay slightly

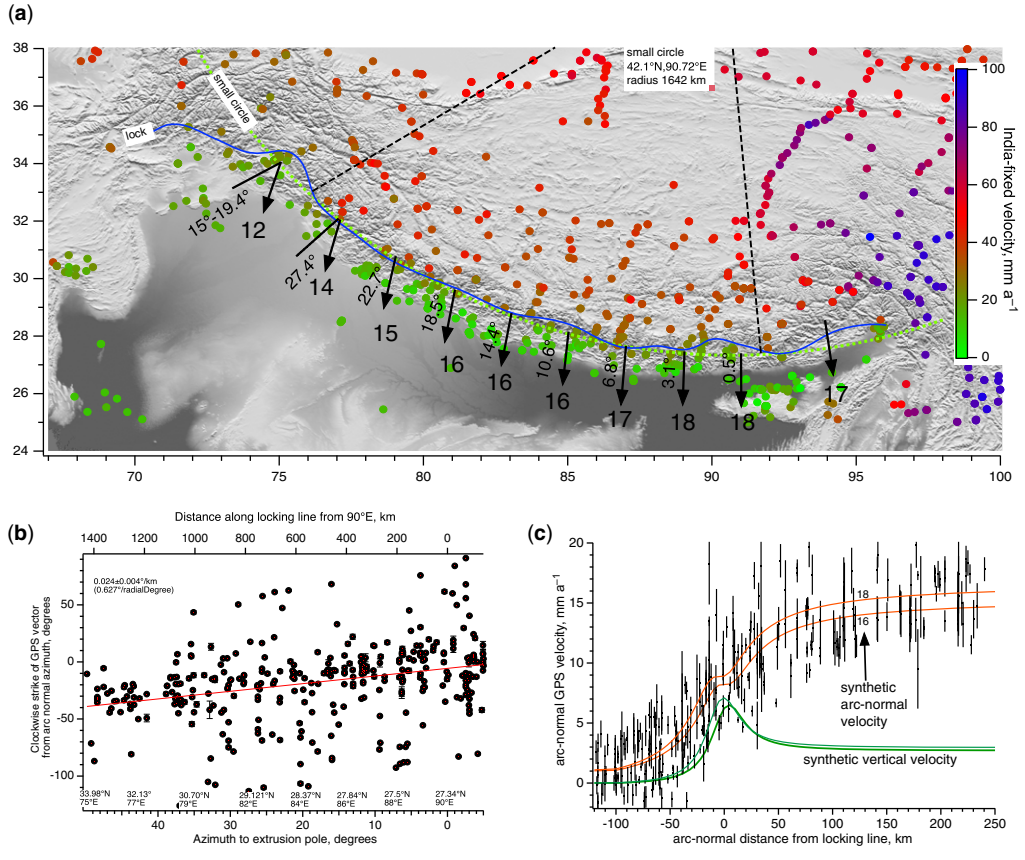

Fig. 2. (**a**) India-fixed GPS north velocities summarized by Vernant *et al.* (2014) and Kreemer *et al.* (2014) are coloured coded to indicate their southwards velocity relative to India. The blue line indicates the 8.5 mm a^{-1} velocity contour which approximately follows the locking line at 18 km depth below the 3.5 km contour. The dashed green line is small-circle fit to this centred on a pole at 42.1° N and 90.72° E with a radius of 1642 km (Vernant *et al.* 2014) used in subsequent plots. (**b**) Deviation of GPS vectors (from arc normal) within the 1 radian quadrant dashed. The weighted least-squares fit to these (red line) is used to calculate the deviation from arc normal velocities depicted as arrows in (a). (**c**) Arc-normal velocities within the small-circle quadrant compared with synthetic velocities for a 6°–9° dipping dislocation locked at 18 km depth, and with convergence velocities of 16 and 18 mm a^{-1} (red lines), and synthetic vertical displacements (green lines).

eastwards due to the clockwise rotation of the Brahmaputra Valley away from the Himalaya about a point south of Sikkim. The Himalayan velocity field is not well defined east of 90° E due to a sparsity of measurements in the mountains (Vernant *et al.* 2014). An average convergence rate of 17 mm a^{-1} is used in the text to characterize Himalayan convergence, with the caveat that a rate closer to 15 mm a^{-1} may be appropriate given that much of southern Tibet does not appear to contribute significantly to the seismic cycle in the Himalaya (cf. Feldl & Bilham 2006).

Vertical deformation rates measured geodetically attain maximum rates of uplift of 6 or 7 mm a^{-1} above the transition zone from creep to locked décollement. These rates are usually inferred from elastic deformation models fit to horizontal GPS data, which are typically much lower noise than the vertical GPS signal (Fig. 2c). Direct measurements of vertical motion consistent with these rates have been reported by Jackson & Bilham (1994) from levelling data, and by Grandin *et al.* (2012) using synthetic aperture radar data.

Indo-Asian convergence and seismicity

In contrast to the almost complete absence of earthquakes in the interior of the Indian Plate, seismicity surrounds its edges and is prolific within the Tibetan

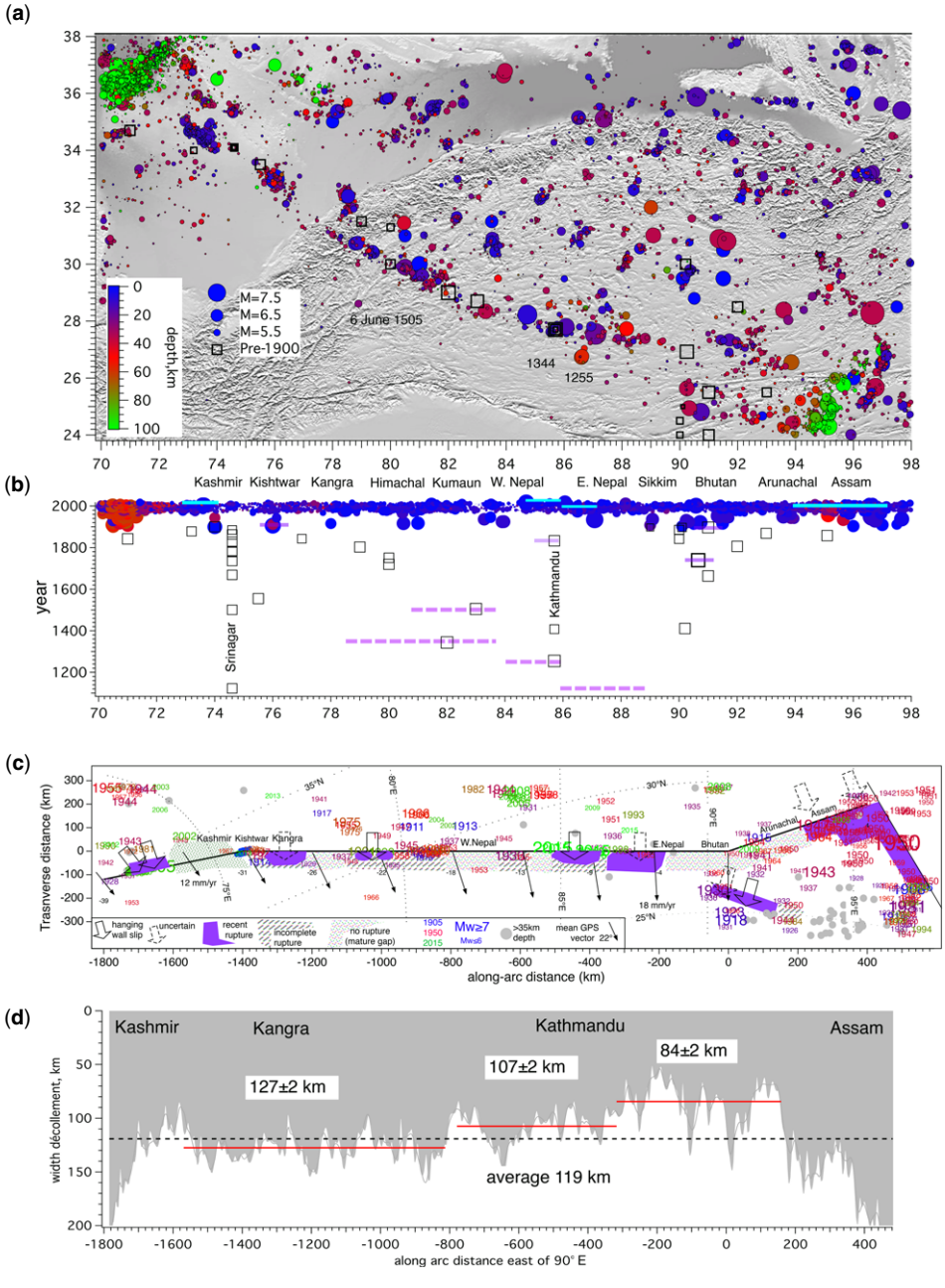

Fig. 3. (**a**) Seismicity of Himalaya and Tibet. (**b**) Time–distance graph showing the rupture lengths of historical earthquakes since 1800 (violet), inferred ruptures (dashed violet) discussed in the text, and the increase in recorded earthquakes since 1900. Red are deeper than 40 km: blue are shallower. (**c**) Polar plot centred at 42.1° N, 90.72° E straightens the Himalaya and illustrates that the locking line closely follows a small circle. Recent earthquakes are dated and colour coded according to depth (scale as in a). Historical earthquakes and unruptured segments of the décollement are colour coded according to the legend below the figure. Incomplete ruptures leave a substantial fraction of the décollement unruptured (see Fig. 4b). (**d**) The same polar plot showing the radial width of the décollement as a function of distance along the arc. The lower edge of the shaded region represents the Main Frontal Thrust; the upper edge the locking line. The red lines indicate along-arc spatial averages with their numerical values.

Plateau (Fig. 3). Most of the earthquakes within the Himalaya occur at shallow depth (<30 km); with deep earthquakes indicating the descent of the Indian Plate into the mantle at the ends of the arc. Earthquakes with depths exceeding 40 km are relatively rare in the continent–continent collision in the central Himalaya and beneath Tibet, indicating the absence of the Benioff–Wadati zone that is characteristic of oceanic plate collisions.

The rate of convergence between the Indian Plate south of the Himalayan foothills and southern Tibet is important because it provides an upper limit for the anticipated rate of seismic productivity for the Himalaya. With an average rate of convergence of 17 mm a^{-1}, the 2000 km-long approximately100 km-wide Main Himalayan Thrust (the décollement separating the Indian and Asian plates) accumulates seismic moment at a rate of *c.* 10^{20} N m a^{-1} (Newton metres per year), equivalent to that released by a $M_w = 7.3$ earthquake. In 10 years, enough moment has accumulated to drive a $M_w = 8$ earthquake, and in a century a $M_w = 8.6$ earthquake. In just 350 years, were no other earthquakes to occur in the Himalaya, a $M_w = 9$ earthquake would be needed to release the accumulated 4 m of Himalayan convergence (assuming a 2000 km-long rupture).

The rate of release of this potential slip, however, is uneven in space and time, and at any one moment there exists a seismic slip deficit along most of the Himalayan arc. With one exception, earthquakes must occur to relieve this growing slip deficit. The exception is known as creep, or aseismic slip, and is discussed below. Large earthquakes are more efficient at releasing the accumulating slip deficit because their large rupture areas (*c.* 100 × 50 km) permit large amounts of slip (≥5 m). Thirty $M_w = 6$ earthquakes must occur to match the energy released by a $M_w = 7$, and 1000 must occur to match the energy released by a $M_w = 8$ earthquake. For this reason, although many small earthquakes occur daily in the Himalaya with magnitudes of $M_w \leq 4$, in practice only the largest of earthquakes permit the Indian Plate to slide beneath the southern edge of the Tibetan Plateau. Since 1600, only two $M_w > 8$ earthquakes are known to have occurred in the Himalaya: in 1934 ($M_w = 8.4$) and in 1950 ($M_w \approx 8.6$). A third great earthquake occurred beneath the Shillong Plateau south of Bhutan in 1897 ($M_w = 8.2$). Of the eight earthquakes since 1600 with magnitudes in the range $7 < M_w < 8$ documented in the Himalaya, six have occurred since 1900 (1905, 1936, 1947, 2005 and two in 2015). It is probable that the historical record is incomplete prior to 1800 but there is little reason to suppose that $M_w \geq 7$ earthquakes are missing since then, given the reasonably good coverage of the region by newspapers, administrative reports and travellers' accounts in the nineteenth century.

Three types of *shallow* seismicity are manifest in the Himalaya (Fig. 4). Indo-Tibetan convergence results in strain concentration near the transition from locked décollement to steady aseismic creep beneath the plateau. Small earthquakes ($M_w < 3$) occur daily in this region accompanied by the occasional $4 < M_w < 5$ felt earthquake (Fig. 4a). More rarely (every 10–20 years), a north-dipping $6 < M_w < 7$ reverse fault will rupture in this region. Yet more rarely, major earthquakes incompletely rupture the décollement (Fig. 4b). These earthquakes, exemplified by the Gorkha 2015 $M_w = 7.8$ earthquake, release strain near the transition zone and transfer it to their point of rupture termination. Earthquakes with this mechanism are inferred to have occurred in 1803, 1833, 1905, 1916, 1936 and 1947. Infrequently, the entire Himalayan carapace slips southwards during a great earthquake (Fig. 4c). In these great earthquakes, elastic strain is depleted in the north and is dissipated entirely as extension of the carapace, accompanied by a surface rupture at the Main Frontal Thrust. These great earthquakes (most recently in 1950) have the capacity to release the updip relict strain abandoned by incomplete ruptures (Mencin *et al.* 2016; Bilham *et al.* 2017).

The earthquake ruptures shown in Figure 4 all conspire to absorb Indo-Asian convergence. Not illustrated in Figure 4 are earthquakes that occur within the descending Indian Plate. These intermediate-depth earthquakes arise from flexural and compressional stresses caused by India's downwards descent beneath the southern edge of Tibet. An example of such an earthquake is the 50 km-deep $M_w = 6.8$ Udaipur earthquake of 21 August 1988 on the Nepal–India border SE of Kathmandu. In addition, several north-striking, sub-Himalayan faults can be recognized from their offset of sediments in the Gangetic plain that appear to weakly influence seismicity in the Himalaya and southern Tibet (Dasgupta *et al.* 1987). The most active of these is the Kopili shear zone that strikes NNW through western Bhutan, which may have sustained a $M_w \approx 7$ earthquake in 1943 in the Brahmaputra Valley.

Historical earthquakes in the Indian Plate below the Main Himalayan Thrust cannot easily be distinguished from décollement earthquakes, even when accounts of widespread damage are available, sometimes accompanied by accounts of prolonged aftershock sequences. For this reason, some historical earthquakes no doubt include earthquakes that should not be associated with décollement slip or rupture of the Main Frontal faults.

Sources of information on pre-instrumental era earthquakes in the Himalaya

Prior to the availability of instrumental data in *c.* 1900, two sources of information record the

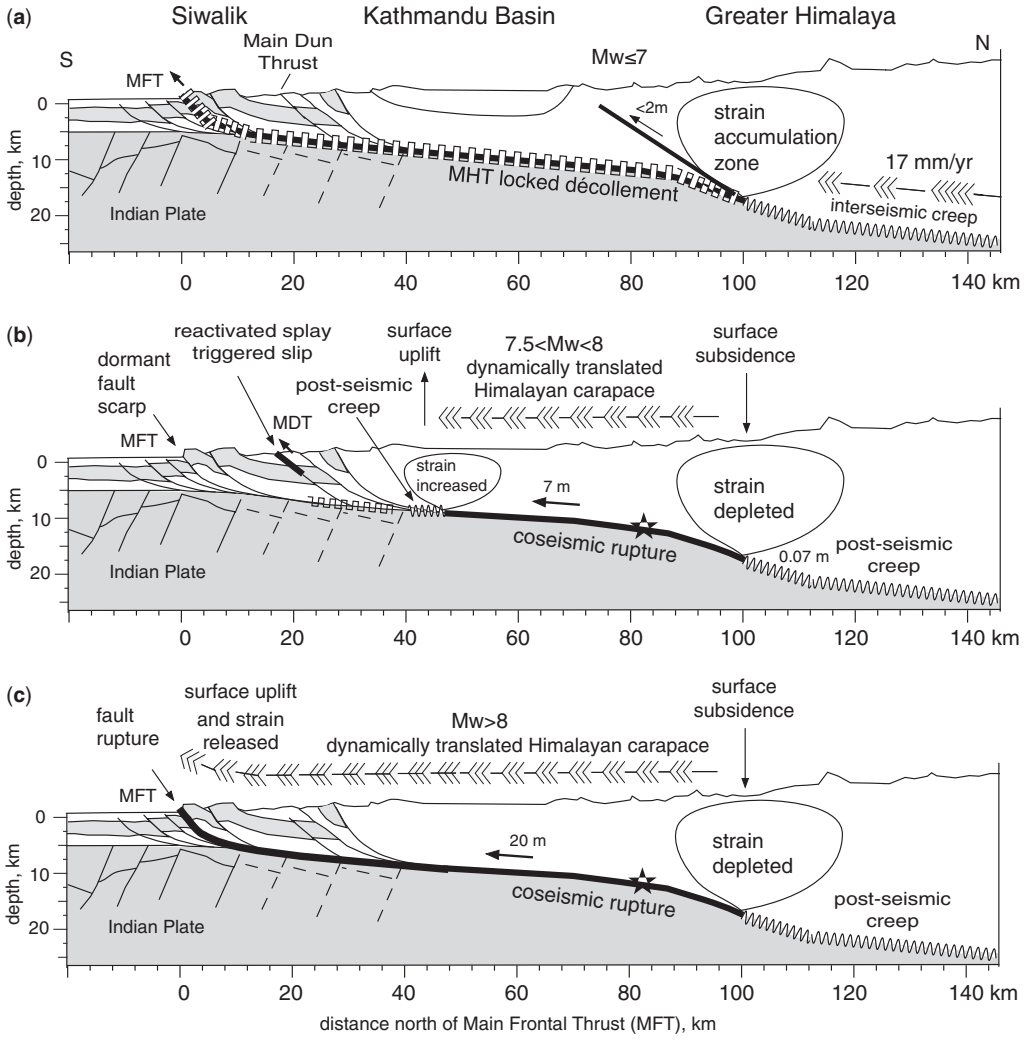

Fig. 4. Geometry of the slip in Himalayan earthquakes (section from Mencin *et al.* 2016). Updip blind thrusts from oil exploration seismic lines (Bashyal 1998). The square wave indicates locked, the bold line indicates rupture and the sine wave indicates aseismic slip. (**a**) The region of interseismic strain accumulation is the locus of microseismicity and occasional moderate earthquakes occurring as high-level thrusts. (**b**) Incomplete rupture in the 2015 Gorkha M_w 7.8 earthquake, with subsequent induced post-seismic creep (4 min–4 years). No slip occurred on the Main Frontal Thrust (MFT) but triggered surface slip was recorded on the Main Dun Thrust. InSAR (interferometric synthetic aperture radar) imagery shows that this occurred in the form of decaying creep for 26 km along strike with no slip below *c.* 5 km. The slip increased over a few weeks to ≥5 cm and then ceased (Elliott *et al.* 2016). (**c**) Complete rupture as inferred to occur in great earthquakes (e.g. in 1505 and 1950 $M_w \geq 8.6$). Occasionally these may activate blind thrusts south of the MFT.

passage of historical earthquakes in the Himalaya: archival documents, newspapers and travellers' diaries (Iyengar *et al.* 1999; Bilham 2004), and excavations of earthquake-related features such as surface liquefaction or the offset of surface faults (palaeoseismology). Both sources tend to accentuate the largest or most damaging earthquakes, and these are typically décollement earthquakes with mechanisms similar to those depicted in Figure 4. Archives from ancient kingdoms in Kashmir and Nepal yield a persistent but patchy record of earthquakes for the past 1000 years, but few of these records permit estimates of magnitude or location since most of the materials describe earthquakes felt only by populations in Srinagar and Kathmandu, respectively. Minor local earthquakes are typically

indistinguishable from distant larger earthquakes unless the account mentions prolonged sequences of aftershocks.

Some irreplaceable historical records have been lost quite recently: Bhutan archives were destroyed by fires started by the 1897 Shillong earthquake (White 1909), and archives from Assam were deliberately destroyed by rulers anxious to erase links to perceived unsavoury ancestors (Gait 1906; Choudhury 1985). Due to their widely distributed locations along the southern edge of the Tibetan Plateau, archives from Tibetan monasteries provide a favourable setting for assessing the magnitude of the largest earthquakes, from the survival of simultaneous requests for repairs submitted to a central administration. In contrast, frequent territorial wars in parts of the Himalaya and northern India have not offered ideal conditions suitable for the survival of ancient documents. The historical record is thus uneven in space and fragmentary in time (Fig. 3b). As new palaeoseismic findings arise, from trench excavations of the Main Frontal faults of the Himalaya typically dated to accuracies of no better than ±50 years, links have been sought between these dates and chronologies of known historical earthquakes.

The paucity of early written records means that earthquakes before 1000 CE are known almost entirely from their palaeoseismic signatures. A few earthquakes in mythical form or in religious works have the potential to be equated loosely with palaeoseismic findings. For example, one of the several major earthquakes associated with significant events in the life of the Buddha (Ciurtin 2009) may correspond to a rupture of the Himalayan frontal thrust at Ramnagar bracketed by ^{14}C dates between 570 and 467 BCE by Malik *et al.* (2017). Recent excavations at Lumbini in Nepal lend support to the timing of the Buddhist chronicles being centred in the sixth and fifth centuries BCE (Coningham *et al.* 2013).

The dates of collapse and repair of temples provide additional clues that have been used to infer the times of historical earthquakes (Rajendran *et al.* 2013). These records must be used with caution since the absence of repairs may not necessarily signify the absence of major earthquakes. This is because surviving structures are typically anomalously resilient to shaking (survival of the fittest), and minor damage may often not be considered worth an immediate fix by temple supervisors. Massive stone temples in Kashmir have clearly suffered from incremental wasting during successive earthquakes, where each earthquake has exacted relatively modest damage to the composite edifice, but the sum total of 1200 years of earthquakes has resulted in a ruinous state. The entrapment of dateable materials by collapsed temple blocks, if they remain undisturbed by archaeologists or vandals, permits incremental damage to be associated with known earthquakes: for example, the 1123 earthquake in Kashmir (Bilham & Bali 2013). On the protective envelope of his 1903 glass negative of Pandrethan Temple, Kashmir (74.860° E. 34.056° N), R.D. Oldham remarks that most of the visible damage to this temple occurred before the 1885 Kashmir earthquake (he saw the damaged temple in 1883); an observation that can be verified by comparing his photograph with Burke's 1868 photograph of the same temple (Bilham *et al.* 2010). Incremental damage is evident in pre- and post-1885 photographs of the Sankaragaurisvara and Sugandhesa (34.1530° N, 74.5622° E) Kashmir temples (Bilham & Bali 2013). Similarly Middlemiss, in his May 1905 photograph of the Bishweshwar Mahadev Temple at Bajaura (31.8473° N, 77.1646° E) in the epicentral region of the April 1905 Kangra $M_w \approx 7.8$ earthquake, relates his discussion with the local temple priest who pointed to minor damage in 1905 compared to significant lateral shifting of temple blocks from former undated earthquakes (Szeliga & Bilham 2017).

In the same way that cities or ancient buildings retain a record of strong shaking, lake deposits record strong shaking in the form of layers of disturbed sediments identified as turbidites (seismites) that accumulate as gravity flows on lake floors (Stolle *et al.* 2017; Ghazoui *et al.* 2018). With sufficient numbers of lake records it would, in principle, be possible to estimate the magnitude of major earthquakes from the spatial distribution of synchronous seismites. Unfortunately, lakes with a long seismic record tend to be rare in the Himalaya because the erosional runoff is so abundant as to fill basins rapidly. Brian Hodgson, in his pioneering studies of Himalayan languages, noted that words describing large bodies of water were rare, and none included a word for ocean. The rapid infill of the colluvial wedge of a fault scarp has been used to advantage to date the time of faulting in locations where dateable materials are entrapped (Bilham *et al.* 2013; Murphy *et al.* 2013).

Prior to the 2015 Gorkha earthquake, we had scant information about shaking intensities in the mezzo-central regions of $M_w > 7$ Himalayan earthquakes. A rule-of-thumb opinion was that intensity 8 shaking signified typical intensities above the rupture zone ($\geq 0.5g$), with numerous assessed locations of intensity 10. In the 2015 $M_w = 7.8$ Nepal earthquake, abundant observations of unexpectedly low shaking intensities above the 150 × 60 km rupture surface were recorded. Accelerations in the 2015 earthquake were of long duration (1–3 min) and with significant fling (incremental translation of 1–7 m causing people to have difficulty standing) but averaged less than EMS (European macroseismic scale) (Grünthal 1998) intensity 7 above the rupture zone (Mencin *et al.* 2016; Adhikari *et al.* 2017;

Bilham *et al.* 2017). Intensity 7 corresponds to 0.18*g*–0.34*g*. It is probable that the intensity ≥ 8 shaking observed above Himalayan ruptures in previous earthquakes (1833, 1905 and 1934) may have been the result of ridge amplification, as was observed in a handful of locations above the 2015 rupture. The low shaking intensities in 2015 resulted in fewer significant landslides than anticipated for a M_w = 7.8 earthquake (Kargel *et al.* 2015).

While discussing damage to archaeological features, two ancient structures are of special interest: the once >50 m-high Kesariya Stupa (26.334° N, 84.855° E) and the >72 m-high Qtub Minar (28.524° N, 77.185° E) in Delhi, *c.* 100 and 200 km from the Himalayan front, respectively. The Kesariya Supa was constructed as a brick stupa in *c.* 700–250 CE above an earlier earthen stupa, but the structure had been decaying for centuries. When it was first recognized by archaeologists in the early twentieth century, it was close to 30 m high. Shaking in the 1934 earthquake reduced it to its current height of *c.* 23 m. Its location close to the 1255 CE Nepal earthquake, and the inferred great east Nepal earthquake of *c.* 1100 CE (Wesnousky *et al.* 2018), suggests that it may have sustained damage in those earthquakes also; however, the structure was exhumed by archaeologists in 1998 and no dating of collapse layers appears to have been attempted.

The Qtub Minar has been repaired several times since its initial construction in 1220 CE and completion in 1370 CE. The Qtub is the highest medieval building on the Indian continent and is occasionally cited for its vulnerability to Himalayan earthquakes. Despite its height and masonry construction, its 14 m-wide base and 3 m-wide summit results in a 1.2 s fundamental period when stimulated by wind (Ramos *et al.* 2006). It is alleged to have been repaired in 1332, 1505 and 1803, close to, or coincident with, the years of major earthquakes. Figure 5 shows the proximity of the Minar (Delhi) relative to known significant historical earthquakes. It was also damaged by lightning in 1326, 1368 and 1803. Inscriptions engraved on parts of the Minar uniquely date repairs following the 1368 lightning strike and repairs to the upper two storeys that commenced on, or were completed by, 23 September 1503. The inscription above the fourth storey doorway describes repairs in 1368, but importantly mentions no earthquake (Blakiston 1922; Page 1926, p. 7); and the 1503 repairs predate, or may have been in progress during, the great Himalayan earthquake of 6 June 1505 that is inferred to have severely damaged Agra, 230 km to the SSE. Alleged earthquake damage to the Minar prior to 1332 (Pande 2006) is not mentioned in inscriptions on the tower. For additional discussion concerning possible reconstruction following the earthquake felt in Nepal in 1344 see Rajendran *et al.* (2018*b*). Moreover, some confusion surrounds the source of the frequently repeated mention of damage to the Minar in the 1 September 1803 earthquake (Dasgupta & Mukhopadhyay 2014, 2015). Cunningham (1865) writing more than half a century after the earthquake states, 'On the 1st August 1803, the old cupola of the Kutb Minar was

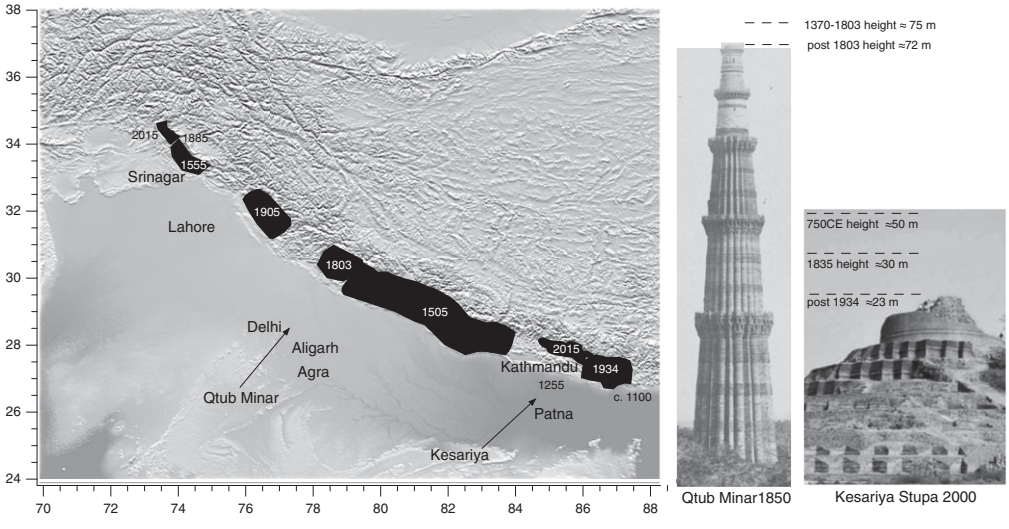

Fig. 5. Location of the Qtub Minar and the Buddhist Kesariya Stupa relative to the nearby Himalayan earthquakes. The omission of the multifluted ornamentation of the lower three tiers in higher levels of the minar has been interpreted as a result of post-seismic 14th century reconstruction (Rajendran *et al.* 2018*b*). The Qtub is alleged to have lost its summit cupula in the 1803 earthquake, and the uppermost 7 m of the Stupa collapsed in the 1934 earthquake.

thrown down, and the whole pillar seriously injured by an earthquake'. The 1803 earthquake is assessed to have shaken Delhi (EMS = 5) and Aligarh (EMS = 6), 160 km to the SE of Delhi (Szeliga *et al.* 2010), and damage to the Minar, whose balustrades were in a dilapidated state prior to the earthquake (Blunt 1794) as depicted in Daniell's 1898 scene (Archer 1980), would not be unexpected. The 1803 earthquake is the closest of the historical earthquakes to have occurred near the Minar (Fig. 5); however, there is no mention of damage to the Minar in the nearby 15 July 1714 Delhi earthquake that destroyed parts of the old fortifications to the city (Iyengar 2000). Given these uncertainties, it is probable that damage to the Qtub Minar occurred in 1803 and in other earthquakes, but it is unlikely that repairs to the Minar were undertaken punctually following historically damaging earthquakes.

Historical earthquakes 844–1900

Earthquakes prior to 1897 are mostly known from accounts of their felt effects (Table 1). Where these accounts specify damage, it is possible to assign a numerical value on a Mercalli, MSK (Medvedev–Sponheuer–Karnik) or EMS intensity scale (e.g. Grünthal 1998). Where a favourable spatial distribution of these intensities is available, a magnitude may be estimated. It is certain that many earthquakes are missing, especially for those with magnitudes of less than $M_w = 7$. For earthquakes after 1900, instrumental data are complete for $M_w > 7$ and possibly complete for $M_w > 6.5$ (cf. Stevens & Avouac 2015). Qualitative descriptions of early Himalayan earthquakes have been quantified in the past two decades to provide new insights into Himalayan earthquakes.

Case studies of five pre-instrumental earthquakes are discussed chronologically to illustrate these new quantitative findings, followed by five post-instrumental earthquakes. For many of these earthquakes, intensity data are plotted in polar coordinates with the logarithm of distance as the radial ordinate. This permits a comparison of earthquakes of different magnitudes and rupture area on identical sized plots; and, in some cases, permits the rupture propagation direction to be estimated.

Case studies of significant earthquakes

In this section I discuss accounts of earthquakes 1500–1900, and constraints inferred from early instrumental data 1900–1960. Earthquakes prior to 1500 are insufficiently described in historical accounts to justify detailed discussion.

It is customary to describe the location of an earthquake by providing its epicentral coordinates. However, all the earthquakes we shall be discussing are not point locations but rupture areas of considerable size, often bracketing 1° or more of longitude or latitude, and many occurred before *c.* 1900 when it became possible to use seismic arrivals to determine mainshock coordinates. To place the rupture areas of each of these earthquakes in a graphically comparable form, I have adopted a polar plot centred on the rupture area plotted in logarithmically decaying distances from an arbitrary, or intensity-guided, epicentre. Intensities close to or above the rupture are thereby weighted more highly near the centre of the plot than are distant observations around its edges. The plots show either observed intensities or, with greater utility, residuals from predicted intensities using an estimated magnitude and a calculated rate of decay of intensity with distance.

1500–99 Earthquakes in Afghanistan, Kashmir and Garhwal

On 6 June 1505 at about dawn (6 am) a great earthquake, or a sequence of major earthquakes, shook almost one-quarter of the Himalayan arc and contiguous parts of southern Tibet from east of Dehra Dun to the Thakola graben in Nepal (Figs 5 & 6). A month later, on 6 July 1505, an earthquake occurred near Kabul that is inferred to have ruptured one of the faults of the northern Chaman transform system bounding the western edge of India. Fourteen years later, in 1519, a second major earthquake occurred to the NW of the 6 July 1505 Kabul earthquake of which we know little, except that the duration of the mainshock and aftershocks lasted many hours. This may have resulted from slip on the Chunar Fault or it may have been a deep Hindu Kush earthquake. The details of the Kabul earthquakes are described in Ambraseys & Bilham (2003*a*, *b*) and their subsequent conflation by historians with the 1 June earthquake in the central Himalaya is discussed by Jackson (2000) and Ambraseys & Jackson (2003).

Although the 6 June 1505 earthquake damaged several monasteries in Tibet and the Thakola graben region of Nepal, and villages in southern Tibet north of Kathmandu, no record of this earthquake has survived in Kathmandu. Shaking was also reported from the town of Agra on the southern edge of the Gangetic Plain. Prior to Sikander Lodi's move of his capital from Delhi to Agra, the city was of minor importance. Its fort at Badalgarh was damaged by the earthquake, and its reconstruction in 1505 (Lal 1980) was accompanied by expansion of the city to become a suitable residence for Sikander Lodi and his ministers and military leaders to administer his expanded dominions. All accounts describing the earthquake in Agra contain similar passages from

Table 1. *Chronological list of significant Himalayan earthquakes including palaeoseismic earthquakes with approximate dates where no known historical account exists*

Date year: month:day	Latitude (° N)	Longitude (° E)	Low M_w	High M_w	Source and commentary
844:00:00	34	74.8	6.5	7.5	Srinagar, Kashmir. Great earthquake occurred during the night – landslide dammed Jhelum at Khadanyar near Baramulla (Stein 1892, 1898; Bilham & Bali 2013) (Fig. 7)
1123:00:00	34	74.8	6.5	7.5	Srinagar, Kashmir. (Stein 1892, 1898; Iyengar & Sharma 1996, 1998; Iyengar *et al.* 1999), Sugandhesa Temple damage (Bilham & Bali 2013) (Fig. 7)
1100 ± 50	27	*c.* 86.5	8.5	9	No historical record (Wesnousky *et al.* 2019)
1223:1 2:24	27.7	85.3	6.5	7	Nepal (Pant 2002)
1225:06:07	27.7	85.3	7.5	8.5	Nepal (Pant 2002). One-third of the population of Kathmandu killed. (Sapkota *et al.* 2013)
1344:09:14	27.7	85.3	7.5	8.2	Nepal (Pant 2002; Bollinger *et al.* 2016). Epicentral longitude ±1°
1400 ± 50	30	82	8.0	8.5	Western Himalaya (Kumar *et al.* 2001, 2006)
1501:09:24	34	74.8	6.5	7	Srinagar, Kashmir. Three months of aftershocks (Bilham & Bali 2013)
1505:06:06*	30	82	8.2	8.9	Guge, eastern Nepal and Kumaon (Jackson 2000; Ambraseys & Jackson 2003)
1505:07:06	34	71	7	7.9	Kabul, Afghanistan (Ambraseys & Bilham 2003*a*, *b*)
1519:01:03	35	71.5	7	7.5	Bajaur, Afghanistan (Ambraseys & Bilham 2003*a*, *b*)
1552					Refers to the 1555 earthquake. Misinterpretation of the Prinsep (1858) p. 312 entry on the events in the 3 year reign of Ibrahim II
1555:09:00*	34.25	74.8	7.6	8	Kashmir. Baramula 34.25° N, 74.3° E; Srinagar 34.15° N, 74.8° E; Bilarah 33.8° N, 75.1° E; Anantang 33.75° N, 75.2° E; Mareg 33.7° N, 75.6° E; Maru Pergam 33.65° N, 75.7° E (Iyengar & Sharma 1996, 1998; Iyengar *et al.* 1999; Ambraseys & Jackson 2003; Bashir *et al.* 2009; Bilham & Bali 2013). Earthquakes for 7 days. Landslides, liquefaction and aftershocks (Bashir *et al.* 2009; Bilham & Bali 2013)
1669:06:23	34	74.8	6.5	7	Srinagar, Kashmir. The buildings rocked like cradles. No loss of life (distant event?) (Bashir *et al.* 2009; Bilham & Bali 2013)
1678 (1779?)	34	74.8	6.5	6.8	Srinagar, Kashmir. Persistent shaking. Reconstruction needed (Bashir *et al.* 2009; Bilham & Bali 2013)
1683:00:00	34	74.8	6.5	6.8	Srinagar, Kashmir. Shocks continued for a long time, which caused panic among masses. The quake victims constructed new houses (Bashir *et al.* 2009; Bilham & Bali 2013)
1714:05:04	27.5	89.6	8	8.2	Bhutan (Hetényi *et al.* 2016). Two historical accounts, felt reports and trenching.
1736:03:24	34	74.8	6.5	7	Srinagar, Kashmir. 'Buildings of the city and hamlets razed to the ground'. Aftershocks for 3 months (Bashir *et al.* 2009 list this event as 1735)
1752:00:00	31.5	79.8	6.5	7	Ambraseys & Jackson (2003) list this event as 1751
1779:00:00	34	74.8	6.5	7.5	(Srinagar and villages in Kashmir Valley) flattened and aftershocks for 14 days. 'destroyed houses in city and villages with much loss their life'. Aftershocks for 6 weeks: Bashir *et al.* (2009) list this event as 1778; Oldham (1883) lists it as 1780.
1784	34	74.8	6.5	7.5	Srinagar, Kashmir. People thrown. Shocks persisted for 6 months. Possibly 1785,

(*Continued*)

Table 1. *Chronological list of significant Himalayan earthquakes including palaeoseismic earthquakes with approximate dates where no known historical account exists* (*Continued*)

Date year: month:day	Latitude (° N)	Longitude (° E)	Low M_w	High M_w	Source and commentary
1803:09:01*	31.5	79	7.5	7.9	Gangotri, Srinagar (Gharwal), Almora (Ambraseys & Jackson 2003; Rajendran *et al.* 2013, 2015)
1808:06:04	27.7	85.3	6.5	7	Nepal (Pant 2002), 21 aftershocks
1828:06:28	34	74.8	6.5	7.5	Srinagar, Kashmir (Vigne 1844), 1200 houses collapsed, 15 days of aftershocks (Bashir *et al.* 2009)
1833:08:26*	28.83	78.58	7.7	7.8	Nepal (Bilham 1995; Szeliga *et al.* 2010)
1842:02:19	34.42	70.83	7.5		Jalalabad (Szeliga *et al.* 2010)
1842:03:05	30.28	80.62	7.2		Gharwal (Szeliga *et al.* 2010)
1845:08:06	26.09	90.89	7.1		Shillong (Szeliga *et al.* 2010)
1852:03:31	28.09	79.17	7.0		Gharwal (Szeliga *et al.* 2010)
1863:00:00	34	74.8		6	Srinagar, Kashmir (Bashir *et al.* 2009) Lawrence (1895) indicates 1864
1866:05:23*	27.12	85.26	7.4		Nepal (Szeliga *et al.* 2010)
1878:03:02	34.48	72.18	7.4		Hazara, Pakistan (Szeliga *et al.* 2010)
1885:05:30	34.54	74.68	7.1	7.5	Baramulla, Kashmir (Jones 1885*b*; Bashir *et al.* 2009; Szeliga *et al.* 2010)
1897:06:12*	25.13	90.07	8.1	8.3	Shillong (Szeliga *et al.* 2010; England & Bilham 2015)
1905:04:04*	32.636	76.788	7.8	7.9	Kangra (Szeliga *et al.* 2010; Szeliga & Bilham 2017)
1908:12:12	26.948	96.773	7		
1916:08:28	29.73	80.745	7		
1934:01:15*	27.55	87.09	8.4		Bihar, Nepal (Chen & Molnar 1977, 1983)
1936:05:27	28.378	83.32	6.9		Nepal
1943:10:23	26.705	93.829	7.2		
1947:07:29*	28.63	93.73	7.3		Chen & Molnar 1977, 1983)
1950:08:15*	28.363	96.445	8.7		Assam (28.33° N, 96.76° E: Chen & Molnar 1977)
1964:10:21	28.065	93.798	6.8		
1966:03:06	31.525	80.487	6.7		
1975:01:19	32.393	78.536	6.8		
1988:08:20	26.712	86.627	6.9		Udaypur >50 km depth
1991:10:19	30.753	78.823	6.8		
2005:10:08*	34.451	73.649	7.6		Muzafferapur, Pakistan
2011:09:18	27.756	88.141	6.9		
2015:14:25*	28.15	84.71	7.8		Gorkha, Nepal

Prior to 1900, coordinates indicate felt locations or trench locations, not epicentral coordinates. For many historical earthquakes only one report exists, and epicentral longitudes are not known better than 1°. A range of magnitudes is provided for pre-instrumental earthquakes, and case studies are devoted to earthquakes marked with an asterix. A zero month or day indicates that only the year is known.

Ferishta, or an earlier unknown source, stating that several earthquakes occurred, that the tallest buildings in the city became the lowest (i.e. heaps of rubble) and one mentions that several thousands of the inhabitants were buried under the ruins Although the details of structural collapse are vague, they are not easily disputed because damage to the fort comes from an independent historical source; however, some accounts begin with the phrase 'The hills began to shake', which poses a problem since there are no hills within 30 km of Agra. It is probable that this phrase was introduced as the result of conflation with Bábar's account of the Kabul earthquake 1 month later (Ambraseys & Jackson 2003).

Several accounts, presumably derived from a missing original account, speak of *successive* earthquakes shaking Agra on 6 June 1505. This is unusual for what might almost be considered a teleseismic location, and again may have arisen from aforementioned conflation with the July Kabul earthquake. However, the multiple earthquakes described in Agra accounts have parallels with descriptions in mezzo-seismal Tibetan sources. The following accounts are abstracted from Jackson (2000), using his chronology dated 7 June and 8 June. The dates in Ambraseys & Jackson (2003) are described as follows 'The fifth or the sixth day of the fifth lunar month of the wood-ox year in the 9th Tibetan sixty-year cycle' corresponding to '6 or 7 June 1505':

> 7 June 1505 Marang, Globo/Mustang (83.4E, 28.5N) When the sun rose … five great earthquakes arose of almost unbearable intensity. Many monasteries and palaces collapsed to the earth.

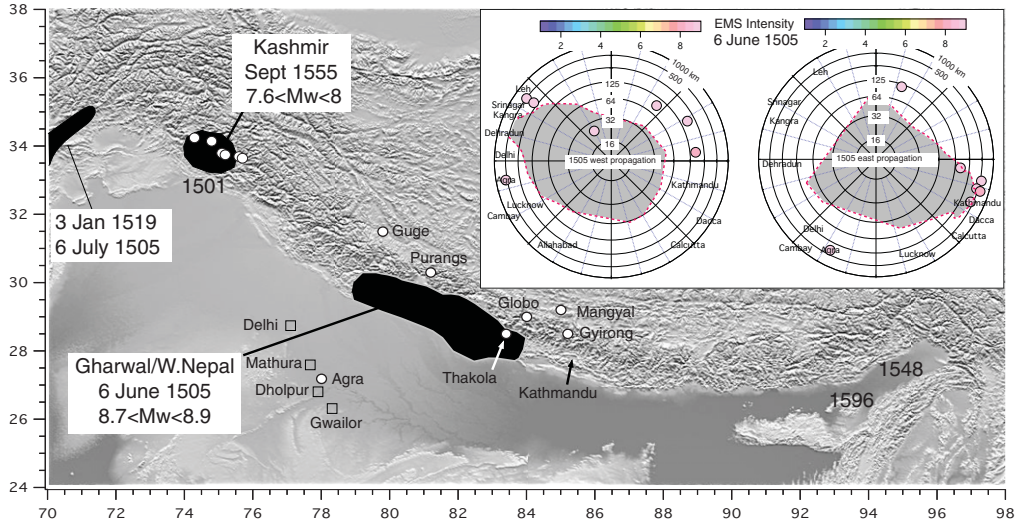

Fig. 6. The location of sixteenth century earthquakes, and reported damage from the 6 June 1505 and 1555 earthquakes. White circles clustered near inferred rupture zones (shaded black) indicate conformed reports; open squares are accounts of dubious validity. Dated events with no rupture areas are the location of accounts from one location only with no indication of severity. The inset polar plots are shown for westwards (nucleation at 28.3° N, 83.5° E) or eastwards (nucleation at 30.5° N, 79.5° E) propagation for the 6 June 1505 $8.7 < M_w < 8.9$ earthquake, assuming it was a single event (see the text). The radial direction from each hypothesized nucleation point is represented by the log of the distance in kilometres from the hypothetical epicentre at the centre of the polar plot, and the azimuth indicates the proximity and direction of major cities and the (in this case, sparse) location of intensity observations. The grey area within the dashed red line represents the rupture area (from Table 2) using the same projection and permits a first-order evaluation of the possible influence of rupture propagation directivity, relative to reported observations of shaking intensity. That the earthquake was not reported in Kathmandu, where sediment amplification would have been pronounced, provides weak evidence that the earthquake ruptured westwards (see the text).

Table 2. *Estimated bounds of the 6 June 1505 $8.7 < M_w < 8.9$ Garwhal/Nepal rupture (latitude GN°, longitude GE°) and the September 1555 Kashmir (latitude KN°, longitude KE°) ruptures (see the text)*

1505 Gharwal, western Nepal				1555 Kashmir	
GN°	GE°	GN°	GE°	KN°	KE°
29.6	79.0	28.9	83.2	34.2	74.1
29.5	78.9	29.1	82.9	34.0	74.0
29.2	79.8	29.4	82.5	33.7	73.9
29.0	80.4	29.5	82.3	33.5	74.1
28.7	81.0	29.6	82.0	33.3	74.6
28.6	81.3	29.7	81.8	33.2	74.9
28.4	81.5	29.7	81.6	33.2	75.2
28.0	81.9	29.8	81.3	33.5	75.5
27.7	82.5	29.9	81.1	33.8	75.5
27.8	82.9	30.0	80.7	34.2	75.2
27.8	83.1	30.1	80.4	34.3	74.9
27.7	83.9	30.2	80.2	34.4	74.7
27.8	84.0	30.2	79.9	34.4	74.5
28.0	84.2	30.3	79.8	34.4	74.3
28.4	84.2	30.4	79.6	34.2	74.1
28.6	83.7	30.5	79.4	34.2	74.1
28.7	83.4	29.6	79.0	34.0	74.0

8 June 1505 Between early morning and evening 14–15 earthquakes shook the region between Guge 79.8E, 31.5N and Mangyul GungThang (85E, 29.2N) including Purangs (81.2E, 30.3N) and Globo (84E, 29N). The region from Globo westward and southward, including the Kali Gandaki region of central Nepal was more severely shaken than Mangyul GungThang. In the Tibetan mountains north of Kathmandu (85.2E, 28.5N) houses collapsed but there were fewer casualties.

Hitherto, it has been assumed that the date sequence 6, 7 and 8 June is the result of historical entry errors similar to the conflation that subsequently occurred with the 6 July Afghanistan earthquake, a lunar month later. But the historical entries admit the possibility that they describe a sequence of earthquakes. Even if the rupture were a single event, as hitherto considered probable, the 1505 rupture, like all great earthquakes, would have consisted of a mainshock followed by major aftershocks. Assuming unilateral propagation of a single *c.* 550 km-long rupture, the rupture propagation pulse could have taken as little as 4 min to reach Thakola from Guge, or vice versa. A minimum magnitude of the event was estimated as 8.2 by Ambraseys & Jackson (2003) and Bilham & Ambraseys (2005) based on an intensity

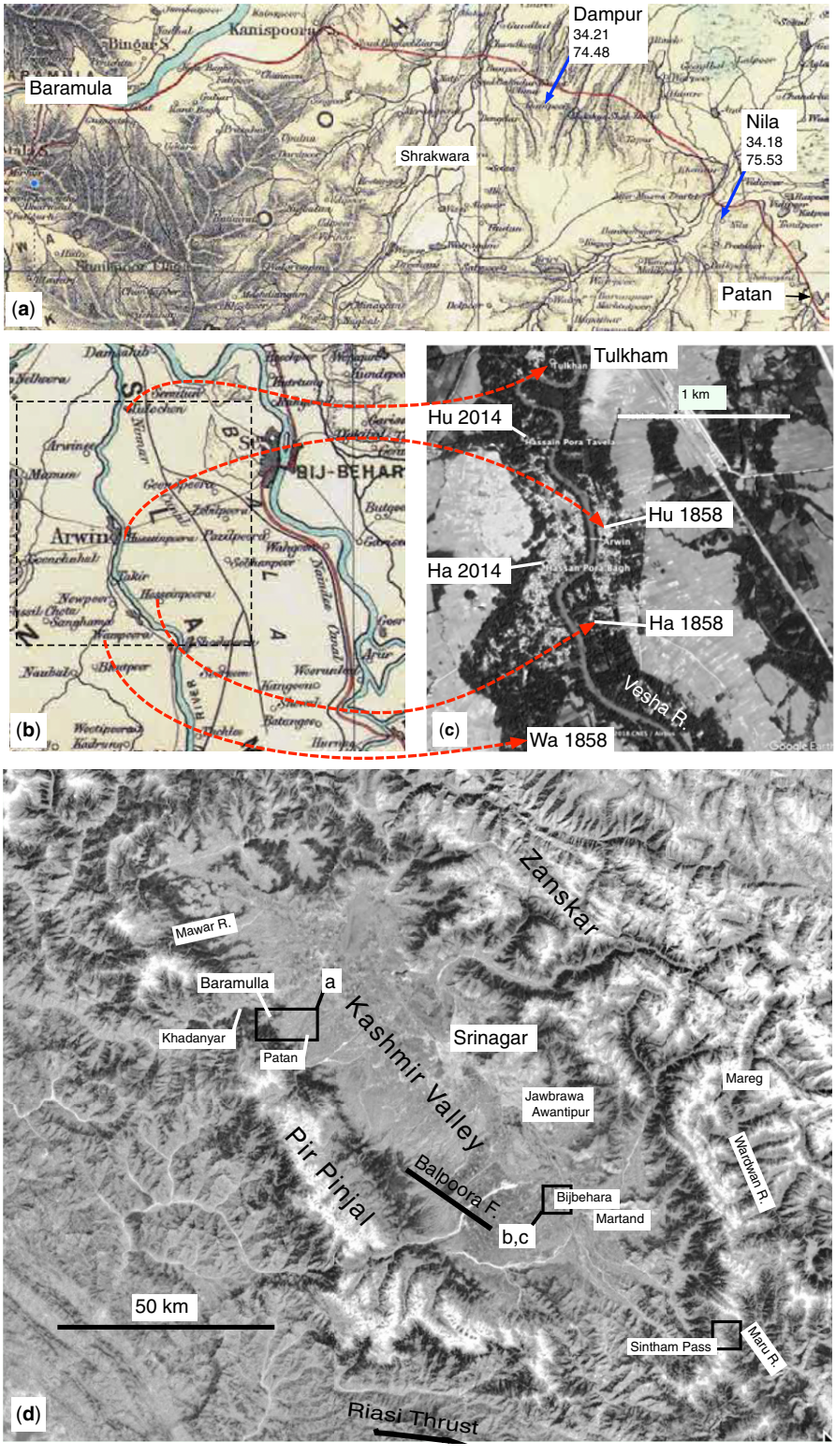

scaling relationship, which saturates for large earthquakes, and is thus a minimum estimate. Given a rupture area of 450–550 km long and *c.* 100 km wide with 10–15 m of slip, the actual magnitude of the 1505 earthquake as a single rupture was more likely to have been $8.7 < M_w < 8.9$. Distinct aftershocks approaching or exceeding $M_w = 7.8$, and numerous smaller earthquakes, would be expected to follow such a large slip event. Agra lies no closer than 250 km from the Himalaya; however, its riverine setting, and its location in a region of thinning sediments near the southern edge of the Gangetic Plain, makes Agra especially prone to surface-wave amplification from waves from the Himalaya shelving as they approach the southern margin of the Ganges sediments. Similar amplification was recorded near Monghyr in the 1934 $M_w = 8.4$ earthquake (Pandey & Molnar 1988). Hence it is possible that Agra was shaken not just by a $M_w > 8.6$ mainshock, but also by one or more $M_w > 7.6$ aftershocks.

The case for the 1505 earthquake would be strengthened were there, within the >500 km-long arc of the rupture, an extensive independent sequence of palaeoseismic trenches confirming a throughgoing rupture on the Main Frontal Fault. Palaeoseismic trenches claim to have sampled its surface rupture with slip of 4–10 m (Yule *et al.* 2006; Bollinger *et al.* 2016; Hossler *et al.* 2016; Malik *et al.* 2017). However, the palaeoseismic dates interpreted (and reinterpreted) by these authors admit at least a ±50 year uncertainty in the dating of ruptured sedimentary layers, and therefore are unable to distinguish between a single massive rupture or a sequence of ruptures, or even that the causal earthquake occurred in 1505.

Another vexing, but not fatal, problem is that the earthquake was not recorded in Kathmandu histories. The absence of an historical account is not unusual because records can easily be lost or destroyed in subsequent centuries, and for many of Nepal's early earthquakes a single line of text is all that remains of evidence for their occurrence. Moreover, along-strike shaking is known to be attenuated significantly in the Himalaya. For example, the 2015 Gorkha earthquake was felt strongly in Kathmandu where the rupture terminated, but it was hardly felt in Pokhara 70 km west of the Barpak epicentre. However, it is considered likely that eastwards propagation of the 1505 rupture would have been associated with significant directivity with long-period basin resonance in Kathmandu, and would have probably been recorded by Nepali sources had this occurred. In contrast, had the earthquake nucleated near Pokhara and propagated westwards, this would have increased directivity effects in Agra, and lessened the chances of it being felt in Kathmandu (Fig. 6 inset). Weak eastwards directivity in the intensity distribution was noted in the Gorkha earthquake (Adhikari *et al.* 2017). The distribution of observed intensity locations is insufficient to evaluate its propagation direction, but the above reasoning would suggest it propagated from east to west.

Rajendran *et al.* (2013) took issue with speculative reports of damage at Dholpur, Gwalior and Mathura cited by Iyengar *et al.* (1999) and Ambraseys & Jackson (2003) on the basis that they are known only from an historical novel written in Hindi by Verma (1889–1969), whose sources in 1950 are unknown and perhaps imaginary. For this reason these locations are omitted from the polar plots of Figure 6. Less well founded is their concern at the absence of reports of damage to the Qtub Minar in Delhi in 1505, which, as mentioned above, was at the time possibly undergoing reconstructive maintenance (Fig. 5).

The 1 June 1505 earthquake remains veiled with uncertainties, and is poorly constrained by its historical sources. That it occurred on the Main Himalayan Thrust is probable, for if it were a single rupture there is no known alternative, sufficiently large, structure to host an earthquake with dimensions approaching or exceeding 500 km. Its eastern edge must have been close to the Thakola graben, perhaps extending as far east as Jomoson (84° E), with milder damage extending further east to 85° E (Kyirong north of Kathmandu). Its northern edge is assumed to be the locking line roughly following the 3.5 km contour, and its southern edge would have been the Main Frontal Thrust where evidence for surface rupture has been postulated (Yule *et al.* 2006). Its western

Fig. 7. Maps of the Kashmir Valley. (**a**) Section of Montgomerie (1858) map showing villages of Nila and Dampur mentioned in one of several accounts of the 1555 earthquake (location a in d). The Nila location is also mentioned as venting methane in an account of the 1885 Kashmir earthquake. (**b**) Segment from 1858 map with a dashed box showing the location of the 2014 Google Image (**c**). The villages Hussainpur (Hu), Hossainpur (Ha) and Dampur (Wampur, Wa) near Arwin allegedly switched sides across the Vesha River in 1555. The Vesha floodplain is approximated by the dark forest cover. With the exception of a more pronounced meander near Tulkhan, the path of the Vesha River has changed little since 1858. The present village of Wanpora may correspond to the village of Dampur (Wampur) mentioned in Ferishta's account of the legend. (**d**) Location map. The village of Khadinyar near Baramulla lies close to the earthquake-induced landslide that in 844 CE dammed the Jhelum and flooded the valley up to Bijbehara (Bilham & Bali 2013). Bilham *et al.* (2013) described a minor normal fault near the summit of the Sintham Pass that slipped near this time (*c.* 700 CE ^{14}C detrital date). The Sughandesa Temple near Patan was damaged in an earthquake in 1123 CE and again in 1885 (Bilham & Bali 2013).

edge may have extended as far as 78.5° E near Tehri and Srinagar in Gharwal; however, the damage in Guge could equally have been a local triggered earthquake north of the Himalaya. Table 2 lists the approximate bounding coordinates of this area with uncertainties of *c.* 30 km in the east, and *c.* 20 km north and south, but with considerable uncertainty in the west, which is constrained by a single report of damage in Tibet.

Kashmir, September 1555, 7.6 < M_w < 8.0. Iyengar & Sharma (1998) reproduced original and translated accounts of the 1555 earthquake in Kashmir (Figs 6 & 7). Additional accounts are reproduced in Ambraseys & Jackson (2003). The wording of the several accounts of the earthquake are sufficiently similar to suppose that they are all sourced from an earlier account, perhaps written by the contemporary historian Suka, and hence cannot be considered independent observations. The damaging earthquake appears to have been one of a sequence of events, with a mainshock and numerous aftershocks, that occurred over a period of 7 years starting in 1554 or 1555 shortly after the valley had been annexed by Babur's son Humayun. The earthquake occurred at around midnight, collapsed many houses in Srinagar and toppling some into the river, and was accompanied by fissuring and ground cracks.

A puzzling account ubiquitously repeated by historians for this event that has yet to be quantitatively explained is related to the two villages, now variously named Hussainpura, Husseinpoora, Nilu or Jalu, and Hassanpura, Hosseinpura, Adampur or Dampur, that allegedly switched positions across the Vesha River near Arwin during the night of the earthquake. Nila (34.18° N, 75.53° E) and Dampur (34.21° N, 74.48° E) are located 7 km apart on Montgomerie's 1858 map south of the old road from Patan to Baramula (Fig. 7a). However, these locations are 84 km NW of the Vesha River, and lie on elevated but relatively even terrain above the floodplain separated by a small valley. Thus, these appear to be spurious locations conflated with the 1555 earthquake. Intriguingly, Jones (1885*a*, *b*) reported a fissure at Nila to be emitting methane after the 1885 earthquake and an offset of the nearby Baramula–Patan road (Fig. 7a).

Tarikh-i-Hassan (Ghulam Hassan 1954) includes a verbose description of the 1555 legend, and the author, Pir Ghulam Hassan, who lived from 1833 to 1898, identifies the legend with the names Husseinpur and Hassanpur. He would have had access to Montgomerie's 1858 map, which shows these two villages on the east side of the Vesha (Fig. 7b) in the relatively featureless floodplain of the Jhelum near Bijbehara. The flatness of the surrounding terrain makes it unlikely that gravity sliding would have been responsible for the translation of the two villages. The most likely explanation is that an avulsion of the river was triggered by liquefaction or lateral spreading towards the incised river. Downstream collapse of the banks of the Vesha would permit its banks to flood and to take a new course. Currently, the Vesha is incised in a narrow channel within sediments approximately 5 m below the level of the fields adjoining the river (Fig. 7b). The mystery of what occurred during the earthquake is further confused by the current locations of the two villages (*c.* 33.78° N, 75.07° E) being mapped *c.* 1 km apart both on the west bank of the Vesha (Fig. 7c), whereas in 1858 they were mapped on the east bank of the river roughly 500 m SE of their present positions. That the locus of a village may shift with time is indicated by the changes in the named location of Tulkham. Between 1858 and 2014, the meander near Tulkham apparently shifted to the east of the present village identified by that name.

The 1555 earthquake is generally considered the largest earthquake to have been described by historians in Kashmir, but this may be because the curious village-translation legend narrated above recurs in many histories, and is the only earthquake prior to 1885 for which damage is described in more than one location (Fig. 6). Major earthquakes occurred in 1501, 1669, 1736, 1779, 1784, 1828 and 1885, and damaged buildings in Srinagar, and all were associated with aftershocks lasting for weeks or months for which we have scant information. The recent period between 1885 and 2005 in Kashmir for which we have a reliable history is thus atypical in that it is devoid of major earthquakes.

Ambraseys & Jackson (2003) identified six locations in the Kashmir Valley that were damaged by the 1555 earthquake (Table 2), although there is much uncertainty about the precise coordinates of half of them. They equate the most northwesterly of these six sites with Baramulla, 50 km west of Srinagar, and the most southeasterly (Jadra or Maru Pergam) tentatively 120 km SE of Srinagar near Khandkot on the River Chenab (SE of Fig. 6d). Several possible landslide locations lie in the Wardwan Valley that may have buried a village of 6000; however, the location is so uncertain that Jadra may refer to Montgomerie's village of Jaidner or Jabair (now Jawbrawa: 33.93° N, 75.00° E) below the steep hills that rise 1 km above the Kashmir valley floor north of the Temple at Avantipur. The bedrock region of the Martand Temple (33.74° N, 75.22° E), just 15 km ESE of Hussainpur/Hassanpura on the hills above Anantnag, is mentioned as having been shaken less vigorously by the 1555 earthquake (e.g. intensity ≤7), protected by the sanctity and proximity of the Martand Sun Temple (Fig. 6d); although the temple itself is supposed to have been ruined by Sikander (the Iconoclast) a century earlier.

The GPS convergence vector in Kashmir (12.5 ± 1 mm a^{-1} at N175° W) is almost 45° oblique to the Zanskar and Pir Pinjal range front, which led Kundu *et al.* (2014) to suggest that the Karakoram Fault is responsible for partitioning the *c.* 5 ± 1 mm a^{-1} shear component of the GPS vector. The long-term slip rate on the Karakoram Fault is insufficient to absorb this slip and, although a case can be made to interpret sparse data nearby, the geodetic shear strain component is not localized near it (Zheng *et al.* 2017). Alam *et al.* (2015) speculate that the Kashmir Valley represents a relict dextral pull-apart basin with an invisible dextral fault along its axis. There are several problems with this suggestion, not the least being the absence of strike-slip mechanisms in local earthquakes, and the absence of evidence for strike-slip faulting in the mountains beyond the ends of the valley. Shah (2016) offers a litany of additional problems. In the absence of identifying a major strike-slip, the Riasi thrust system (Fig. 7) or a high-level thrust must host an oblique slip component.

If all six sites of the felt locations have been correctly identified and were shaken by approximately intensity 8, they are consistent with a NW–SE-striking rupture with a length of *c.* 170 km. If the earthquake occurred on a décollement type thrust beneath the Zanskar or Pir Pinjal Range, its magnitude assuming a downdip width of 50–100 km and a slip of 2–5 m would have been $7.8 < M_w < 8.2$. If Baramula and Maru Pergam are omitted from consideration, the remaining sites have a spatial distribution of 80 km along-strike which would reduce the estimated magnitude to M_w 7.8, possibly to as low as M_w 7.6 if the rupture were steep, and the rupture area reduced in width, as in the recent 2005 Kashmir earthquake. Mugnier *et al.* (2017) argued that this is more likely, and that great earthquakes may not occur on the décollement beneath Kashmir, and instead NW–SE shortening is accommodated on steeply dipping thrust faults. They base this conclusion on an analysis of the several surface offsets of the Riasi Thrust, the thrust fault underlying the southern margin of the Pir Pinjal. This interpretation would be consistent with the depth of the décollement inferred by Schiffman *et al.* (2013), but is less compatible with the broad zone of seismic decoupling inferred from the GPS velocity field here (Stevens & Avouac 2015). Geodetic data exclude the possibility of localized strain concentration beneath the NE edge of the Pir Pinjal. The 1555 earthquake currently has no known surface rupture, but Shah (2013, 2015) described a thrust fault mapped on the NE flank of the Pir Pinjal that may have hosted the 1555 earthquake. An alternative explanation is that a north-dipping thrust fault beneath the Zanskar Range could have slipped in 1555, with its surface rupture subsequently buried by rapid sedimentation from the Jhelum. The only surface fault of note in the Kashmir Valley is the Balpora reverse fault (Fig. 7) that dips to the SW and is estimated to have a low rate of slip (<1 mm a^{-1}), and which has not slipped in the past 1000 years (Madden *et al.* 2010).

The large range of possible magnitudes ($7.6 < M_w < 8.2$) for the 1555 earthquake follows from the scant observational data available and the absence (as yet) of palaeoseismic evidence for a surface rupture. The rupture area depicted in Figure 6 is thus conjectural and the footprint of the rupture may be significantly less if the rupture occurred on a steeply dipping blind thrust, or more if the rupture extended to Kishtwar to the SE. Such data as are available are limited to the vicinity of the Kashmir Valley, and had the earthquake exceeded $M_w > 7.8$ it is considered unlikely that it would have escaped mention in the records of the Mughal administration whose revenues were documented at length in the A'in Akbari of Fazl-i-Allami (see Sarkar 1978) some 40–50 years after the earthquake. A rupture much longer than 150 km is considered unlikely, and the magnitude of the earthquake of 1555 is likely to have been $M_w < 8$.

1600–1799: 200 years with few major earthquakes?

In the seventeenth and eighteenth centuries, few earthquakes are recorded as having occurred in the Himalaya (Fig. 8), and although numerous earthquakes must have occurred, only those in Kashmir, with one exception, were sufficient to cause damage and for these we have solitary reports. The exception is the Bhutan earthquake, which occurred on 4 May 1714, and was registered by felt reports in Bhutan and in Assam (Fig. 7). The absence of major earthquakes in the Central Himalaya 1600–1803 is probably real because several histories have survived from these times; however, the absence of written notifications of earthquakes is never a conclusive indicator of seismic quiescence.

The details of the Bhutan earthquake were considered by Hetényi *et al.* (2016), who based their estimate of magnitude of $M_w = 8.0 \pm 0.5$ on five felt reports and two trench excavations that bracket a minor surface rupture between 1642 and 1836 (Le Roux-Mallouf *et al.* 2016) (Table 3).

Nineteenth century earthquakes

In the nineteenth century, the historical record undergoes a dramatic increase in the numbers of earthquakes recorded, described and studied (Fig. 9). For the first of these, 1 September 1803 in the Garwhal Himalaya, numerous damage accounts exist

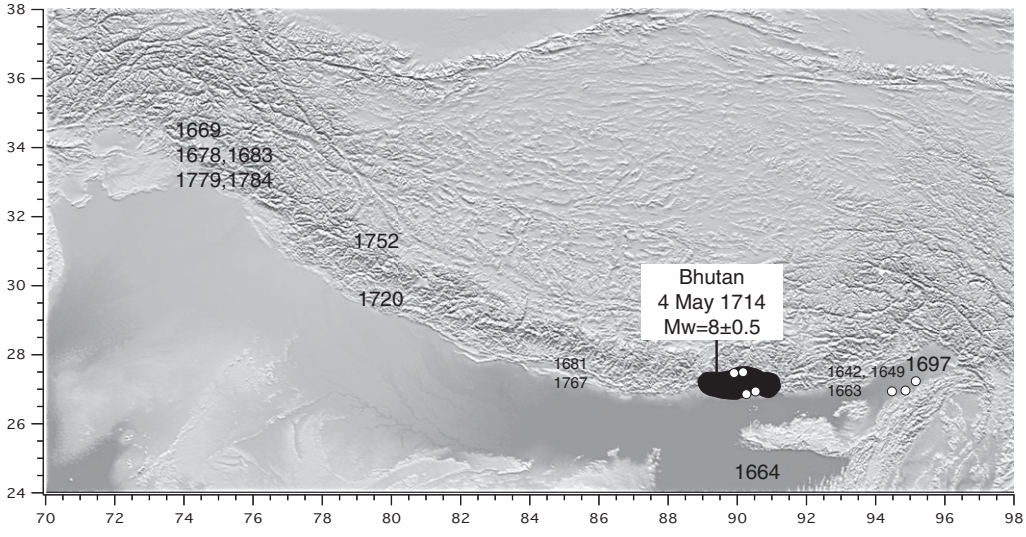

Fig. 8. Seventeenth and eighteenth century earthquakes. With one exception, the earthquakes are known from single accounts and thus permit no estimate of magnitude. The exception is the 1714 Bhutan $M_w = 8.0 \pm 0.5$ earthquake (Hetényi *et al.* 2016) felt north and east of the epicentre, and associated with dated slip in two trenches (white circles).

from explorers, military officers, travellers' accounts and reports in newspapers: 25 reports have been evaluated by Martin & Szeliga (2010) and 34 by Ambraseys & Douglas (2004). Historical accounts have been reproduced by Dasgupta & Mukhopadhyay (2014), and archaeological damage and geological implications were assessed by Rajendran *et al.* (2013).

Garwhal (Almora/Srinagar), 1 September 1803 (01:30 local time), 7.6 < Mw < 8. The earthquake caused church clocks (set by the local midday sun) to stop at 01:17 in Allahabad and at 01:35 in Calcutta, where the sloshing of water tanks caused fish to be tossed onto banks (the p. 388 entry in the *Calcutta Gazette* for 8 September 1803 is erroneously entered 1 week late). Fissuring and liquefaction phenomena were extensive in Mathura, located between Aligarh and Agra, and a woman was killed by a falling tile. Another was put to death upon suspicion of infidelity due to the mutually scant clothing of her and her rescuer (*Asiatic Annual Register* 1804, p. 100). A potentially long-duration military siege came abruptly to an end that day, with the capture of the Fort of Aligarh presumably as a result of distress to the resisting Mahratta forces in the early morning hours (Thorn 1818). The four-pillared cupula of the Qtub Minar in Delhi was destroyed and the structure of the column was much weakened. Although the earthquake was close to Srinagar, Garwhal, it may have damaged Srinagar, Kashmir, where several houses and the spire of the Khanqah-e-Moalla mosque collapsed, and ground fissures occurred (Ahmad *et al.* 2009). However, the absence

Table 3. *Bhutan earthquake intensity observations (I) and approximate bounds for ruptures (latitude BN°, longitude BE°) from Hetényi* et al. *(2016)*

Location	Latitude (° N)	Longitude (° E)	I	BN°	BE°	BN°	BE°	BN°	BE°
Wangdue	27.5	89.9	8	27.5	88.9	26.9	90.3	27.6	90.0
Bahgara	26.9	94.4	6	27.1	88.9	26.9	90.5	27.5	89.7
Charaideo	26.9	94.9	6	26.9	89.0	26.8	90.9	27.5	89.1
Tinkhong	27.2	95.2	6	26.8	89.3	27.1	91.2	27.5	88.9
Sarpang Trench	90.3	26.9	8	26.8	89.4	27.5	91.2	27.5	88.9
Gelephu Trench	90.5	26.9	8	26.7	89.9	27.5	90.7		

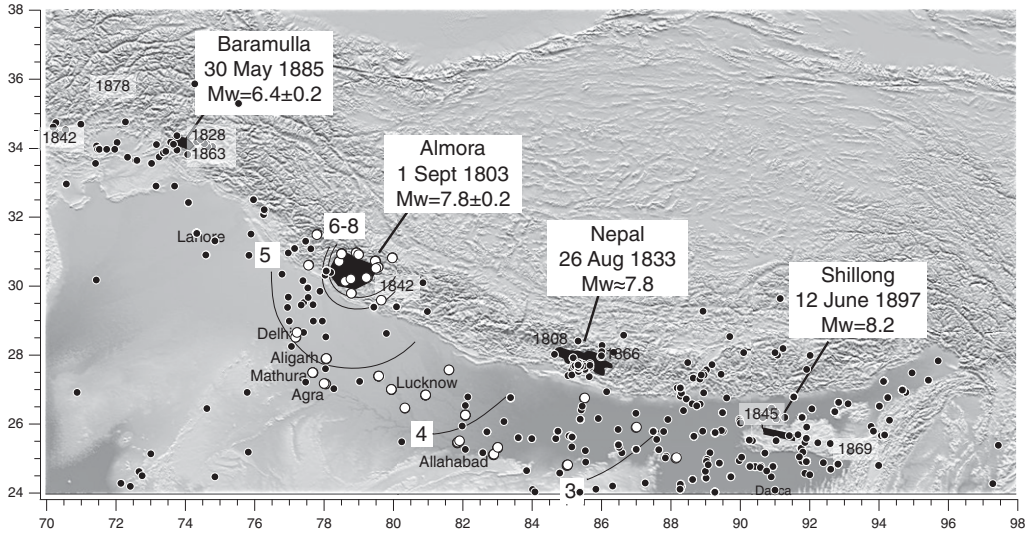

Fig. 9. Nineteenth century earthquakes. Approximate location of the 1803 rupture and its felt reports (white circles), and the location of all nineteenth century felt reports (1800–99, black dots) from Martin & Szeliga 2010. Approximate EMS intensity contours for the 1803 earthquake are shown.

of a specific day and month may imply that the year of this account (Ahmad *et al.* 2009) could have been conflated with an earlier earthquake.

The epicentre of the 1803 earthquake (Fig. 10) lies in the Gharwal Himalaya near Uttarkashi (then Barahat), where in the summer of 1808, just 5 years after the earthquake, Raper (1810) provides a verbose description of damage during his team's search for the source of the Ganges. At the time of the earthquake and for the next 12 years the epicentral region was occupied by Gorkha forces, hence subsequent news remained sparse. Fraser (1820) reported primitive repairs to the Badrinath temple in 1819, and, according to Rajendran *et al.* (2013), ancient temples between Chamoli and Uttarkashi were all repaired following the earthquake. However, a cluster of temples to the SE appear to have been damaged and partly repaired after earlier earthquakes (and some remain in ruins even now), a possible contender being the 1505 rupture that presumably terminated near this longitude. Felt intensities above the Gorkha 2015 rupture averaged about 6.6, which provides weak justification for approximating the 1803 rupture by an envelope that includes the sparse intensity 7 observations. When this is done, the 1991 and 1999 Uttarkashi and Chamoli earthquakes are found to be approximately located at each end of the inferred 1803 rupture patch (Table 4). The 260 m-high Tehri Dam, which was designed to resist shaking in a $M_w = 7.2$ earthquake, lies within the inferred 1803 rupture zone. A precise repeat of the 1803 earthquake would shake the dam with EMS intensity ≥7 (0.3*g*) for approximately 5 s, with a 'fling' exceeding 4 m (Bilham 2016) approximately normal to the face of the dam. Calculations reveal that this might lead to crest settlement threatening the integrity of the dam (Sengupta 2010).

Given the location of the strongest shaking and the probable area of the rupture, the direction of propagation in the 1803 earthquake was probably from the NW to the SE. According to the analysis of Szeliga *et al.* (2010), the epicentre coincided with the epicentre of the Uttarkashi earthquake, where most damage was reported in 1803. In Figure 11, we adopt this epicentre (30.7° N, 78.7° E) and project the rupture area and intensity observations radially from this point. Consistent with nucleation in the NW and directivity to the SE, residuals are largely low (−2 EMS units) to the NW and high to the SE. The high (+2 EMS units) residuals at Agra, Mathura and Lucknow are probably the amplified response to surface waves shelving near the southern edge of the Ganges Basin, as was observed in the 1934 earthquake (Pandey & Molnar 1988).

The conjectural rupture zone is depicted as an incomplete rupture of the Main Himalayan Thrust in Figure 10 terminating updip 20–50 km north of the Main Frontal Thrust. Three intensity observations near the southern edge of the inferred rupture, however, attain intensities $6 < \text{EMS} < 8$ that are consistent with slip approaching or rupturing the Main Frontal Thrust (Fig. 10). The palaeoseismic record of the 1803 Almora/Srinagar earthquake is currently disputed. Malik *et al.* (2017) reported evidence for a

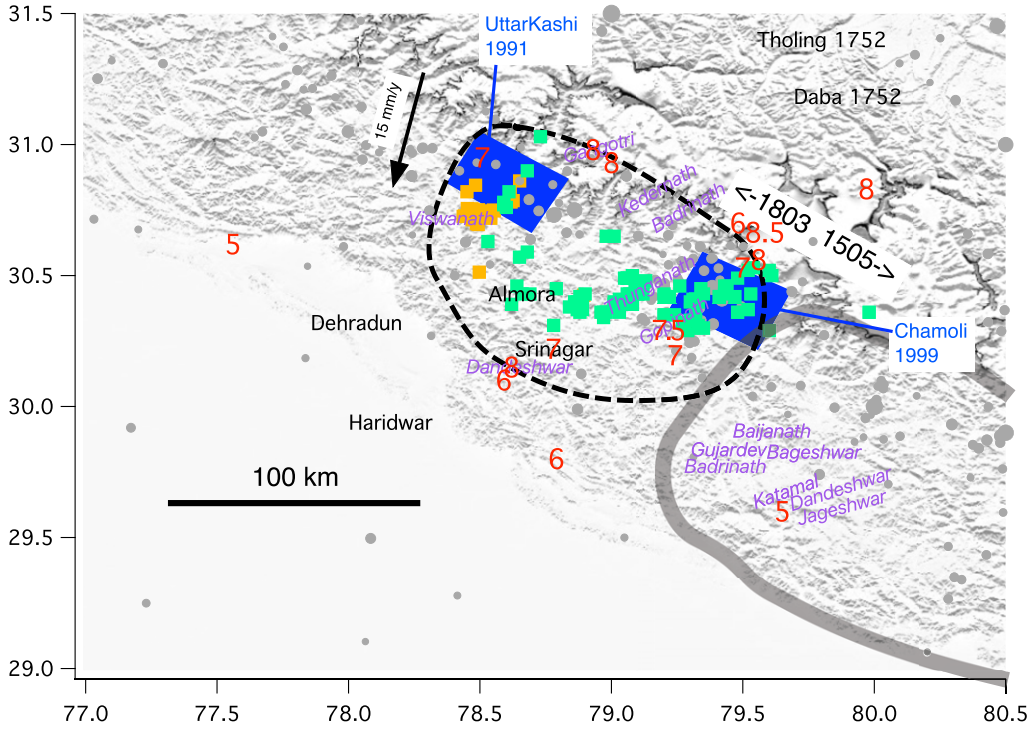

Fig. 10. The inferred epicentral region of the 1803 earthquake (dashed) is loosely drawn to encapsulate the EMS intensity 7 observations (red numbers) and named temples (violet italics) repaired after 1803 (Rajendran *et al.* 2013). The repair or ruin of temples to the SE of the depicted rupture is not specifically associated with the 1803 earthquake. The rupture areas of the Uttarkashi 1991 and Chamoli 1991 earthquakes are shaded blue, and their intensity ≥7 felt locations are shaded by orange and green squares, respectively. The conjectural west end of the 1505 rupture is outlined with light grey shading. The arrow depicts the local convergence rate and direction.

surface rupture in 1505 and 1803. Rajendran *et al.* (2018*a*) found no surface rupture in 1803 in a nearby trench.

Is it possible that the four earthquakes depicted in Figure 10 influenced each other in the sense that earthquakes after 1505 responded to residual localized slip deficits? The 1505 earthquake would have resulted in stress near its western termination that would have been reduced by the 1803 earthquake. In the same way, the 1803 earthquake may have incompletely released stress in the region between the 1999 Chamoli earthquake and the 1505 rupture; and the 1991 Uttarkashi earthquake would represent the release of stress concentrated near the western end of the 1803 rupture (Fig. 12). Figure 12a illustrates an elliptical distribution of slip magnitude typical of theoretical ruptures. There is some evidence to suggest that rupture distributions can be skewed to a more triangular distribution.

Does the developing slip potential (Fig. 12b) from the local 15 mm a^{-1} GPS-derived convergence rate support this scenario? Supposing that the Chamoli and Uttarkashi each slipped 1 m (Satyabala & Bilham 2006; Xu *et al.* 2016), this would represent only one-third of the 2.9 m slip potential developed since 1803: that is, the earthquakes in the 1990s released insufficient slip to annul the accumulating slip potential since 1803. In contrast, the 1803 rupture zone, had it a zero slip potential in 1505, may

Table 4. *Approximate coordinates bounding the rupture of the 1803 earthquake (used to plot rupture zones shown in Figs 10 & 11)*

Latitude (° N)	Longitude (° E)	Latitude (° N)	Longitude (° E)
30.8	79.0	29.9	78.9
31.0	78.6	30.1	79.3
30.8	78.3	30.4	79.5
30.4	78.1	30.6	79.5
30.0	78.4	30.8	79.0

The area indicated is much the most uncertain of the several large earthquakes that have occurred since 1800. The epicentre from maximum damage and directivity consideration is inferred to have been at 30.7° N, 78.7° E, with rupture propagation to the SE.

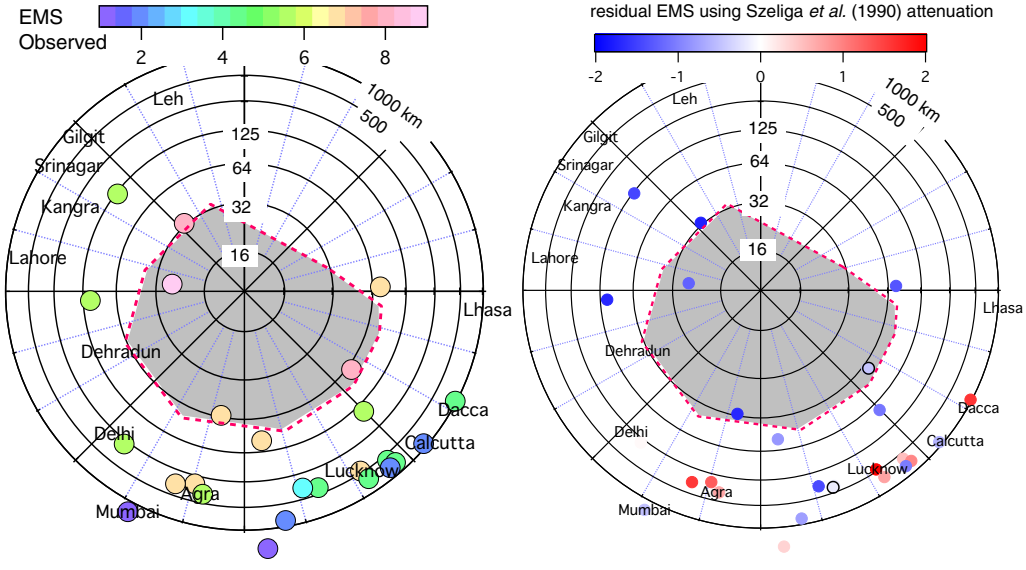

Fig. 11. Polar log–distance plots showing the conjectural rupture zone and observed and residual EMS assessments for the 1803 Almora/Srinagar earthquake. The residual is the difference between the observed EMS value and that predicted by the Himalayan attenuation curve developed by Szeliga *et al.* (2010). SE rupture propagation is evident from the residual plot (right), and is consistent with their calculated epicentre near Gangotri and Uttarkashi (Fig. 10).

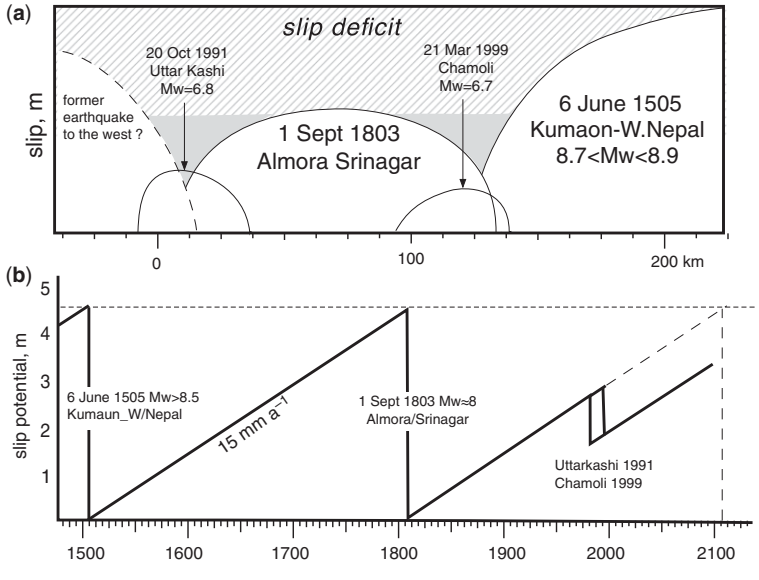

Fig. 12. (**a**) A cartoon of sequential slip in the 1505, 1803, 1991 and 1999 earthquakes depicting the static slip residual resulting from contiguous or overlapping elliptical slip distributions. Assuming the 1991 and 199 earthquakes reduced the wedge-shaped grey slip residuals between the larger earthquakes, the hatched region shows considerable slip potential remains to which must be added the growing 1.5 m/century slip potential from the convergence rate. (**b**) The time sequence of the growing slip potential assuming zero strain after the 1505 earthquake at these longitudes. The region between the 1991 and 1999 earthquakes includes a slip deficit that will grow by *c.* 2100 to 4.5 m. The current slip deficit is sufficient to drive a $7 < M_w < 7.3$ earthquake in the Almora/Srinagar/Tehri region.

have released its entire 4.5 m slip potential as a M_w = 8.0 earthquake. However, we have supposed that the 1803 rupture was not ruptured in 1505, and hence the 4.5 m slip we have invoked may represent a minimum slip deficit in 1803. The slip deficit prior to failure may have been twice this and, if its rupture zone is correctly depicted in Figure 7, its magnitude would have been M_w = 8.2. Bilham *et al.* (2017) discuss reasons why it may not be possible to support much more than a 2–3 m slip potential near 79° E, and in that discussion we assume a much more compact rupture area for the 1803 earthquake consistent with the improbably low magnitude (M_w = 7.5) obtained by Szeliga *et al.* (2010).

Thus, even with this overly simplistic model based on admittedly sparse data, neither the 1803 earthquake (with an inferred slip of ≤4.5 m) nor the Chamoli/Uttarkashi earthquakes were sufficiently large to release the accumulating slip deficit in the Garwhal/Kumaon Himalaya. Moreover, an earthquake with up to 3 m of slip between the 1991 and 1999 earthquakes is necessary to release the slip accumulated since 1803. If its downdip width is 20 km, and the entire slip deficit between the two earthquakes is released this decade, its magnitude would be $M_w \approx 7.3$. If it releases 30% of the slip deficit and slips 1 m, its magnitude would be $M_w \approx 7$. In a later section of this chapter, the consequences of a pervasive and growing slip deficit along the Himalaya will be discussed.

Nepal, 26 August 1833 (c. 11 pm local time), $M_w \approx$ 7.8. Although there has been much discussion of the magnitude and location of the 1833 Nepal earthquake, a comparison between the 1833 and 2015 (Martin *et al.* 2015) intensity observations reveals that they resemble each other to such a degree that distinguishing the two can only be undertaken with difficulty (Mencin *et al.* 2016 supplement). Previous comparisons have been driven by investigators attempting to identify the epicentre of an earthquake, rather than its mean rupture location. In the polar plot shown in Figure 13, intensities from identical locations are shown. Since there are approximately as many excess residuals as deficient residuals, the use of the 1833 intensity data to refine an unique location or magnitude different from the Gorkha earthquake requires independent information that we are currently lacking. An acceptable working hypothesis is thus that the 2015 earthquake is a replica of the 1833 earthquake, and that its magnitude was M_w = 7.8, and that the mean slip in the Gorkha earthquake represents the slip potential of *c.* 3.3 m that accumulated between the two earthquakes as a result of observed Indo-Tibetan GPS convergence at a rate of 15–18 mm a^{-1}.

However, there are differences. The 1833 earthquake was preceded by two foreshocks that were sufficiently large to alarm the local population and to bring them out of doors, saving in the process many lives during the mainshock. The second foreshock occurred just 15 min before the mainshock. No warning occurred in 2015. Each of the 1833 foreshocks may have been equivalent in magnitude to the 2015 M_w 7.3 aftershock east of Kathmandu, located along the locking line to the west or east of

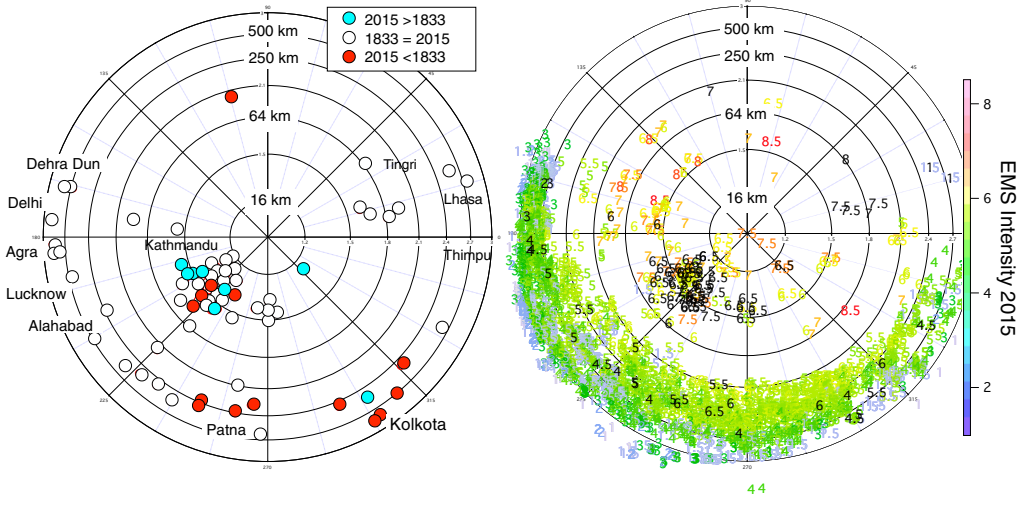

Fig. 13. Polar plot comparing the intensity distributions of the 1833 and 2015 earthquakes (from Mencin *et al.* 2016). The left-hand plot shows only those locations for which an intensity was evaluated both in 1833 and in 2015; whereas the right-hand plot numbers all the 1833 observations in black, and the 2015 observations in colour.

Kathmandu. Although initially there was some suggestion in the distribution of intensities (Szeliga *et al.* 2010) that the 1833 epicentre may have been located to the east or NE of the Kathmandu Valley (possibly near the 2015 aftershock), this was biased by the scant distribution of felt intensities in Tibet. Newly translated Tibetan sources indicate that damage occurred also to the NW of Kathmandu in 1833 (Martin *et al.* 2015).

Accounts in the Kathmandu Valley of tens of seconds of shaking and difficulties in standing during the 1833 earthquake (Bilham 1995) resemble those recorded by video cams in 2015, and which are now known to be the result of long-period resonance of the sediments in the valley floor. Like the 2015 Gorkha earthquake, the 1833 earthquake was an incomplete rupture of the Main Himalayan Thrust; and like the Gorkha earthquake, contractional strain must have been increased near the southern edge of the rupture, including the region near Kathmandu.

The 1833 earthquake was followed by an aftershock sequence that after a few weeks decayed to a low rate. A distinct aftershock was noted in 1835. For the 1835 earthquake, we have a single report and no macroseismic data, which suggests that its magnitude may have been $M_w < 6.5$. Thirty-three years after the 1833 earthquake, in 1866, a significant earthquake shook Kathmandu that was felt in Calcutta and Bombay, and 28 other locations, and was estimated as $6.8 < M_w < 7.4$ by Szeliga *et al.* (2010) but with significant uncertainty in its location and no information on its depth. A single report of EMS shaking intensity 7 results in a crescent-shaped uncertainty region that encircles its felt report location in the Kathmandu Valley. The 1866 location uncertainty contour intersects the locking line in the same location as the 12 May 2015 $M_w = 7.3$ Dolocka aftershock. A second weaker solution (Szeliga *et al.* 2010) permits a location near the Ganges, which is considered an unlikely locus for a large earthquake. It is also possible that the earthquake may have occurred at depth within the Indian Plate between these two calculated epicentres, similar to the 21 August 1988 Udaipur $M_w = 6.9$ earthquake. Of the three options, the most likely location for the significant 1866 aftershock is considered to be close to the Dolocka aftershock (Fig. 14).

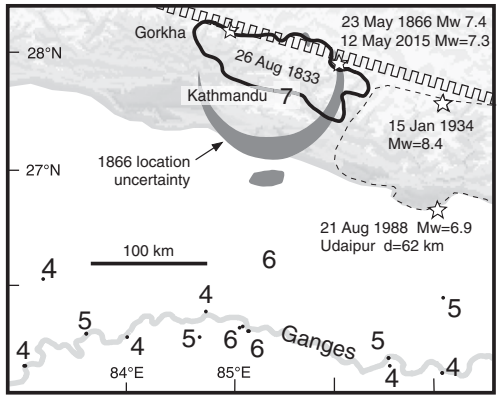

Fig. 14. The crescent-shaped uncertainty in the location of the 1866 $M_w \approx 7$ aftershock (Szeliga *et al.* 2010) surrounding Kathmandu results from the weak geometrical distribution of felt EMS intensities (numbered) mostly along the Ganges. The square wave depicts the locking line. If the 2015 Gorkha rupture area is adopted as a proxy for the 1833 rupture; the 12 May 2015 aftershock would be consistent with a recurrence of the 1866 earthquake.

Baramulla, Kashmir, 30 May 1885 (02:45), M_w = 6.4 ± 0.2. The earthquake stopped the residency clock in Srinagar at 02:45 local time on Sunday 30 May 1885 (Figs 9 & 15). Although some accounts mention 5 am, according to the Rev. Knowles it was still dark when his two-storey building in Srinagar creaked for 30 s. An account from near Murree (33.9° N, 73.39° E) from a man lying awake mentions that it occurred at 3:40 am (11:40 pm GMT) and lasted for 7–10 s. His bungalow shook and creaked, shedding small pieces of plaster (intensity 5–6) with strong aftershocks at 10:45 and 11:05 that caused a sedan chair to rock. Ambraseys & Douglas (2004) assigned a date and time to the mainshock of 29 May 02:45 (a day too early).

The earthquake wreaked enormous structural damage to settlements in the Kashmir Valley with a death toll of the order of 3000 people and a greater number of cattle. Most of the damage occurred in Baramulla and Srinagar.

Duke (1888) mentioned two earthquakes felt in the previous month that year at Baramulla. The first occurred at night on 7 March and the second

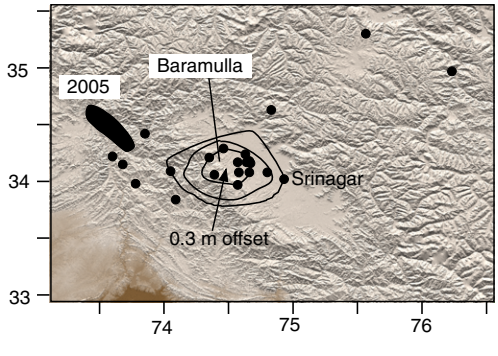

Fig. 15. The 1885 Kashmir earthquake and felt locations (solid circles) showing approximate isoseismal contours for EMS intensities 5, 6 and 7 surrounding Baramulla.

on 14 March. No building damage is ascribed to either, although the second earthquake resulted in a minor landslide that blocked the road between Chata (Chatter: 34.33° N, 73.47° E) and Dulai (34.25° N, 73.48° E) in the steep gorge of the Jhelum *c.* 10 km south of Muzaferrabad, 60 km west of Baramulla. Collet (1898, p. 88) mentioned aftershocks continuing with diminished vigour for the following 12 months:

> The shocks which commenced on 30 May, were followed in the first hour by 6 severe shocks, followed by 19 more, making 25 shocks in 37 hours, and for some days afterwards they continued at a rate of 3 or 4 every 24 hours. They gradually became less frequent, but were occasionally severe, and with less frequency took place for more than 12 months afterwards. Jones (1885*b*) who was dispatched by the Geological Survey of India to the epicentral region in late June mentions a large aftershock on 16 August.

In the biography of Arthur Neve, a surgeon based in Srinagar, his brother provides a brief account of the earthquake (Neve 1928), which is unfortunately sparse on specific damage to structures. The account mentions extensive surface fissures near the Jhelum River, a substantial landslip that buried 40 of the 47 inhabitants of the village of Laridura (34.139° N, 74.352° E), in the hills south of Baramulla, and, intriguingly, a fissure that crossed the Patan–Baramulla road (Fig. 5d), whose location is now lost, with an offset of 30–60 cm. It is near here, at Nila (34.18° N, 75.53° E), that the account of methane emanating from a fissure is related to have occurred (Fig. 5a). It is unknown whether this offset, whose strike is unspecified, represented fissuring or primary faulting. There is no documented evidence elsewhere for primary faulting in the earthquake, contrary to claims by Ahmad *et al.* (2014), who, among other errors, erroneously interpreted the Laridura landslide headscarp as a fault scarp. Incremental damage to the medieval temples in Patan and Srinagar is evident in pre- and post-earthquake photographs (Bilham *et al.* 2010; Bilham & Bali 2013)

Jones (1885*a*, *b*), wrote two official accounts of the earthquake and although he lists fewer than a dozen locations where damage intensities were evaluated, his second article includes hand-interpolated maps of meizoseismal and far-field isoseismal contours, based on a scheme devised by Mallet. Unfortunately, he died from Malaria a year after the earthquake and his original notes have been lost. Martin & Szeliga (2010) and Ambraseys & Douglas (2004) list 20 and 37 locations, respectively, where the felt effects of the earthquake could be quantified, some of which are shown in Figure 15. The magnitude of the earthquake has been estimated from these intensity data as $6.3 < M_w < 6.6$, a relatively modest earthquake for its considerable damage.

Shillong, 12 June 1897, $M_w = 8.2$: a blind thrust with 25 ± 5 m of subsurface slip. Although located 100 km south of the Himalaya, the 1897 Shillong earthquake is important because it was the first major Indian earthquake to be studied in detail by geologists and geodesists (Table 5). It was recorded by a dozen early seismometers in Europe, which ultimately led to Richard Oldham quantifying the diameter of the Earth's core (Oldham 1906). The earthquake occurred in the late afternoon in sunshine shortly after prolonged rain, and as a result many people were outdoors. This may account for the relatively modest death toll (*c.* 1542) despite it being the largest earthquake in India for almost four centuries. Masonry buildings near the epicentre and for an extensive region in the surrounding plains were destroyed. The earthquake was responsible for minor damage in Calcutta, where prolonged shaking caused considerable alarm. Subsidence of the Brahmaputra Valley north of the epicentre resulted in easier passage along the Brahmaputra for several weeks following the earthquake. Uplift of the northern edge of the plateau was so rapid that rocks were, in places,

Table 5. *Subsurface coordinates for the Oldham Fault, Shillong 1897 earthquake $M_w = 8.2$*

Old latitude (° N)	Old longitude (° E)	ChedN	ChedE	ChedN	ChedE	ChedN	ChedE
25.9	90.68	25.907	90.629	25.846	90.675	25.907	90.629
25.7	91.59	25.896	90.638	25.837	90.675	25.896	90.638
25.5	91.57	25.886	90.647	25.827	90.676	25.886	90.647
25.7	90.66	25.876	90.656	25.818	90.676	25.876	90.656
25.9	90.68	25.866	90.665	25.809	90.677	25.866	90.665
		25.856	90.674	25.781	90.677	25.856	90.674

The first two columns indicate the subsurface bounds of the Oldham fault. The strike of the subsurface fault was N110° E, its length 79–95 km, and it slipped from 31 km to 6 km depth with mean slip 25 m. The coordinates of the surface expression of the 24 km-long Chedrang normal fault that slipped 11 m are listed in the six right-hand columns (England & Bilham 2015).

propelled from the surface, and its gradient was so severe that lakes were formed partly from the backwards tilt of streams on the plateau surface.

The epicentral effects of the earthquake were recorded by Tom LaTouche, who has left an extensive narrative of the earthquake (Bilham 2008) and provided Oldham (1899) with many of the quantitative details from the epicentre used in his 1899 memoir. LaTouche related that at the time of numerous aftershocks, telegraph operators observed that electrotelluric currents interrupted or reversed the current of grounded single-cable circuits but 'when a second wire was used instead of the earth as a return circuit, no effect of the kind was observed' (Oldham 1899, appendix A, 267–268). La Touche constructed a crude seismometer, modelled on a design of Gray's described by Milne (1886, p. 23), that recorded dozens of hodograms of aftershocks for the following 3 years; the results from which were summarized by Oldham (1900). LaTouche's original hodograms are archived in the British Library (LaTouche 1899).

A dozen early seismometers were operating globally in 1897 but none with sufficient timing or amplitude accuracy to determine precise location or magnitude. Geodetic measurements were available from before and after the earthquake that provide a unique determination of its slip parameters. When these were initially analysed more than a century after the earthquake (Bilham & England 2001), the slip was found to be unexpectedly large (*c.* 15 m). Moreover, the earthquake had not occurred on the Dhauki Fault, the prominent north-dipping thrust fault bounding the southern edge of the Shillong Plateau, but had ruptured an unknown SSW-dipping blind thrust obliquely traversing the northern edge of the plateau. In the absence of a name, the fault was named the Oldham Fault. The subsequent availability of additional geodetic data and a careful evaluation of Oldham's mapped Chedrang Fault, which with upwards of 11 m of normal faulting marks the western edge of the subsurface rupture, revealed that 25 m of slip had occurred between 6 and 31 km depth for more than 80 km along strike (England & Bilham 2015). The predicted vertical uplift of the northern edge of the plateau from the triangulation solution exceeds 12 m in places. This is consistent with villagers' reports of line-of-sight changes of distant views in the north, although there exists one apparently inconsistent account of line-of-site changes near Tura. Geodetic measurements of uplift of 0.6–7.3 m were quantified north of the city of Shillong (Fig. 16).

The surface projection of the fault corresponds to a line of steepened stream gradients on the thickly forested north-facing slope of the plateau (Clark & Bilham 2008; England & Bilham 2015). No palaeoseismic study of the sag ponds entrained by the

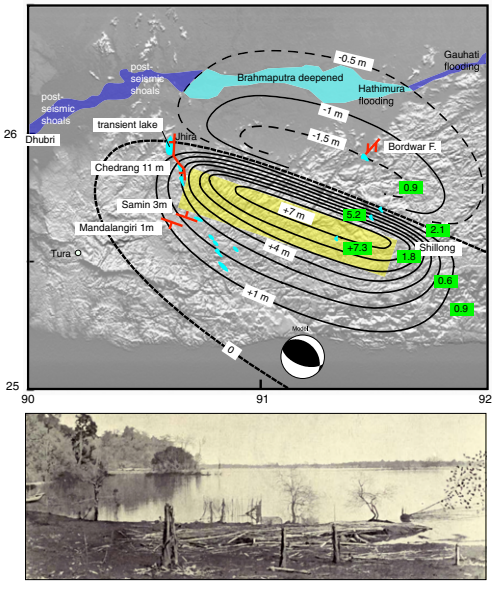

Fig. 16. Uplift contours from one of several synthetic models consistent with horizontal triangulation changes before and after the 1897 Shillong rupture (England & Bilham 2015). Green boxes show (independent) observed vertical uplift relative to trigonometrical points on the southern margin of the plateau consistent with the synthetic model. Light blue to the SE and south of the rupture indicates transient lakes or the subsidence reported by Oldham (1899). Below the map is Oldham's (1899) photograph of the impounded (5 m deep) transient lake near Jhira, reproduced from Marr (1900). Red lines indicate faulting reported by Oldham (1899) with the sense of motion. To avoid running aground on shoals, a pilot was usually hired by captains steering shipping along the Brahmaputra between Dhubri and Gauhati. For many months after the earthquake this stretch of the river (light blue) was free from shoals and pilotage was not required.

southernmost segments of Chedrang fault has yet been attempted, although a number of palaeoseismic events have been dated in sediments near the Krishnia River (Sukhija *et al.* 1999), where a coseismic lake several kilometres long and 500 m wide formed in 1897, and persisted until 1908 (Marr 1900; Playfair 1909) (Fig. 16). North–south extension and minor subsidence in the Brahmaputra Valley excludes the possibility of the 1897 surface rupture north of the plateau (Rajendran *et al.* 2004; Bilham 2006; England & Bilham 2015). In 1930, the Dhubri $M_w = 7$ earthquake occurred to the west of the Chedrang Fault, presumably on the westwards extension of the Oldham fault system.

Oldham described two other faults that slipped in 1897: the ≥5 km-long, WNW-striking Samin Fault to the south of the Chedrang Fault; and the

north-striking Bordwar Fault north of the eastern end of the subsurface Oldham rupture. Geologists have been unsuccessful in locating the Samin Fault, but there are several morphological expressions of normal faulting down to the north near villages with names similar to Samin. Synthetic slip on the 11.2 km-long Bordwar Fault in response to slip on the Oldham Fault is calculated to be approximately 25 cm left-lateral with no vertical offset. The absence of vertical offset is consistent with Oldham's description (pp. 148–151 in Oldham 1899). Horizontal motions near this fault are also consistent with this being a location where Sal trees were overturned and snapped off by accelerations in 1897, and where conspicuous landsliding was localized close to the fault zone. A 1.75 km hillside fault is visible close to his description of the NE end of this fracture. It crosses a NW-facing hillside spur from 25.930° N, 91.480° E to 25.942° N, 91.490° E, with morphology that suggests more than 10 m of long-term slip down to the SE. The SW termination of this fracture possibly corresponds to the hill-crest depression at 25.899° N, 91.441° E above what is now called the Barduar Tea Garden No. 2, corresponding to Oldham's indicated location, although 3 km from the designated coordinate listed in his geographical index. The inferred fault between these extreme NE–SW limits has a length of 6.8 km and strike N44° E. It is recorded to have no significant vertical offset (≤0.3 m). It appears that no one has subsequently examined these faults since Oldham mapped them.

A significant earthquake occurred *c.* 50 km to the west of the Oldham and Chedrang faults 33 years after the 1897 earthquake (the 1930 Dhubri M_w = 7.1 earthquake: Gee 1934) that presumably occurred in response to stresses developed in 1897. No corresponding earthquakes are known on the SE projection of the Oldham Fault, which was presumably stressed significantly by slip in 1897. In 1869, a damaging historical earthquake occurred *c.* 200 km to the ESE: the $M_w = 7.4$ Cachar earthquake at 93.0° N, 25.5° E (Oldham 1883; Ambraseys & Douglas 2004). The absence of any known major earthquake between the 1869 and 1897 earthquakes may indicate that the intervening region, including the city of Shillong (2011 population if 143 000), is one of high seismic hazard (Fig. 8). It will be noted that Shillong is almost in line with the 1897 rupture, but some 20 km to its SE, implying that accelerations recorded by displaced monuments in 1897 (Bilham 2008) were probably not as severe as those experienced to the north or directly above the rupture. A future earthquake on the SE extension of the Oldham Fault with similar slip would presumably shake Shillong with higher accelerations than in 1897, due to the anticipated directivity effects associated with wave propagation.

Twentieth and twenty-first century Himalayan earthquakes

By 1900 it became possible to record $M_w \geq 7$ earthquakes occurring almost anywhere in the world, but it took a few more years to improve the density and accuracy of seismometers to make possible routine estimates of not just position and depth, but precise earthquake magnitude. The subsequent burst of information is readily apparent in Figure 3, where the number of earthquakes recorded per century in the Himalaya (and elsewhere) increases more than 1000-fold starting around 1900. Until 1900, only the largest earthquakes appear in the historical record. After 1900, it is apparent that for every $M_w = 6$ earthquake that was felt, 10 times as many $M_w = 5$ occur, and 100 times as many $M_w = 4$, and 1000 times as many $M_w = 3$, etc.

The huge numbers of these smaller earthquakes, however, are ineffective at permitting India's advance beneath southern Tibet. For that to happen, it is essential that great earthquakes occur. The two great earthquakes of the twentieth century were the largest in four centuries: 1934 ($M_w = 8.4$) and in 1950 ($M_w \geq 8.6$), and, in principle, we should know more about them than any earthquakes in the history of the Himalaya, but these two largest earthquakes predated two remarkable advances in earthquake science – the standardized worldwide seismic recording and the development of space-based geodesy (GPS and InSAR). As a result, most of the information we have from these earthquakes has required similar methods to those used to study historical earthquakes.

Not only are earthquakes and felt reports of the twentieth century the largest in 400 years (Fig. 17), but as a result of increased population densities and changes in construction methods we begin to see Himalayan earthquakes being accompanied by many thousands of fatalities.

Kangra, 4 April 1905 (00:50 GMT: c. *6 am local time), $M_w = 7.8$.* The earthquake occurred without foreshocks in the early hours of the morning when the local populations were in their homes. It resulted in *c.* 20 000 deaths in the Kangra Valley and surroundings, and was felt weakly in Calcutta and Bombay. Two detailed accounts of the earthquake were compiled by Middlemiss (1905, 1910), who reported surface fissures near Dharmsala (Szeliga & Bilham 2017), a short normal fault near Barwar (31.712° N, 77.251° E), but related no surface rupture of the Himalayan frontal thrusts. The earthquake did considerable damage to the irrigation channels in the Kangra Valley, and destroyed or damaged several substantial bridges and ancient monuments. One unusual account is of an

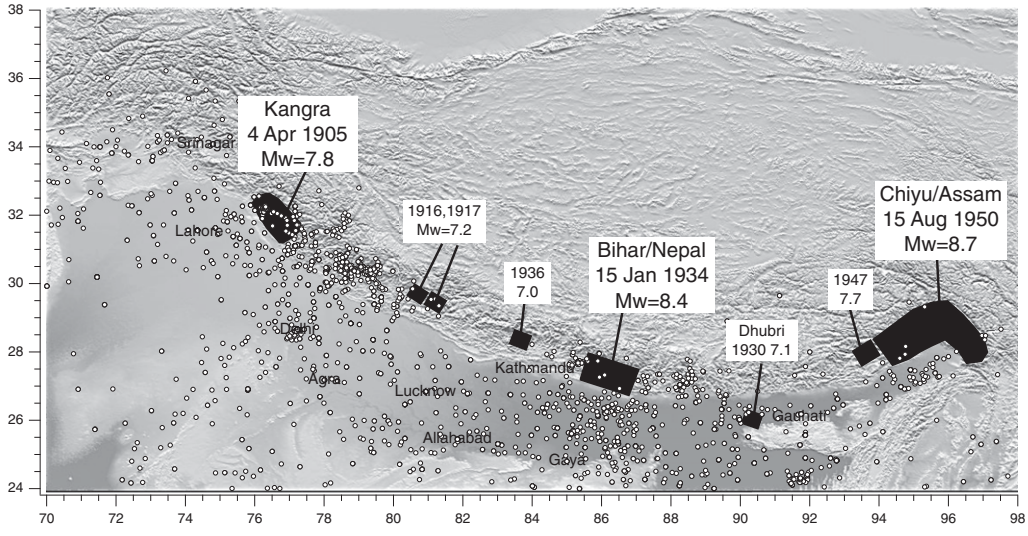

Fig. 17. Twentieth century felt reports (dots), major earthquakes and two great earthquakes.

apparently precursory increase in the Jawalmukhi Temple methane seep:

> Normally, the flames were a few inches high. But on the 4th of April, they rose not feet, but yards. For the moment, the worshippers were delighted. The flames rose to above 12 feet and started flowing out on the ground like water. Some men were injured by this matter. Suddenly, an earthquake occurred, whose direction seemed to be north to south
>
> (Baduwi 1905 (in Urdu) translated in electronic supplement to Szeliga & Bilham 2017).

The Kangra earthquake was recorded by a dozen seismometers worldwide, from which an instrumental magnitude of $M_w = 7.8$ has been assessed (Ambraseys & Bilham 2000). The $M_w = 7.9 \pm 0.1$ re-evaluated International Seismological Center catalog Version 5 catalog (http://www.isc.ac.uk/iscgem/) epicentre at 32.597° N, 76.916° E lies near the western edge of the mezzo-central region mapped by Middlemiss (1910), who identified a second region of high-intensity shaking near Dehra Dun that has confused subsequent investigators (discussed below). The epicentre was probably close to the region of maximum shaking at Dharmsala at 32.22° N, 76.32° E near the Kangra Valley Fault (32.359° N, 76.025° E–32.088° N, 76.443° E) described by Malik *et al.* (2015) (Fig. 18). However, if the Kangra earthquake was entirely due to slip on this 60 km-long strike-slip fault, as conjectured by Malik *et al.* (2015), and if we assume it slipped uniformly to a depth of 15 km, it would have had to have slipped more than 20 m to account for a $M_w = 7.8$ earthquake. No date is assigned to an estimated *c.* 10 m offset of the fault identified by these authors at 32.372° N, 76.012° E, but supposing that it slipped dextrally by this amount in 1905, its magnitude would be $M_w \leq 7.6$.

In contrast, the Kangra Valley Fault is assessed from geodetic data to have slipped in a dextral sense no more than 0.1 ± 0.6 m during the earthquake (Szeliga & Bilham 2017), with most of the deformation accounted for by a minimum of 1.3 ± 0.3 m of thrust faulting and probable mean thrust slip of up to 5.1 m. These two observations can be approximately reconciled by invoking 50–66% partitioning between pure thrusting on the Jawalamucki Thrust (or sub-parallel frontal thrusts) and strike-slip faulting on the Kangra Valley Fault. If this ratio prevails for former earthquakes, it may be possible to use slip on the Kangra Valley Fault to estimate the thrust component of slip of former thrust earthquakes. For example, the ratio would require that the 10 m offset of the Kangra Valley Fault was not associated with the 1905 rupture, but with a former earthquake with 15–20 m of thrust faulting.

A puzzling feature of the Kangra earthquake was Middlemiss' identification of a region of high intensities near Dehra Dun (Middlemiss 1910). This has variously been interpreted as a second earthquake (Hough *et al.* 2005*a*, *b*) or as the existence of a continuous *c.* 300 km-long rupture between Dharmsala and Dehra Dun (Seeber & Armbruster 1981; Chander 1988), an interpretation that appeared to be supported by uplift at Dehra Dun measured by first-order levelling after the earthquake. The levelling data have since been shown to have been perturbed by systematic errors, which when suppressed show no evidence for uplift at Dehra Dun, consistent with the absence

of horizontal deformation in trigonometrical lines near Mussourie (Bilham 2001). Re-evaluated intensities for the earthquake reveal that the region of anomalous intensities is diffused over a large region to the SE of the rupture and attenuated to the NW, suggestive of directivity caused by the rupture propagating to the SE (Fig. 19).

The SW bounds to the rupture are conjectural since no surface rupture occurred (Fig. 18). Szeliga & Bilham (2017) estimated the approximate NW and SE bounds of rupture using the mean EMS 5.6 intensity kriged contour observed above the Gorkha rupture as a proxy for the lateral reach of subsurface rupture. They constrained the SW bound geodetically (Table 6), and assumed the northern limit was the locking line defined by the 3.5 km contour (Stevens & Avouac 2015). A late aftershock (28 Feb 1906) brought down traditional buildings (Middlemiss 1910, p. 395) and caused additional fatalities at the western extremity of the contoured region (Fig. 18).

Bihar/Nepal (27.55° N, 87.09° E), 15 January 1934 (2:43 pm), M_w = 8.4. In the half century following the 1934 earthquake, due to the extensive damage to cities and villages in the Gangetic Plain (Dunn *et al.* 1939), its epicentre was believed to be located beneath the Ganges in the Bihar province of India, corresponding to an early epicentral location by Gutenberg & Richter (1954). This erroneous location persists in several recent catalogues. Approximately 10 500 deaths are often reported for the earthquake, but this excludes the number of fatalities reported from Nepal. Brett (1935) reported 7253 deaths in Bihar. The death toll in Nepal exceeded 8500 (Pandey & Molnar 1988). In a 1934 speech in Bihar, Gandhi attributed the suffering, damage and the loss of life incurred in the earthquake to divine chastisement for India's failure to eradicate the concept of the caste of untouchables. The Kesariya Stupa (26.334° N, 84.855° E), 5 km north of the Ganges, was reduced in height by 7 m to 23 m as a result of the earthquake.

The exclusion of foreigners from Nepal (1815–1950) had prevented the installation of Survey of India triangulation stations along the Himalayan foothills, whose remeasurement would have constrained the southern edge of the rupture. This exclusion also delayed news of the extensive damage in

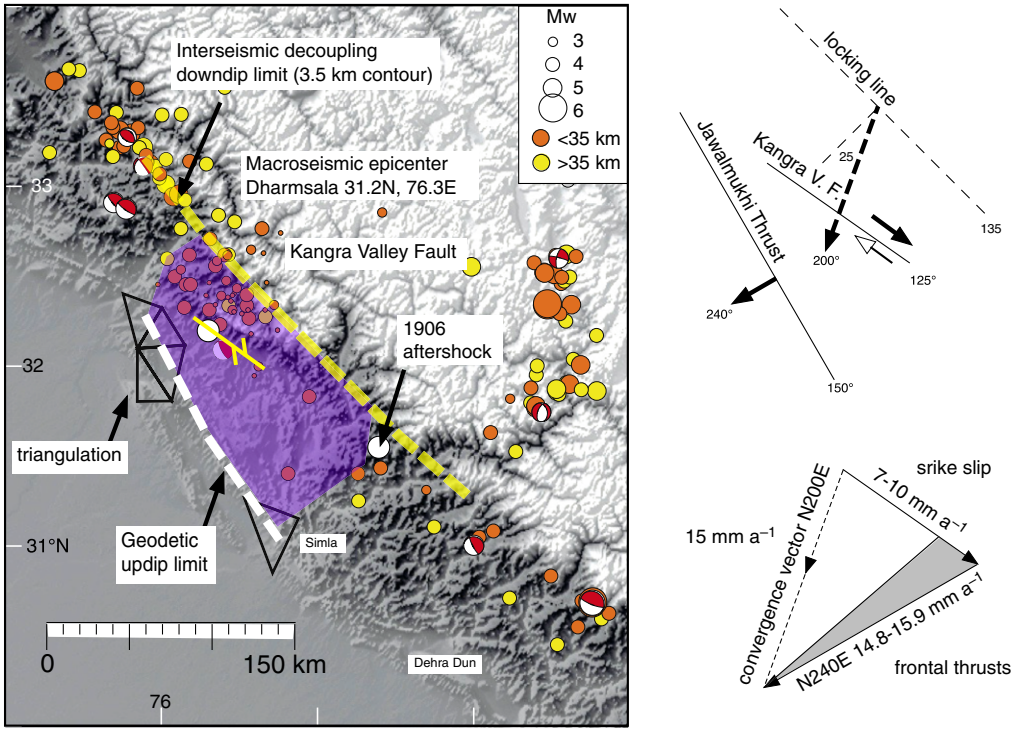

Fig. 18. Bounds of rupture for the Kangra 1905 earthquake (Table 6) shown by violet shading. Mean GPS convergence vectors (*c.* 15 mm a^{-1}) are indicated by arrows (from Fig. 2). The mainshock and principal aftershock are separated by *c.* 150 km (cf. Gorkha 2015 earthquake). Slip partitioning between the Kangra Valley Fault and the frontal thrust faults varies from 50 to 66% depending on the strike of the fold belts currently active (shaded range in vector summation is shown in the lower right).

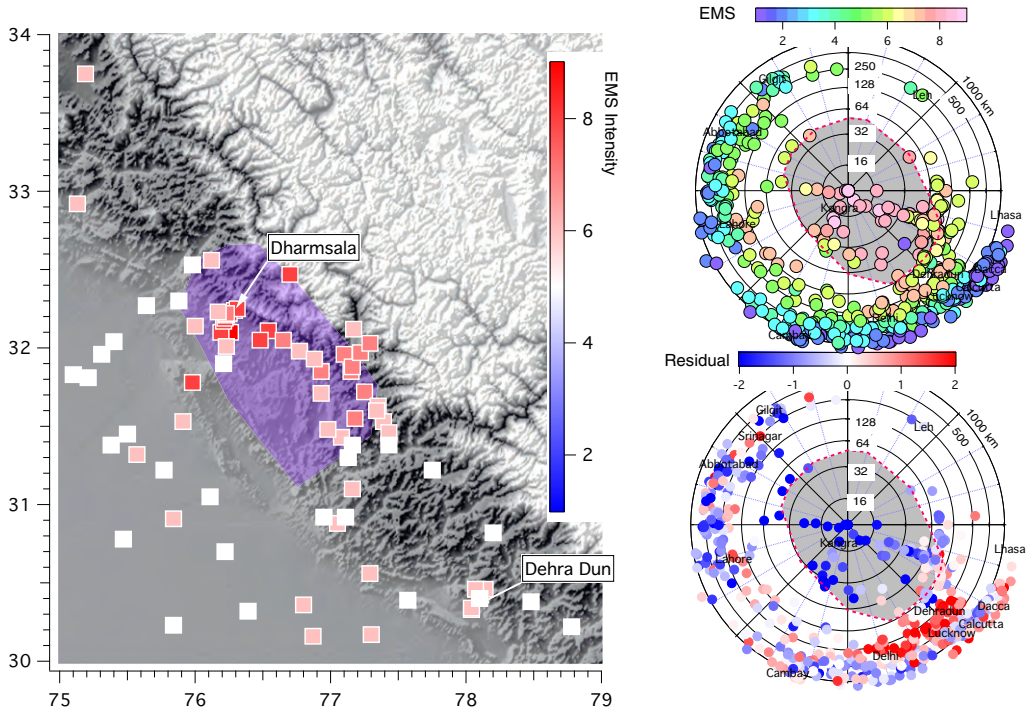

Fig. 19. EMS intensities (Martin & Szeliga 2010; Szeliga & Bilham 2017) for the 1905 Kangra earthquake and log polar plots (on the right with the rupture zone in grey outlined by a red dashed line) centred on Dharmsala. Residuals (lower right) from removing synthetic amplitudes predicted by Himalayan attenuation parameters (Szeliga *et al.* 2010) suggest amplification towards the SE and attenuation to the NW, consistent with directivity caused by nucleation near Dharmsala and propagation 125–150 km to the SE. High intensities near Dehra Dun have hitherto been interpreted to have resulted from a triggered deep earthquake near the base of the Indian crust (Hough *et al.* 2005*b*, Hough & Bilham 2008).

the epicentral region of eastern Nepal from reaching the outside world (Rana 1935; Pandey & Molnar 1988). Damage near the epicentre was barely mentioned by members of the first British expedition to approach Everest from the south a year after the earthquake (Hunt 1953).

The instrumentally relocated 1934 epicentre lies approximately 10 km south of Mt Everest (Fig. 20) at 27.55° N, 87.09° E (Chen & Molnar 1977), although many catalogues mistakenly retain Richter's early erroneous Bihar epicentre almost 200 km to the south. Using a dip of 20°, a seismic moment of 1.1×10^{28} dyne cm is derived. However, using a shallower, more probable dip of 5°, consistent with recent focal mechanisms and current knowledge of the décollement geometry, the seismic moment from the earthquake is calculated to be 4.1×10^{28} dyne cm, yielding a magnitude of M_w = 8.4 (Molnar & Chen 1983; Molnar & Deng 1984). Assuming a rupture area of 130×100 km^2, the mean slip in the earthquake would have been *c.* 10 m. However, despite its relatively recent occurrence, the longitudinal and latitudinal bounds of slip, and hence the inferred slip in the earthquake, continue to be the subject of much speculation, and few objective constraints.

Palaeoseismic excavations of the Main Himalayan Thrust (Bollinger *et al.* 2014, 2016; Sapkota *et al.* 2013) claim that surface rupture occurred in the 1934 earthquake at Sir Khola (85°52′ E), a stream that cuts through the Himalayan Frontal Thrust. The lower levels of this exposure show clear evidence for thrust recent faulting. However, Wesnousky *et al.* (2018) examined the exposure and reported that a shallow layer of pre-1934 surface sediments at this site, and nearby, remained

Table 6. *Coordinates encapsulating the inferred rupture area of the 1905 Kangra earthquake*

Latitude (° N)	32.66	32.49	32.22	31.78	31.58	31.36	31.17	31.18	31.62	32	32.35	32.48	32.6	32.66	32.66
Longitude (° E)	76.42	76.7	76.94	77.34	77.35	77.14	76.82	76.7	76.321	76.08	75.9	75.98	76.15	76.321	76.42

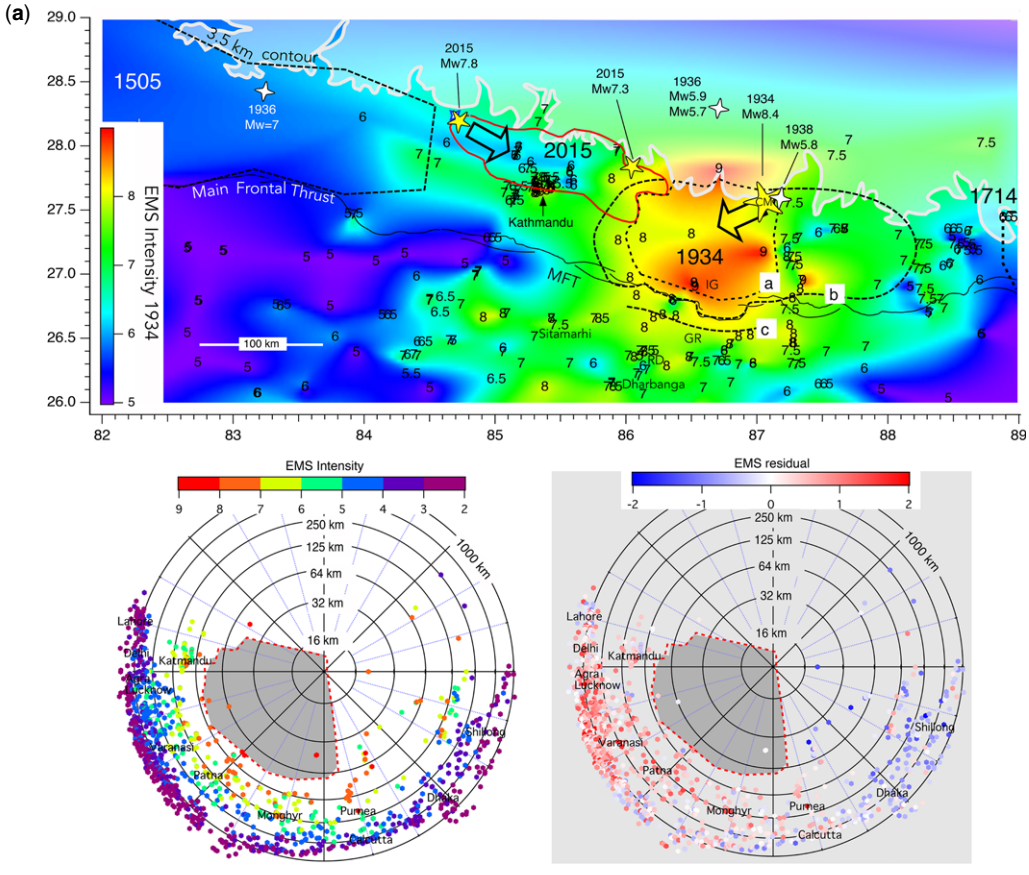

Fig. 20. (a) Intensities observed in the 1934 Mw 8.4 rupture (from Ambraseys & Douglas 2004; Martin & Szeliga 2010) with nearby 1505, 1714 and 2015 rupture zones, dashed where inferred. The size of epicentral stars correspond to approximate mainshock location uncertainties. Various epicentral locations for the 1934 earthquake are indicated by letters: RD=Dunn *et al.* (1939), GR=Gutenberg and Richter (1949) which they rounded to the nearest half degree, IG=ISC/GEM v.5, CM=Chen & Molnar, 1977. White stars depict M > 5.7 aftershocks (ISC/GEM v.5) in the four years following the earthquake. Three 1934 scenario ruptures areas (a, b & c) are depicted (see the text). Large arrows show inferred rupture propagation directions. Dunn *et al.* (1939) propose that the mainshock was a major subevent, west of the nucleation phase, that occurred 11 s after the first arrival. Assuming a 2.6 km/s rupture propagation velocity its location would be c. 30 km west of the CM epicenter. Polar plots (below map) reveal apparent 1934 directivity to the SW related to rupture propagation in scenario a. Amplification in the Ganges sediments is partly responsible for positive residuals to the SW, but the absence of amplification in the SE quadrant at all distances is presumed to arise from directivity to the SW, consistent with scenario a and the location of the dominant subevent west of the nucleation event.

undisturbed by the 1934 rupture. Not only is a rupture plane absent in these covering sediments, but there is no evidence for a prominent surface scarp (c.f. Bilham & Yu (2000), and Jayangondaperumal *et al.* (2013)) that might be expected from several metres of surface slip in the 1934 earthquake.

Although no geodetic control crosses the rupture zone, first-order spirit levelling lines in northern Bihar were remeasured shortly after the earthquake (Burrard 1934; De Graaff-Hunter 1934; Bomford 1937). In addition, more than 800 intensity observations are available for the earthquake (Martin & Szeliga 2010). Subsidence of up to 1.1 m in the region was found to correspond to maximum shaking intensities south of the Nepal–India border (Hough & Bilham 2008), but due to its substantial spatial variability, the subsidence was attributed not to elastic deformation but to lateral spreading, and extensive surface venting associated with liquefaction of subsurface layers. Assuming an along-strike distance of 160 km and using a typical scaling relationship (using a low magnitude of $M_w < 8.1$), its

(**b**)

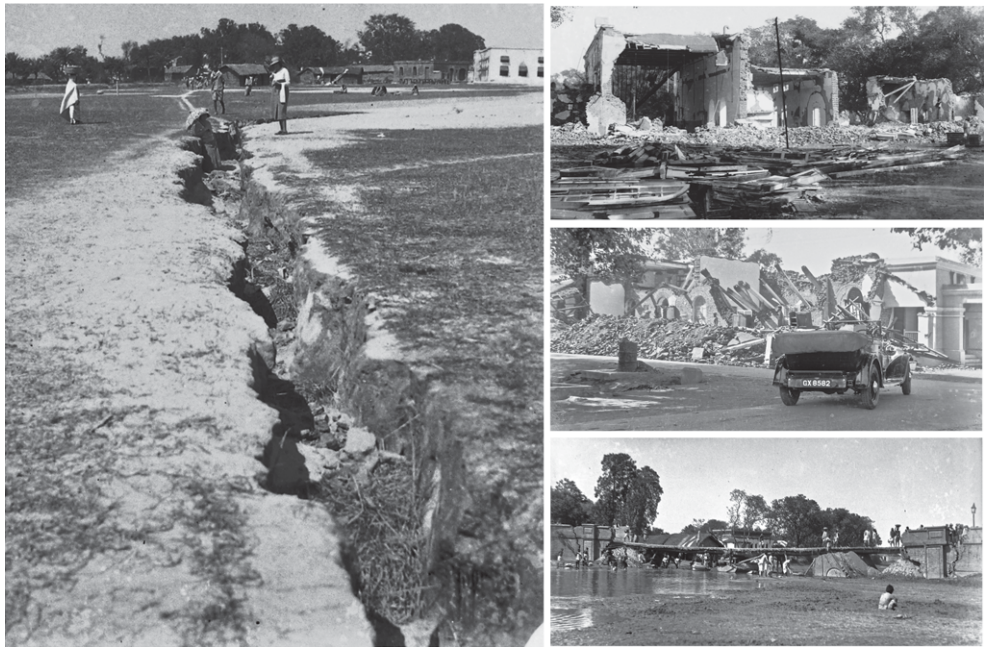

Fig. 20. *Continued*. (**b**) Scenes from the 'slump belt' of the Bihar province of India after the 1934 Bihar/Nepal earthquake. Sitamarhi (left at 26.58° N, 85.48° E), was long considered close to the epicentre of the 1934 earthquake. A typical fissure was 80 m long, 2.5 m wide and filled with sand to within 1m of the top (Dunn *et al.* 1939, p. 149, and p. 210). Extensive lateral spreading and sand venting occurred during liquefaction of sediments in the Ganges Plain south of the rupture.

western edge was estimated to lie at 85.5 ± 0.2° E and its eastern edge at 87.0 ± 0.2° E.

In the absence of a surface rupture (Auden 1935), or abundant aftershock data, or horizontal geodesy before and after the earthquake, a more precise estimate for the bounds to the 1934 rupture remains elusive. Three possible rupture scenarios are depicted in Figure 20 based on maximum felt intensities above and near the rupture. Each is bounded to the north by the locking line approximately following the 3.5 km contour. The minimum rupture area in scenario a is bounded to the west by the 2015 Nepal earthquake rupture at 86.1° E (assuming that the 1934 and 2015 ruptures abutted each other) and to the east by an apparent reduction of observed intensity near 87.2° E from EMS < 8 to EMS ≈ 7 (Table 7). This longitude includes the instrumentally determined mainshock epicentre. The rupture zone in this minimum rupture estimate terminates north of the Main Himalayan Thrust and measures roughly 100×85 km^2, corresponding to mean slip in an $M_w = 8.4$ earthquake of 17 m. The arrow indicates the direction of rupture propagation required by nucleation from the NE corner of this rupture.

Scenario b assumes that some overlap of the 2015 Nepal rupture occurs to the west, consistent with a

Table 7. *Minimum estimated bounds to rupture for the 1934 Nepal earthquake (scenario a in Fig. 20)*

Latitude (° N)	Longitude (° E)
27	86.09
26.8	86.7
26.82	86.9
26.9	87.1
27	87.15
27.3	87.12
27.6	87.17
27.66	87.1
27.66	87
27.7	86.8
27.74	86.7
27.68	86.6
27.73	86.35
27.62	86.3
27.62	86.2
27.63	86.1
27.6	86.06
27.5	86.08
27.4	86.05
27.37	86
27.3	85.97
27.1	86.03

The epicentre was near 27.55° N, 87.09° E.

decay in slip in the 2015 rupture here, and that the eastern edge of the rupture extends 100 km to the east of the mainshock. Scenario b more than doubles the minimum rupture area considered in scenario a, doubles its length (requiring bi-lateral rupture as occurred in the Kashmir 2005 earthquake) and reduces mean slip to about 8 m.

Finally, scenario c admits a further possibility: that the southern edge of the 1934 rupture extended south of the Himalayan Frontal Thrust. This scenario is possible because a number of blind thrusts and subsurface anticlines have been imaged in seismic reflection lines in the Terai of Nepal (Fig. 4). They extend 1–10 km south of the Main Himalayan Thrust (Bashyal 1998; Kayastha *et al.* 1998; Almeida *et al.* 2018). The Main Himalayan Thrust has evolved southwards, successively incorporating these blind thrusts as they grow in amplitude and eventually rupture the surface. The jagged surface path of the Main Himalayan Thrust fronting the Siwalik Ranges includes numerous overlapping strands that testify to this complex process. If the 1934 rupture had terminated on one of these buried structures, it would characterize a class of great earthquakes inaccessible to palaeoseismic investigations of the Main Frontal Thrust.

Scant data are available to choose between these three possibilities (or any combination thereof). Wesnousky *et al.* (2019) considered that a previous earthquake in eastern Nepal occurred at *c.* 1100 and was associated with slip of up to 14 m. In the absence of intervening earthquakes, the geodetic convergence rate here (15–18 mm a^{-1}) would have developed a slip deficit of 12.5–15 m at the time of the 1934 earthquake, similar to that calculated in scenario a, but more than that in scenario b or c. However, slip in scenarios a or c would have to dissipate as dilatational compression in the subsurface, and folding of the surface, either north of the Main Himalayan Thrust, as in the Nepal 2015 earthquake, or as blind thrusting south of the Main Himalayan Thrust. Widening the downdip width of the 1934 rupture to 110 km, for example, and retaining the same *c.* 100 km-long, along-strike length, would require mean slip of 13 m similar to the pre-1934 slip deficit. Almeida *et al.* (2018) speculated that slip in recent earthquakes may have been absorbed south of the Main Frontal Thrust by slip on the blind Bardibas thrust near 86° E.

In contrast to the compact rupture depicted in scenario a, the extended bilateral rupture of scenario b is permitted by the observation that intensities above the Nepal rupture zone averaged approximately EMS 6.5, similar to observed intensities in eastern Nepal (Fig. 20), similar to observed intensities in eastern Nepal (Fig. 20). An eastward propagating rupture is reported by Singh & Gupta (1980), but they invoke a more westerly mainshock location. It is possible that bi-lateral rupture occurred in 1934 to the east and west of the 87.09° E epicenter Subsurface rupture termination is again required in scenario c (because no slip has been reported from the Main Himalayan Thrust (Wesnousky *et al.* 2019)) but in this case the mean slip of less than 6 m required by the moment release and scaling considerations (Stirling *et al.* 2013) would have removed only half the 1934 slip deficit. This is thus considered less likely. A possible alternative scenario is that slip west of the mainshock was much larger than slip to the east, a scenario that would require an future earthquake to release the slip deficit in eastern Nepal and Sikkim.

Clearly, distinguishing between these several possible geometries requires data that we currently do not have, however, it is worth noting that a subsurface blind termination of the 1934 earthquake south of the Main Frontal thrust may account for the unusually pronounced shaking in the "slump belt" near the Ganges in 1934. This region of pronounced lateral spreading and sand venting was primarily responsible for the 1934 Nepal earthquake being known for decades following the earthquake as the "Bihar" earthquake.

Although the contiguous rupture zones shown in Figure 20 (1505, 2015, 1934 and 1714) have large uncertainties (shown as faint dashed lines), two areas appear to have not slipped for some considerable period of time. An area to the south and west of Kathmandu, which Bollinger *et al.* (2016) and Rajendran *et al.* (2018*b*) argue may have slipped in 1344, and a region to the east of the 1934 earthquake, which previously ruptured in about 1100 C.E. (Wesnousky *et al.* 2019).

The Chayu/Assam earthquake, 15 August 1950 (19:39 local time), M_w *= 8.7.* The 1950 earthquake is the largest seismically recorded earthquake to have occurred on the Indian subcontinent, or in any mid-continent region (Fig. 21). First-hand accounts of the earthquake are related by Kingdom-Ward and his wife (Kingdom-Ward 1952, 1953, 1955), who were camped near the village of Rima on the Lohit River (27.5° N, 97.0° E) above the rupture zone. The shaking started at 7:39 pm and lasted for 5 min, and resulted in numerous landslips, many which dammed tributary streams causing local rivers downstream to briefly run dry. Days or weeks later these dams were breached, resulting in debris flows that clear-cut the lower valleys of forest and conveyed enormous volumes of rock, sand and tree trunks to the Brahmaputra Valley. Mathur (1953) estimated the landslide volume mobilized by the earthquake as 47 km^3, which resulted in the injection of a considerable sediment load to the Brahmaputra that took many years to flush through its lower courses (Sarker & Thorne 2006).

Seismic studies of the earthquake revealed both a dominant thrust component and a subsidiary strike-slip component (Ben-Menahem *et al.* 1974; Molnar & Chen 1983). The complexity of the rupture is appropriate for its occurrence at the eastern syntaxis of the Himalaya, where the northern end of the dextral transform that marks the eastern transform boundary of the Indian Plate meets the convergence along the Himalaya. Due to difficulties in access and its sparse population, the 1950 Assam earthquake was not well documented at the time of its occurrence, and remains the least well studied of all major earthquakes in the Himalaya. Until quite recently, there was no evidence that the earthquake had ruptured the surface. Recent investigations describe features that may represent a 200 km-long surface scarp associated with the earthquake, but details at the time of writing are unavailable (Burgess *et al.* 2012; Coudurier-Curveur *et al.* 2016, 2018; Priyanka *et al.* 2017).

Observations of its felt intensity were largely confined to a narrow quadrant to the SW, and because many felt locations are located on thick sediments that are likely to have amplified shaking, the distribution of anomalous intensities provides no reliable indication of rupture propagation direction (Tandon 1954). However, since the epicentre is located near 96.5° E, the long duration of the shaking reported by eyewitnesses presumably occurred during westwards rupture propagation, with a minor component of rupture propagating to the south.

Three years before the Assam earthquake, on 9 July 1947, a M_w 7.7 earthquake occurred near its western edge (28.63° N, 93.7° E). The rupture zone of a rare M_w 7.7 earthquake abutting that of the 1950 earthquake (Figure 21 and Table 8) just 3 years before the largest earthquake in 450 years argues for a common cause. Static strain triggering is considered unlikely because the 1947 rupture would have been no closer than 250 km to the 1950 epicentre; and if this mechanism is to be invoked, an eastwards propagating rupture starting near the locking line near 94° E is likely to have been induced, the opposite of what was observed. Three moderate thrust earthquakes occurred near the inferred junction of the inferred rupture zones in the following two decades. A seismic gap exists between the 1714 Bhutan and 1947 Arunachal earthquakes that has not slipped at least since 1697 and possibly much earlier (Fig. 21).

Kashmir (34.49° N, 73.63° E), 8 October 2005, M_w = 7.6. A number of $M_w < 7$ earthquakes were to occur after the 1950 earthquake, but the next major earthquake in the Himalaya occurred in the westernmost Himalaya. The 2005 earthquake nucleated at approximately 15 km depth as a bilateral rupture propagating to the surface as a 75 km-long rupture (Figs 22, 23 & 24), with mean slip of 4.2 m, and maximum subsurface slip of 14 m and surface slip of *c.* 8 m (Avouac *et al.* 2006; Pathier *et al.* 2006). The earthquake occurred at 8:40 am local time when numerous poorly constructed schools were occupied, which contributed significantly to the record death toll (*c.* 86 000). In contrast to the décollement earthquakes hitherto discussed with dips of typically less than 6°, the dip of the 2005 earthquake was *c.* 30° to the north. The anomalous steepness of the dip renders previous interpretations of Kashmir earthquakes uncertain. It is possible, for example, that the 1555 earthquake ruptured a narrow region beneath the Pir Pinjal extending to the SE from the ends of the 2005 rupture (Mugnier *et al.* 1998). The geodetic velocity field is very broad beneath the Kashmir Valley and does not indicate the presence of a localized transition from locked to creeping decollement that would result in a future steep rupture, unless it nucleated at unexpectedly deep depths (>30 km).

Felt intensities from the earthquake were amplified to the SE in the Punjab and Ganges sediments. Shaking intensities were further enhanced by the SE rupture propagation component of the rupture. The intensity distribution is of value in that it offers clues as to the detectability of historical Kashmir earthquakes in persistent population centres such as Lahore. It is unlikely that Kashmir's numerous historical earthquakes exceeded $M_w = 8$ since no reports of these earthquakes exist outside the Kashmir Valley, subject to the caveat that historical reports may have been lost.

Gorkha (28.15° N, 84.71° E), 25 April 2015 (midday), M_w = 7.8. The earthquake occurred at 12:11 Kathmandu time (Saturday lunch hour) and resulted in considerable damage in the city and throughout central Nepal. The timing of the earthquake on a holiday weekend at noon when many people were not in their homes contributed to the relatively low number of fatalities in the earthquake (*c.* 9000 dead and 22 000 injured), when compared to the number of dwellings that were destroyed (3.5 million people were rendered homeless). Had the earthquake occurred at night 12 h earlier or 12 h later when people were asleep, the death toll would have been much higher.

We know more about the Gorkha 2015 earthquake than about any previous earthquake in the Himalaya due to the availability of precise geodetic measurements and sophisticated seismic analysis methods. The rupture nucleated on the Main Himalayan Thrust at its western edge near Barpak (28.15° N, 84.71° E) (Fig. 25), and propagated eastwards and southwards at *c.* 3 km s^{-1}, translating the Himalayan carapace between Kathmandu and the mountains southwards and upwards at velocities locally approaching or exceeding 1 m s^{-1} (Fig. 26) (Avouac

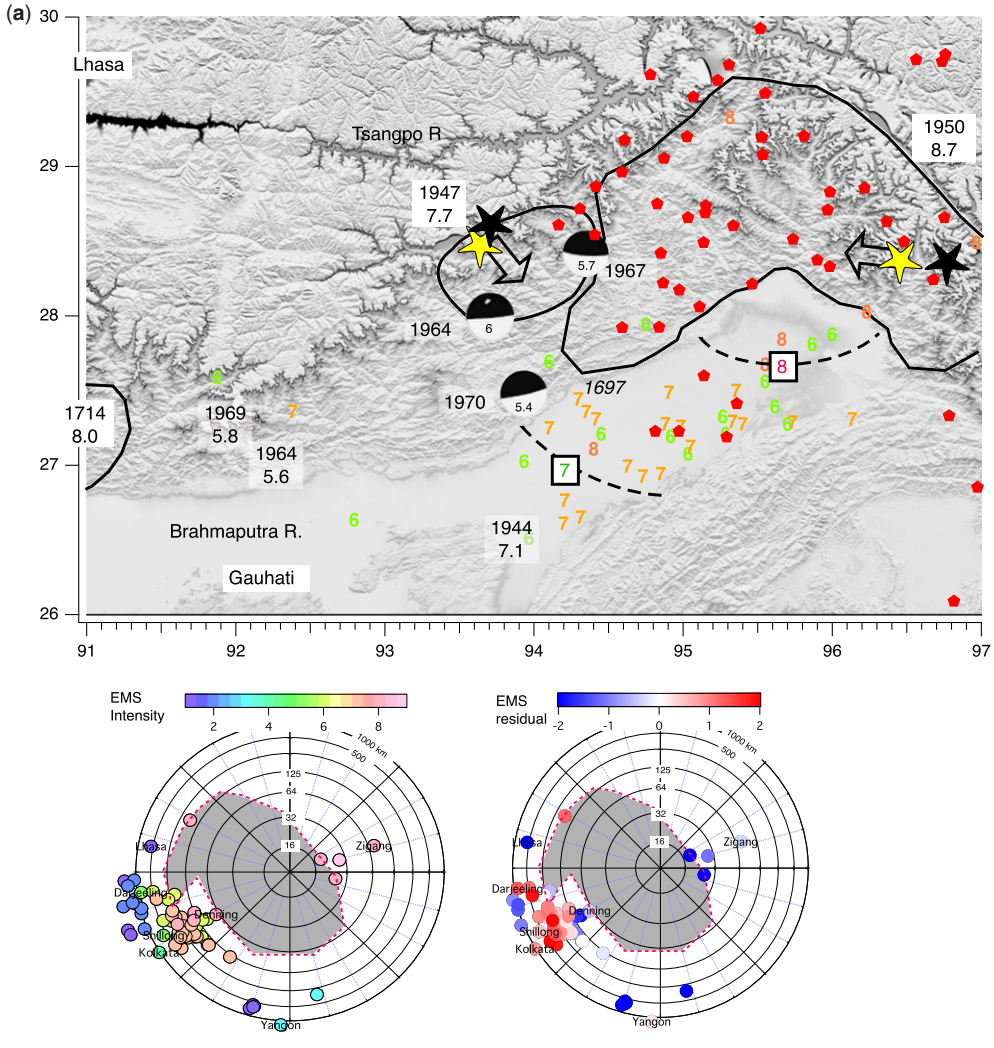

Fig. 21. (**a**) Estimated rupture zones and inferred propagation directions for the 1947 M_w = 7.7 and 1950 M_w = 8.7 earthquakes (the size of epicentral stars approximate the location uncertainties). Yellow and black stars are 1947 and 1950 mainshock locations from ISC/GEM v.5, and Chen and Molnar (1977) respectively. Red pentagons are the first 100 days of 1950 aftershocks from ISCGEM. Numerical EMS intensities and smoothed isoseismal contours are shown for the 1950 rupture. Felt intensities in the polar plots are consistent with westwards propagation in 1950, but high intensities are also influenced by sediment amplification in the Brahmaputra Valley.

et al. 2015; Galetzka *et al.* 2015; Lay *et al.* 2017). In the same way that the Sumatra/Andaman earthquake rapidly unzipped the entire plate boundary northwards followed by slip of the updip plate interface (Bilham 2004), nucleation in the Gorkha earthquake propagated along the channel of highest strain concentrated along the northern downdip locking line. This initiated southwards slip of the Himalayan carapace (Avouac *et al.* 2015). Detailed seismic analyses showed that several patches slipped sequentially (Fan & Shearer 2015; Kumar *et al.* 2017), with the downdip rupture fracturing as a sequence of rapid seismic fractures suggestive of roughness at the base of the plate interface, and with the updip portion of the Main Himalayan Thrust sliding more smoothly towards the south and east (Yue *et al.* 2017). Although most of the sub-events along the northern edge were thrust-type earthquakes, the last of the four major sub-events during rupture propagation is reported to have been strike-slip (Kumar *et al.* 2017).

The irregular shape of the rupture patch and the quest to determine why rupture terminated to the

(b)

Fig. 21. *Continued*. (**b**) Photographs of rail damage near Dibrugarh in the Brahmaputra Valley after the 1950 Assam earthquake photographed by M.C. Poddar (1950). (ii) is a close-up of the engine shed visible in the background of (i). Liquefaction sanding is visible in the foreground of (i) and is responsible for the subsidence beneath the tilted engine. A lateral spreading crack has severed the house in (iii).

south and east, and why it nucleated where it did, have led to several interpretations that suggest the influence of structural control (Grandin *et al.* 2015; Hubbard *et al.* 2016). But, perhaps, the most important observation is that all previous attempts to characterize the bounds of historical earthquake ruptures in the Himalaya, which were known to be speculative, must be viewed now as vastly oversimplified. There is nothing unexpected about this, but it suggests that attempts to determine relationships between contiguous Himalayan ruptures may be more complex than hitherto believed.

For the first time in the Himalaya, instantaneous position data were obtained five times per second from several locations using high data rate GPS position fixes (Galetzka *et al.* 2015). These recorded both the displacement of the Kathmandu Basin (Fig. 26), which took about 30 s, and the prolonged sedimentary resonance of the basin observed as a oscillatory rotation for several minutes with diminishing intensity. The sickle-shaped path of the southern edge of the rupture (Fig. 26a) was quite unexpected, and is our first glimpse into the complexities of how the Himalaya advance over the Indian Plate during major earthquakes. Contemporaneous views captured by video monitors in public places provide the first insight as to why people have difficulty standing on the hanging wall of a dynamically translating shallow thrust fault, and why structures should have a propensity to collapse in the opposite direction to the slip of the hanging wall (cf. Szeliga & Bilham 2017).

More than 3800 accounts of the earthquake were evaluated on the EMS scale by Martin *et al.* (2015), mostly outside Nepal (Fig. 23), and these were supplemented by 291 891 observations of building damage in Nepal (Adhikari *et al.* 2017; McNamara *et al.* 2017). These investigators report an average intensity for the Kathmandu Valley of EMS 6.4 ± 0.9, slightly less than the average shaking intensity above the entire rupture of EMS 6.6 determined by several investigations. Intriguingly, the centre of the valley experienced diminished shaking compared to the edges, but by less than 0.5 intensity units. Outside the valley, EMS intensity 8 was observed only on ridges (Fig. 26e), and along the northern edge of the rupture near the interseismic locking line (Adhikari *et al.* 2017).

Most of the concrete frame structures in Kathmandu survived with minor cracks, but in several

Table 8. *Estimated bounds to the 1950 Assam rupture zone*

Latitude (° N)	Longitude (° E)
27.78	94.88
27.99	95.2
28.15	95.51
28.33	95.9
28	96.29
27.64	96.51
27.71	96.97
27.99	97.15
28.37	97.05
28.73	96.77
29.12	96.42
29.52	95.98
29.47	95.5
29.26	94.97
28.8	94.4
28.3	94.65
27.9	94.1

The northern and eastern bounds are taken to be the mean 3.5 km contour and the Po Qu-Lohit Fault, respectively. The western bound abuts the inferred rupture zone of the 1947 $M_w = 7.7$ earthquake. The SW thrust boundary is adopted from a talk given by Jerome Van De Woerd in 2017 (Coudurier-Curveur *et al.* 2018). The epicentre was given as 28.38° N, 96.76° E in Chen & Molnar (1983) and 28.29° N, 96.66° E in ISC/GEM5.

locations on ridges, or in previously swampy regions near rivers, some structures collapsed or tilted and had to be demolished. The widespread collapse of fieldstone masonry structures above the rupture zone in villages outside the valley is attributable to the lack of cohesion resulting from the use of mud as a mortar (Bilham 2015), and with the ubiquitous absence of tensile bonding between inside and outside walls. A number of ancient masonry temples collapsed in the Kathmandu Valley. The Bhimsen Tower in Kathmandu was totally destroyed. Prior to the earthquake, the tower was the remaining one of a pair constructed in 1825 by a former Prime Minister that collapsed in the 1833 earthquake. Reconstructed after the 1833 earthquake, it escaped damage in 1866, but its upper half had to be repaired following partial damage in the 1934 Bihar/Nepal earthquake.

Fig. 22. View looking north at the 2005 earthquake fault scarp east of Muzafferabad. In the background can be seen some of the many thousands of landslides triggered by the earthquake. Shaking intensity was assessed as EMS 8–9 within 10 km of the surface rupture.

The availability of InSAR and GPS data above and surrounding the rupture zone permits detailed maps of horizontal slip and uplift. All pre-earthquake horizontal surfaces in the city of Kathmandu are now tilted down to the SSW, but by less than 1°. InSAR data reveal that displacement of the surface above the décollement locally exceeded 7 m, with mean slip of approximately half this amount (Elliott *et al.* 2016; Lindsey *et al.* 2015; Wang & Fialko 2015; McNamara *et al.* 2017). The strain gradients newly established in rocks at the base of Himalaya flanking the Main Himalayan Thrust peaked at 5×10^{-4} strain in a north–south direction for 10 km north and east of Kathmandu. This strain is primed for release in another earthquake.

GPS data reveal that 10 cm of afterslip occurred north of the rupture in the 3–6 months following the earthquake, with a minor amount to the south (Gualandi *et al.* 2017; Mencin *et al.* 2016). The absence of significant afterslip or creep outside the main rupture zone to the south, east and west is especially important in assessing the prospects for future major earthquakes (Mencin *et al.* 2016).

Thousands of aftershocks occurred, hundreds of which were felt by the local population (Adhikari *et al.* 2015; Kumar *et al.* 2017). The first 20 days of aftershocks $>M_w = 4$ are shown in Figure 27. A $M_w = 7.3$ aftershock occurred 10 days after the mainshock within a 20 km-diameter patch that had not slipped in the mainshock (Lindsey *et al.* 2015). The location of this major aftershock was close to the location of a late $M_w = 5.7$ aftershock of the 1934 earthquake. Shaking in the $M_w = 7.3$ aftershock locally masked the damage done in the mainshock during subsequent investigations, and brought down many buildings that were still standing near its epicentre, NE of Kathmandu.

The mainshock and aftershocks resulted in many thousands of landslides, rockfalls and ice avalanches, including one that completely destroyed the old village of Langtang, where approximately 200 people perished. The Langtang slide nucleated in an ice field at *c.* 5000 m and descended to the valley floor at 3400 m, being mostly airborne for the last 500 m. The impact velocity of ice particles, rocks and pulverized rock particles has been estimated as 22–99 m s^{-1} (Collins & Jibson 2015), at which

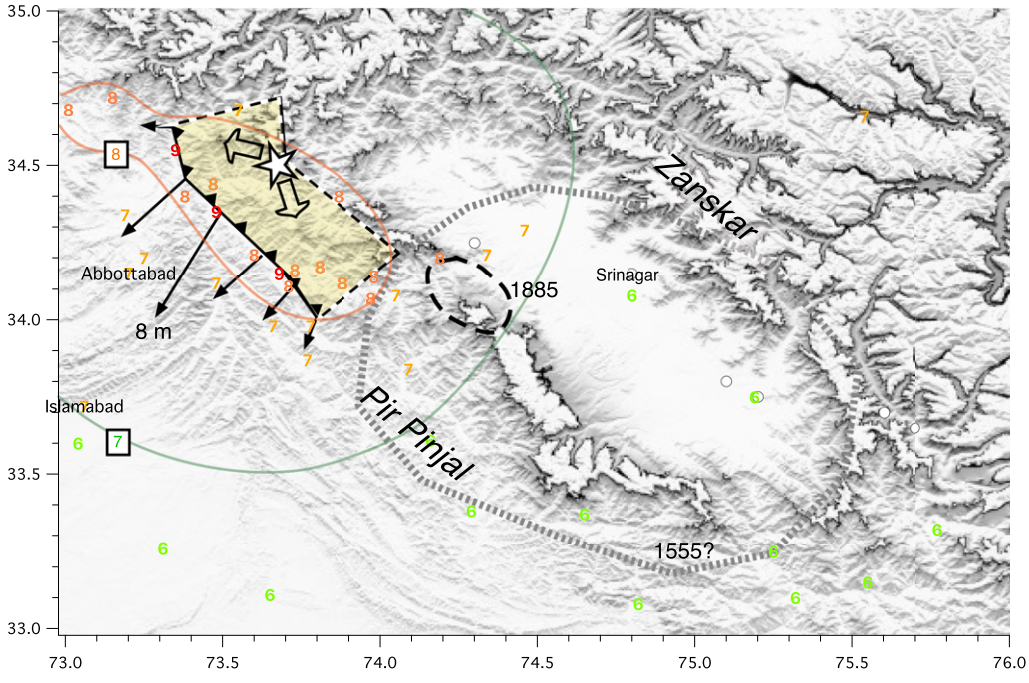

Fig. 23. Kashmir M_w = 7.6, 8 October 2005: subsurface propagation (open arrows) and surface slip (solid arrows, largest surface slip = 8 m) from Avouac *et al.* (2006), with intensity distribution from Martin & Szeliga (2010). EMS intensities 7 and 8 are contoured with individual observations between EMS6 (green) and EMS 9 (red) indicated. The poorly constrained bounds of the 1555 earthquake (dashed) embrace possible slip of a rectangular steeply dipping patch SE of the 2005 rupture, or rupture beneath the Zanskar.

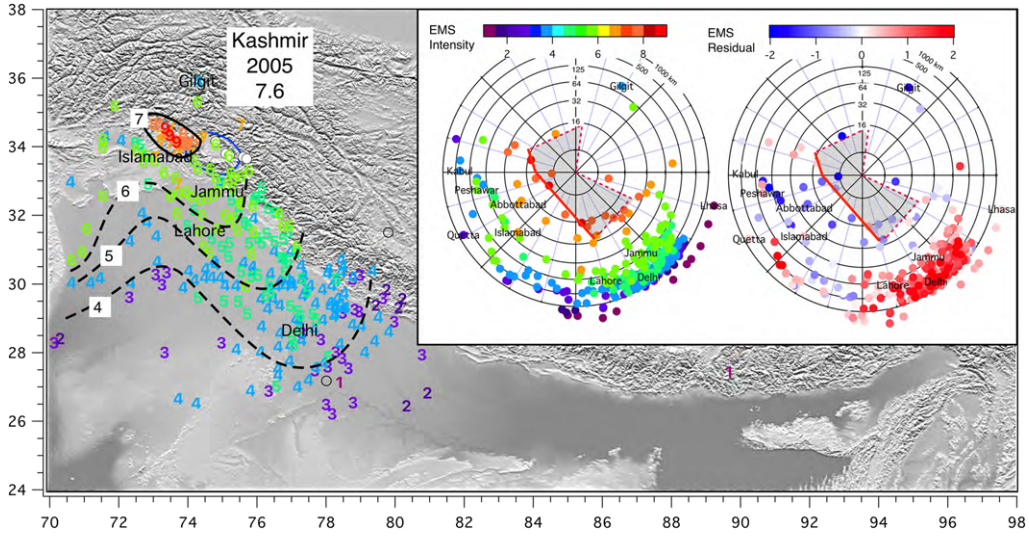

Fig. 24. Polar plots for the Kashmir M_w = 7.6, 8 October 2015. Circles are logarithmically increasing distances from the hypocentre in kilometres. The grey area bordered by a dashed red line indicates the inferred subsurface rupture which ruptured bilaterally and updip. The solid red line indicates the surface rupture. Far-field intensities were amplified by 1–1.5 intensity units in the region of thick sedimentary cover in the Punjab and Ganges basins. Amplification was additionally enhanced by directivity effects during nucleation. Approximate isoseismal contours (EMS 4–7) are shown as dashed lines in map view.

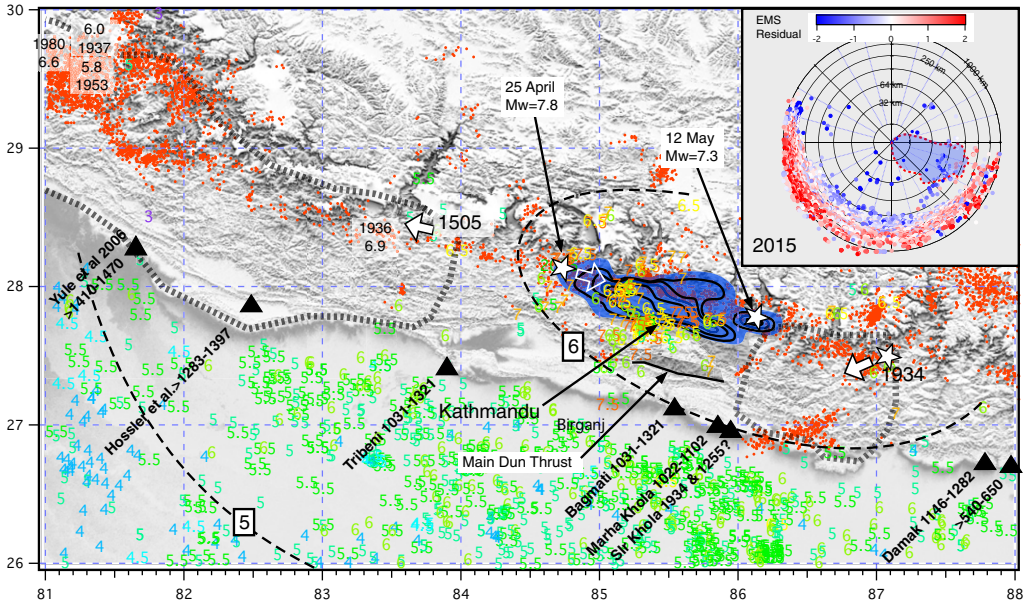

Fig. 25. 2015 Gorkha rupture area and preceding contiguous earthquakes (from ISC/GEM v. 5). EMS-98 intensities are from Martin *et al.* 2015. Intensities above the rupture area average EMS 6.6. Intensities in the Terai south of the rupture average EMS 5, compared to intensities of 6–8 at similar distances from the 1934 rupture (Fig. 18). The polar plot shows anomalous low residuals above the rupture (shaded blue) predicted from the Himalayan attenuation parameters of Szeliga *et al.* (2010). Microseismicity during 1995–99 are shown as red dots. Palaeoseismic trenches are indicated by triangles (from Wesnousky *et al.* 2018).

moment the materials of the slide exploded outwards and upwards at velocities sufficient to propel grazing Yaks airborne for 50 m, and to flatten and rip branches and bark from conifers on the opposite side of the valley. The Langtang ridge experienced EMS intensity 8, but the valley floor, a few kilometres to the south, was shaken by only intensity 7. Video footage of the shaking of masonry houses in the new part of Langtang village, prior to the blast from the landslide, showed uncemented dressed stone walls that were slowly being jostled loose by 1–2 s periodic shaking.

No slip occurred on the Main Frontal Thrust in the northern Terai plains of Nepal, but *c.* 5 cm of slip was triggered on the Main Dun Thrust north of the Main Frontal Thrust (Fig. 23), and a few tens of millimetres of afterslip continued between there and the southern edge of the rupture at decaying rates for 3 months following the mainshock. The triggered slip on 25 km of the Main Dun Thrust occurred dynamically, and its distribution and amplitude is quantitatively similar to the slip that would have occurred had friction on the Main Dun Thrust transiently reduced to zero (Mencin *et al.* 2016 supplement). A field inspection of a small segment of the Main Dun Thrust where maximum displacements were expressed in the InSAR deformation field was unable to identify localized offsets. Instead, a wide zone of deformation populated by sand-venting from east–west fissures was evident. Triggered slip on a thrust fault is unusual, but might be an important process for inducing surface slip on previous blind ruptures in the Himalaya. Given that the triggered slip quantitatively equates to that induced by the incremental increase of strain near Kathmandu after rupture ceased, triggered slip is assumed to have accompanied the stopping phase of the main rupture. However, slip continued to increase aseismically for several days after the earthquake (Elliott *et al.* 2016), indicating that slip at 2–3 km depth had subsequently propagated to the surface.

As mentioned in discussion of the 1833 earthquake, close resemblances can be traced between the 25 April 2015 earthquake and the earthquake that damaged Kathmandu in 1833. The earthquake was felt to similar distances and was reported at some at locations with identical or similar felt intensities. There is no distinct spatial distribution for those intensity observations that differ between the two earthquakes (Fig. 13) and, although much uncertainty about the rupture zone of the 1833 earthquake remains, the simplest interpretation is that the 2015 earthquake was a repeat of the 1833 earthquake. Average slip in the 2015 earthquake was about

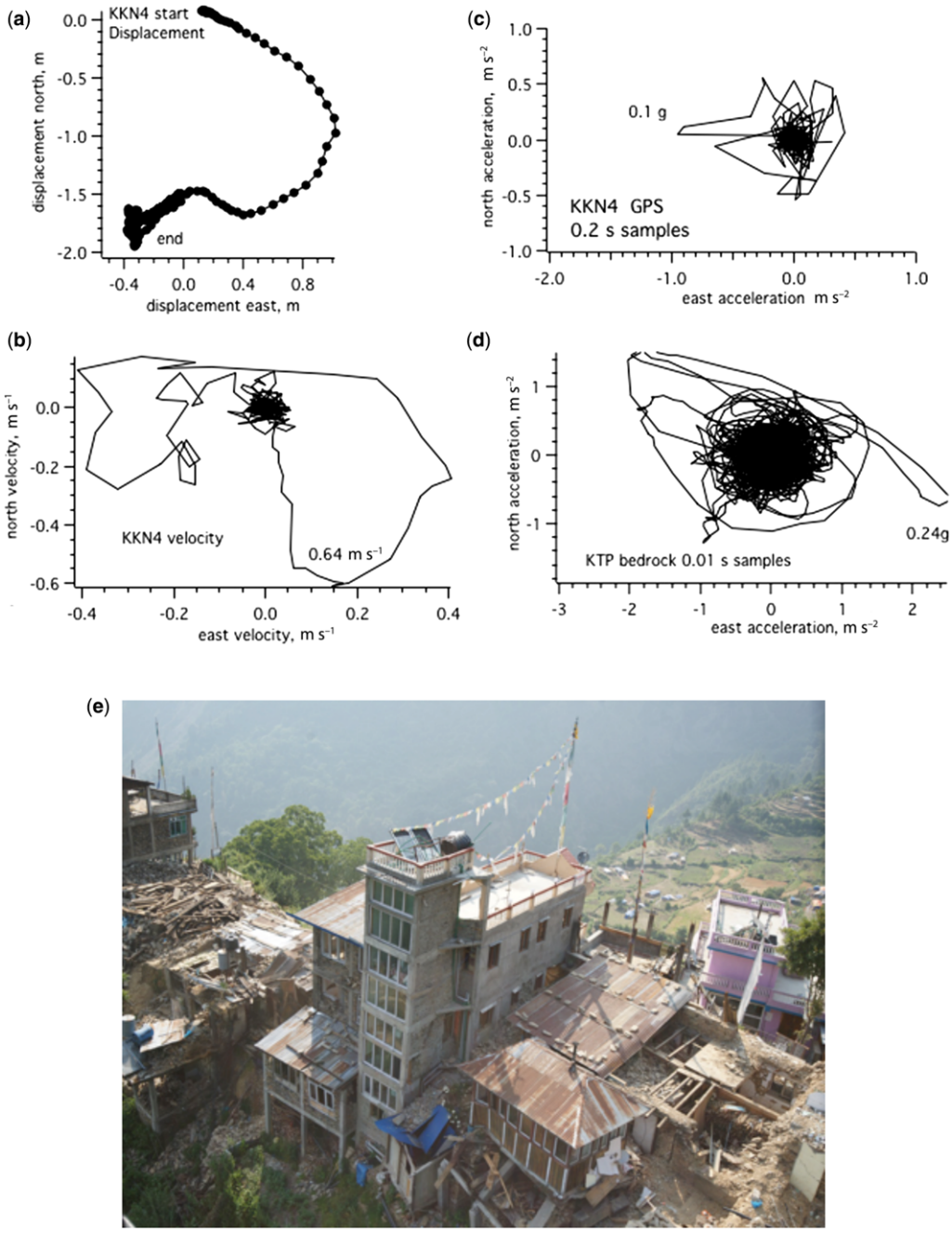

Fig. 26. Bedrock motions from the southern edge of the Gorkha rupture displayed as hodograms (map views of horizontal motions). (**a**) GPS positions sampled every 0.2 s at point KKN4 on the northern edge of the basin reveal the wholesale 1.5 m southwards displacement of the surface rocks of Nepal over the Indian Plate. Simultaneously, the basin rose 1 m more in the north than the south (Galetzka *et al.* 2015). The horizontal displacement is known as 'fling' because of its dynamic non-recoverable offset (in this case more than 1.5 m). (**b**) The GPS velocity at KKN4 is the time derivative of (a). (**c**) KKN4 acceleration, the time derivative of (b). (**d**) KTP acceleration measured by a strong motion accelerometer (Takai *et al.* 2016). (**e**) view of ridge amplification in northern Nepal. The distant village at lower elevation is shaken by lower shaking intensity.

3.5 m, similar to the accumulated 182 year slip deficit following the 1833 earthquake.

In the aftermath of the earthquake, of great concern was the possibility that the 25 April 2015 earthquake may have been a foreshock to the anticipated $8 < M_w < 8.4$ earthquake that historical data suggest the region is capable of sustaining (Bilham *et al.* 1995, 2001). Arguments for such triggering include the observation that 10% of all great earthquakes have historically been preceded by a major foreshock (Jones & Molnar 1976). However, the $M_w = 7.8$ Kangra earthquake was not followed by a larger earthquake, and neither was the 1833 earthquake north of Kathmandu. Bollinger *et al.* (2016) made a case for the 1255/1344 earthquake sequence being similar to the 1934/2015 sequence; however, there is considerable uncertainty about the rupture zones and slip in the first three of these earthquakes.

Palaeoseismic studies of great earthquakes

Active surface faults in northern India had been described by Oldham in the nineteenth century (Bilham 2004; Bilham *et al.* 2013; England & Bilham 2015), but not until 1999 had surface rupture of the Main Frontal Fault been associated with dated earthquakes. Following the initial reports of surface rupture of the frontal thrust faults (Wesnousky *et al.* 1999; Kumar *et al.* 2001, 2006), more than two dozen excavations of surface ruptures along the Himalayan arc have now been reported. Some excavations have provided evidence for multiple earthquakes in past millennia, and in ideal circumstances each new result would provide additional constraint to the along-strike reach and/or overlap of individual palaeoseismic ruptures. Unfortunately, some results question earlier results and as yet no unique history of earthquakes prior to the instrumental period (1900) has been agreed upon. For example, at the critical Sir Khola River section (27.04° N, 85.9° E), SE of Kathmandu, where Sapkota *et al.* (2013) and Bollinger *et al.* (2014) equate subsurface offsets with historical earthquakes in 1255 and 1934, Wesnousky *et al.* (2018) indicate that no disruption of surface layers by the 1934 earthquake occurred.

A further difficulty is that radiometric dating methods are typically accurate to not better than 50 years and, for some radiometric years, duplication and triplication ambiguities greatly extend this uncertainty. As a result, the association of palaeoseismic fissures with dated historical events is often ambiguous. Historical earthquakes on 7 June 1255 (Sapkota *et al.* 2013; Bollinger *et al.* 2016), 14 September 1344 (Mugnier *et al.* 2013; Rajendran *et al.* 2015), 1 June 1505 (Kumar *et al.* 2001, 2006, 2010; Yule *et al.* 2006; Hossler *et al.* 2016), 4 May 1714 (Le Roux-Mallouf *et al.* 2016; Heténi *et al.* 2016), 1 September 1803 (Malik *et al.* 2017), 1905 (Malik *et al.* 2015) and in Assam on 15 August

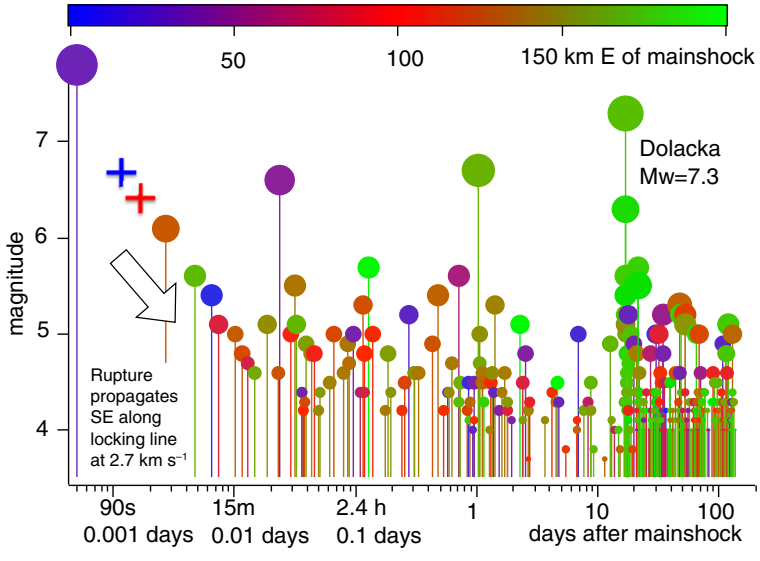

Fig. 27. The first 20 days of aftershocks (log of time since the mainshock) including the $M_w = 7.3$ aftershock show a general eastwards migration of seismic activity. The xx events symbolize the numerous radiating phases that occurred during eastward propagation along the northern edge of the locked décollement in the first two minutes of the rupture. Five aftershocks $\geq M_w = 4$ occur in the first 14 min (0.01 days). More than 553 $M_w > 4$ earthquakes occurred within 45 days of the mainshock.

1950 (Priyanka *et al.* 2017) have been equated with palaeoseismic ruptures. But for even the most recent of these earthquakes (1950), there exists a lack of clarity about the lateral extent of rupture, the relationship of mean slip to observed coseismic offset or, as mentioned earlier, whether or not surface rupture occurred on 15 January 1934 in Nepal (Sapkota *et al.* 2013; Bollinger *et al.* 2016; Wesnousky *et al.* 2018). An extreme example of enthusiastically connecting weakly constrained dates from palaeoseismic trenches is the suggestion by Mishra *et al.* (2016) that the 7 June 1255 earthquake, for which we have a single-line historical account from the Kathmandu Valley (Pant 2002), ruptured 800 km eastwards from 86° E to 94° E. Pierce & Wesnousky (2016) demonstrated that data from six of the seven trench sites invoked in this extrapolation use data with large uncertainties, and that their association with a 1255 rupture is unjustifiable and misleading.

The timing of a palaeoseismic earthquake is bracketed by the age of ruptured sediments and by the age of undisturbed sedimentary cover, which provide minimum and maximum bounds for the time of the causal earthquake. This can be considered an error bar with a mean date and range. However, since the carbon sample being dated is older than the time of sediment deposition, these minimum and maximum bounds represent dates that are earlier than the time of the earthquake by days, months or even decades.

In syntheses of the accumulating palaeoseismic record, the quest has been to identify synchronous events in contiguous trench sites in order to determine the along-strike length of historical ruptures. Several such syntheses are now available (Kumar *et al.* 2010; Bollinger *et al.* 2016; Rajendran & Rajendran 2005; Rajendran *et al.* 2015; 2018*b*; Mugnier *et al.* 2013; Malik *et al.* 2017; Wesnousky *et al.* 2017*a*, 2018). Two common features of the earthquakes can be inferred from palaeoseismic excavations of the Main Frontal Fault: slip is generally remarkably large (upwards of 20 m in some cases); and much of the Himalayan arc ruptured between 1100 and 1600 CE (Fig. 6), a moment release unmatched in the previous or succeeding 400 years (Fig. 28).

That palaeoseismic studies record the passage of truly great earthquakes is not surprising, but slip exceeding 10 m with rupture dimensions of 100 × 200 km imply earthquakes with moment magnitudes with $M_w \geq 8.5$. The 1950 earthquake alone approached this amount of slip in the past 500 years. Prior to this time, there appear to be several. Examples of such earthquakes are shown as grey bars in Figure 28, corresponding to probably synchronous rupture at several trench sites in earthquakes with magnitudes $8.7 < M_w < 9$. One such earthquake is discussed by Wesnousky *et al.* (2018). However, slip exceeding 10 m in historical earthquakes requires a physical explanation. The supposition is that if no earthquake occurs for 1000 years and the convergence rate is 15 mm a^{-1}, the ensuing earthquake must slip 15 m. However, the region that stores the elastic strain released by this earthquake (near the locking line) is *c.* 20 km thick and can store elastic energy only up to its elastic limit, which is *c.* 10^{-4}

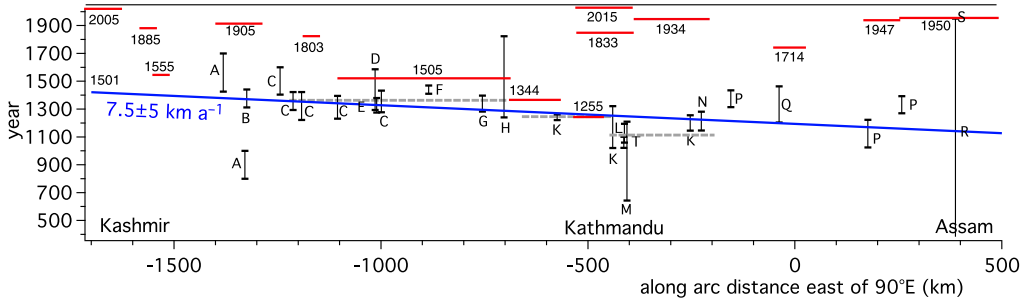

Fig. 28. Historical earthquakes (red) and dated palaeoseismic ruptures of Himalayan Frontal Thrust faults (shown by error bars). Least-squares fits to the east and west Himalaya are indicated with weighted deviations proportional to the range of reported dates at each site. Blue lines are weighted least-squares fit representing a hypothetical west-propagating rupture front with a velocity of 7.5 ± 5 km a^{-1} starting in Assam at *c.* 1100 and arriving at Kashmir >1400 (dates that ignore systematic detrital ^{14}C errors). Grey dashed bars indicate synchronous slip in single earthquakes with surface ruptures exceeding 200 km proposed variously by Mugnier *et al.* (2013), Rajendran *et al.* (2018*b*) and Wesnousky *et al.* (2019). A, Arora & Malik (2017), Malik & Nakata (2003); Malik *et al.* (2003, 2008, 2010*a*, *b*); B, Kumahara & Jayangondaperumal (2013); C, Kumar *et al.* (2006); D, Malik *et al.* (2017); E, Rajendran *et al.* (2015, 2018*b*); F, Yule *et al.* (2006); G, Hossler *et al.* (2016); H, Mugnier *et al.* (1998, 2013); J, Murphy *et al.* (2013); K, Wesnousky *et al.* (2017*b*); L, Lave *et al.* (2005); M, Sapkota *et al.* (2013); N, Upreti *et al.* (2000, 2007); P, Kumar *et al.* (2010); Q, Le Roux-Mallouf *et al.* (2016); R, Jayangondaperumal *et al.* (2011); S, Priyanka *et al.* (2017); T, Wesnousky *et al.* (2018).

strain. For example, if the region of preseismic strain accumulation is only 20 km wide, the maximum slip that can be stored and released, no matter how long the interval since the previous earthquake, is only 2 m (20 km × 10^{-4} strain). Slip exceeding 10 m requires a downdip storage width exceeding 100 km, and it is not certain that such conditions exist in the Himalaya. I shall discuss this further in a following section.

If we admit the possibility that the medieval ruptures correspond to earthquakes that record a propagating sequence of earthquakes, we obtain a westwards propagation velocity of 7.5 ± 5 km a^{-1}, starting in Assam at *c.* 1100 CE, passing 90° E in the year 1212 ± 53, and arriving in Kashmir at *c.* 1400 (Fig. 28). Since the dates are constrained by detrital carbon, they are all too early by an unknown amount. The 1505 and 1515 earthquakes near Kabul on India's western transform occur at the end of this westwards propagation. The 2000 km east–west rupture of the entire Himalaya would have taken 250–400 years, during which time an additional 4–7 m of convergence would have occurred.

Historical earthquakes in the past 200 years have ruptured less than 30% of the Himalayan arc, and those that have unequivocally ruptured the frontal thrusts account for less 13% of the arc. In contrast, medieval earthquakes from 1100 to 1600 CE apparently ruptured 78% of the arc's frontal thrusts.

Several explanations can be invoked as to what may have caused this remarkable slip episode. The first is, of course, that it is merely a statistical fluctuation with no underlying physical cause. Alternatively, a domino effect can be invoked, where each earthquake released many metres of slip and stressed unruptured regions near its extremities, leading to successive failure similar to that which occurred on the 1200 km-long North Anatolian Fault between 1939 and the present time (Ambraseys 1971; Stein *et al.* 1997). Sequential triggering of earthquakes along the strike-slip Anatolian Fault occurred with an average velocity of 15 km a^{-1} with slip of roughly 5 m, roughly double the speed and half the amount of the inferred Himalayan propagation rate and amplitude. Major earthquakes propagated westwards along *c.* 2000 km of the Aleutian subduction zone between 155° W and 170° W between 1938 and 1965 (Johnson *et al.* 1994) at a considerably higher rate (*c.* 70 km a^{-1}).

Another explanation is that the sequence may be the response to an underlying incremental stress regime caused by an increase in plate velocity (unlikely) or a decrease in clamping stress in the Himalaya (ice unloading caused by a warming in climate: Panza *et al.* 2010; Esper *et al.* 2002). Although the details of the earthquakes are currently uncertain, average slip in the twelfth–sixteenth century time interval amounts to approximately 9 m (an arithmetic mean of the observed offsets between 1 and 16 m).

Have recent earthquakes exhibited sequential triggering that might support along-arc propagation? Seismicity in the past four centuries appears to have been anomalously sparse; however, none of the past century of earthquakes has induced contiguous slip in the Himalaya (within a few decades), with the exception of the 1947/1950 sequence (Fig. 21) whose epicentres were separated by *c.* 250 km but whose ruptures probably abutted. The great 1897 Shillong earthquake preceded the Dhubri 1930 $M_w = 7$ earthquake near its western end, and was followed by the 1934 and 1947/1950 sequences, both *c.* 450 km distant, by 37 and *c.* 50 years, respectively, implying a 'communication' velocity of *c.* 10 ± 3 km a^{-1}. Other earthquakes discussed earlier show no simple distance–time relationship, and, in particular, with the exception of aftershock sequences, contiguous earthquakes are not caused by static strain transfer. Clearly, many more earthquakes are required before a case for along-arc propagation can be established.

Limits to Himalayan earthquake magnitudes?

In this section I review some of the challenges in explaining observed slip in great earthquakes, and discuss the maximum credible earthquake that can occur in the Himalaya. Less than 30% of the Himalayan arc has slipped in the past 200 years (and possibly the past 500 years), which means that several great earthquakes are overdue (Bilham *et al.* 2001; Bilham & Ambraseys 2005; Stevens & Avouac 2016) and the possibility of a $M_w = 9$ earthquake in the Himalaya has been proposed (Bilham & Wallace 2005; Stevens & Avouac 2015). Despite the occurrence of the $M_w \geq 8.6$ 1950 Assam earthquake, and palaeoseismic results suggesting that a similar magnitude earthquake may have occurred in eastern Nepal at *c.* 1100 (Wesnousky *et al.* 2018), some authors consider the notion of a $M_w \geq 9$ earthquake in the Himalaya unreasonable. They invoke arguments ranging from the observation that such a large earthquake is unknown in India's history, that creep processes absorb India's convergence, or that physical segmentation of the Himalaya prevents through-going propagation of ruptures longer than a few hundred kilometres (e.g. Srivastava *et al.* 2013; Gupta & Gahalaut 2015; Arora & Malik 2017). However, support for each of the above constraints is subjective or weak, and in some cases, demonstrably wrong. The history of Himalayan earthquakes extends with certainty for only a few hundred years. No shallow creep of the Himalayan décollement has yet been detected geodetically. The segmentation of the Himalaya has certainly limited the growth of recent ruptures, but our view of the

Himalaya may be biased by the shortness of the seismic record, and by the richness of surface geology, that is missing from submarine subduction zones.

The occurrence of a future $M_w \geq 9$ earthquake does not imply that unprecedented violent shaking will accompany such an event. For example, shaking intensities in the Indian Ocean $M_w = 9.2$ earthquake did not exceed Mercalli intensity 8 in the Andaman Islands. The duration of shaking in a $M_w \geq 9$, however, will be much increased compared to a $M_w = 8$ earthquake, and may exceed many minutes. This prolonged shaking is likely to aggravate damage to poorly constructed structures.

Surface slip on frontal thrusts caused by creep or triggered slip?

Although no surface rupture occurred on the Main Himalayan Thrust in the 2015 Nepal earthquake, limited slip of locally more than 5 cm was activated on the Main Dun Thrust (Elliott *et al.* 2016). The splay fault cuts through forest and streams 15 km north of the Main Frontal Thrust (Mugnier *et al.* 1998). Surface slip was triggered dynamically for a 25 km length of the fault during the earthquake down to a depth of *c.* 5 km. A search for this slip was unsuccessful (Mencin *et al.* 2016). Of significance is that InSAR radar scenes and GPS revealed no slip on the underlying thrust plane between the subsurface north-dipping termination of subsurface slip and the main rupture plane (Fig. 4b). The importance of this observation is that a record of $M_w \geq 7$ earthquakes that fail to rupture the Main Himalayan Thrust elsewhere may be recorded as incremental slip on similar splays above the Main Himalayan Thrust. Unfortunately, a 5 cm offset on a thrust fault may be difficult to identify. This is not only because decimetre offsets in surface sediments tend to be somewhat ephemeral, but because thrust faulting is commonly associated with a broad zone of flexural folding (Boncio *et al.* 2018) with no recognizable zone of localized slip. For example, a search for surface offsets on the Main Dun Thrust at 27.24° N, 85.73° E in 2015 in the week following the Nepal earthquake identified no measurable vertical offsets, but revealed several liquefaction fissures with sand venting that may have been associated near-surface strain (Mencin *et al.* 2016).

Creep, elastic limits and the locked décollement beneath the Himalaya

Creep is a process whereby rocks slide past each other without adhesion or friction. For this to occur, the surfaces in contact must somehow be lubricated, either through the presence of high-pressure fluids (water or compressed gases, like carbon dioxide) or because the intrinsic properties of the materials in contact are effectively plastic or viscous by virtue of their temperature or pressure or material properties. At depths below about 18 km, the upper surface of the Indian Plate and the lower surface of the Himalaya attain these special conditions, and the Indian Plate can be considered to descend beneath Tibet at a uniform velocity of about 50 μm/day.

At shallower depths, friction between the Indian Plate and the Himalaya arrests slip between. Before discussing a critical region between the completely locked and the perfectly sliding region, it is necessary to emphasize that any horizontal fault surface, weighted down with more than 5 km of rock above it, has great difficulty in moving at all. A simple mechanical analysis reveals that the friction caused by this enormous weight of rock is so great that any attempt to slowly push the rock southwards over the Indian Plate by forcing it from the north is doomed to failure. Instead, the rock will fracture a new fault towards the surface – a reverse fault or a high-level thrust (Fig. 3). It is easier to break a new fault through 20 km of intact rock than to make the Main Himalayan Thrust slip at depth (cf. Oldham 1921).

This seems to be an odd conclusion given that the Main Himalayan Thrust must, indeed, slip if the Indian Plate is to continue to descend beneath Tibet. But if slip is to occur, friction on the Main Himalayan Thrust must briefly be reduced to vanishingly low levels. We now recognize that when slip occurs, only a small segment of the décollement slips at any one moment. Long before we had measurements that glimpsed the details of this process (Galetzka *et al.* 2015), Richard Oldham (1921) reasoned that perhaps only a part of a thrust fault would move at any one time, thereby loading contiguous parts of the thrust fault 'akin to the crawl of a caterpillar which advances one part of its body at a time, and all parts in succession'. We now know that the segment of the fault on the move measures 1–10 km wide and that this patch slips at rates exceeding 2 km s^{-1}, but the physics of the process that transiently reduces the friction remains uncertain. One possibility is the fault mechanically separates by dynamic processes, another that explosive gas formation arising from the heat of friction forces the surfaces apart, and another that the rock briefly melts (Sibson 1973; Brune *et al.* 1993; Brune & Thatcher 2002; Rice 2006; White 2012). Although the process remains uncertain, no slip on the décollement can occur between the times of dynamic nucleation. Thus, the Himalayan décollement between *c.* 18 km depth and the surface is locked for decades with no possibility of slip. With the exception of parts of Kishtwar and Arunachal provinces, where geodesy remains spare, this has been confirmed by geodetic measurements (Bilham *et al.* 2017).

The elastic energy ($\frac{1}{2}VE\varepsilon_c^2$) that can be stored in rock prior to an earthquake is the product of the volume (V) and strength (E) of the rock times the square of the elastic strain (ε_c) at the moment of failure. Since ε_c is limited to *c.* 10^{-4} (Kanamori & Brodsky 2004; Bilham *et al.* 2017) and E for most rocks is *c.* 3×10^4 MPa, the elastic energy available is $1.5V \times 10^{-4}$ J. A factor limiting the magnitude of primary earthquakes in the Himalaya is the volume, V, available to store this energy. For example, if there were an abrupt transition, just 1 m wide separating the upper surface of the creeping Indian Plate descending beneath the Tibet at 17 mm a^{-1} and the locked décollement at shallower depths, strain would reach the failure strain (0.1 mm in 1 m) in the rock in just 2 days, resulting in more than 180 *c.* $M_w = -1$ earthquakes/year.

Common sense, and the presence of large earthquakes, tells us that transition from locked to creeping décollement is distributed over a considerably wider zone. Surface geodesy and microseismic activity demarcate a broad interseismic decoupling transition zone, where the décollement is neither fully locked nor fully creeping (Fig. 29). On the décollement in this region, some fraction between 1 and 99% of India's 50 μm/day northwards advance occurs as creep, and the remaining fraction is stored as elastic energy near the fault because of friction. The friction in this zone can be considered to be caused by bumps on the décollement (asperities) that are in frictional contact, separated by intervening regions of lower friction or viscous materials, like clays, that continue to slide sluggishly. The zone represents a transition from the creeping décollement to the fully locked décollement and varies in width from less than 10 km to more than 50 km (Stevens & Avouac 2015).

This transition zone assumes special importance because, depending on its downdip width, the rocks above and beneath this region can store more elastic energy than could the rocks above a narrow locking 'line'. In Figure 29, the aspect ratio of dilatational strain contours contiguous with the decoupling zone increases with its width. Although it takes the same 200 years to bring the outlined regions to 20 μstrain, when rupture occurs the length of the compressed 'spring' is longer in the case of a wide zone in Fig. 29, meaning that it can, in principle, drive a Himalayan rupture further in a larger magnitude earthquake. A consequence of its increased width is that it takes longer for strain within this width to accumulate to failure levels. For example, a 60 km-wide decoupling zone takes about 50% longer for its 20 μstrain region to grow to comparable aspect ratio as the 30 km-wide zone in Figure 29, and the net elastic energy stored ever the entire 18 km-thick carapace will double. Thus, larger earthquakes occur at less frequent intervals where the interseismic coupling region is wide (Bilham *et al.* 2017). A convenient rule of thumb is that a 10 km-wide zone can store enough elastic strain to drive a 1 m earthquake (width $\times 10^{-4}$), a 30 km-wide zone can drive a 3 m rupture, and so on. This would imply that observed palaeoseismic ruptures with 10 m of slip would require a more than 100 km-wide decoupling zone.

Estimates of the width of the zone of partial seismic coupling in the Himalaya (Stevens & Avouac 2016) show that such large decoupling widths may exist at the ends of the Himalayan arc, but in the centre of the arc its width averages 20–60 km. This means that earthquakes in the central arc can only release about 2–6 m of slip at the moment of rupture.

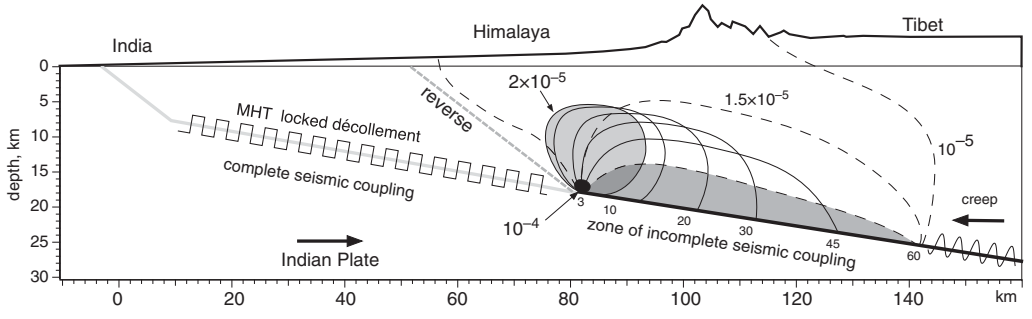

Fig. 29. Schematic descent of the Indian Plate beneath Tibet showing the volume of Himalaya subject to 10 μstrain compression (200 years at 17 mm a^{-1}) for seismic-decoupling transition widths of 3–60 km. The tip of the 3 km-wide decoupling zone reaches 100 μstrain in 200 years (small black area). A 5 km wide shaded area can store elastic strain approaching failure in a much larger region (shaded). A second shaded area extending 60 km down-dip can store significantly more strain before failure (dashed contours show cumulative strain ampliitude after 200 years). Wider decoupling zones take longer to reach 100 μstrain failure levels, but can drive correspondingly larger earthquakes due to their longer downdip widths. The steep reverse fault represents the preferred path for faulting in the presence of a fully locked décollement (c.f. Fig. 4a).

This is insufficient to explain the numerous palaeoseismic ruptures that have been recorded there with 10–20 m of slip.

A paradox thus presents itself. How can we reconcile this theoretical limitation with the numerous documented occurrences of 10–20 m of slip in Himalayan palaeoseismic trench investigations? Feldl & Bilham (2006) proposed that since Tibet is also being deformed by India's convergence, a factor of 2 more elastic strain could be released in a great Himalayan earthquake. This did not occur in the 2015 M_w = 7.8 Gorkha earthquake, nor did afterslip add significantly to coseismic slip in the years following the earthquake (Mencin *et al.* 2016; Gualandi *et al.* 2017). The 2015 Gorkha earthquake, however, provided an important indication as to where additional elastic energy may reside.

Invisible elastic energy

The Gorkha earthquake ruptured from the locking line southwards, but failed to rupture to the frontal faults of the Himalaya (Avouac *et al.* 2015; Galetzka *et al.* 2015. Elliott *et al.* 2016). Its incomplete rupture therefore transferred elastic strain from the Greater Himalaya to the Lesser Himalaya. The resulting strain field is clearly imaged by interferometric geodesy and is quantified by GPS measurements. The strain gradient quantified by InSAR (5×10^{-4}) is at the high end of the range of estimates for failure strain reviewed by Kanamori & Brodsky (2004) and Bilham *et al.* (2017). However, this strain is now invisible to geodetic measurements because it is apparently stagnant. Geodesy reveals only *changes* in strain. The strain established near Kathmandu during the Gorkha earthquake thus remains as an invisible reservoir of 'dark' strain energy because although it can potentially be released in a future earthquake, it cannot be quantified by ongoing interseismic geodetic measurements.

The 1803 ($M_w \approx 7.5$) and 1905 (M_w 7.8) earthquakes in the Himalaya also failed to rupture the frontal thrust faults, thereby also incrementing strain in the mid-décollement region of the Main Himalayan Thrust. In general, we can state that all Himalayan earthquakes that do not rupture to the surface, increment strain south of the locking line (Bilham *et al.* 2017). The corollary is that we know of only three Himalayan earthquakes in the past century that have not incremented strain south of the locking line: the 1950 M_w = 8.6 Assam earthquake; the 2005 M_w = 7.6 Muzafferabad earthquake; and arguably the 1934 M_w = 8.4 Nepal earthquake (which may have loaded the region south of the Main Himalayan Thrust). Only earthquakes that rupture the frontal thrusts effectively release elastic strain by translation of the hanging wall over the Indian Plate.

Ancestral elastic energy and slip in great Himalayan earthquakes

Shortly after the Gorkha earthquake there was concern that the 30–40 km region south of the rupture plane (south of Kathmandu) would slip in a future earthquake. The unruptured area, and its potential slip, was calculated as sufficient to generate a M_w = 7.3 earthquake. This earthquake has not yet occurred. Theoretical and observational arguments suggest that such an earthquake is unlikely, although it may be possible.

A shallow-dipping thrust fault can slip only when friction on the fault approaches zero (Oldham 1921; Davis & Engelder 1987; De Bremaecker 1987). The reason is that even with low coefficients of static friction the forces required to push a several-kilometre-thick block horizontally exceed the strength of the rock and, instead, out of sequence thrusts tend to develop towards the surface upon which slip can more easily occur (Fig. 4e). Once slip has been initiated on a shallow thrust, friction can reduce abruptly to low values by transient separation of the fault surface, by melting of the fault surface or as a result of fluid heating and overpressurization. However, nucleation of slip must first overcome static friction. The conditions for low static friction are that the fault should be lubricated by fluids (high pore pressures) or by viscous materials (salt, gypsum, etc). However, the rapid decay of afterslip south of Kathmandu (Mencin *et al.* 2016) and the absence of afterslip or creep in the 2 years following the earthquake suggest that such conditions do not currently prevail, and that friction on the fault is sufficiently high to inhibit slip. Consistent with the above observation, the 1803 M_w > 7.5 Almora (Fig. 10) and 1905 Kangra M_w = 7.8 (Fig. 18) earthquakes were not followed by subsequent major updip earthquakes.

If this invisible elastic energy is not dissipated as creep, or released in moderate earthquakes, it could be absorbed as plastic deformation of the Himalayan carapace. Few exposures of rocks in the Himalaya are horizontal (Kathmandu was tilted to the south in 2015). Folded strata are ubiquitous.

However, from *in situ* stress studies, it has long been established that crustal rocks can support elastic strains for many thousands, if not millions, of years, much longer than the seismic cycle in the Himalaya. Hence, it is possible to conclude that the large slip in some great earthquakes in the Himalaya may not only be exploiting the elastic energy stored in the interseismic interval preceding their occurrence, but may also be fuelled by elastic energy inherited from ancestral incomplete earthquakes (Mencin *et al.* 2016; Bilham *et al.* 2017). Some great earthquakes may thus nucleate as $M_w \approx 7$ earthquakes, but their ruptures may encounter residual elastic strain stored centuries earlier on the Main Himalayan

Thrust, resulting in a doubling, or quadrupling, in their initial rupture area, or, in the extreme case, resulting in a cascade rupture with area similar to the 1505 earthquake (Fig. 6).

Such a process could reconcile the apparent limitation of the 2–5 m slip potential of earthquakes in the Himalaya, based on typical downdip decoupling widths of 20–50 km. It is possible to argue that this deduced limitation depends only upon the choice of an artificially low ultimate strain at failure. For example, if the failure strain were 5×10^{-4} strain, then earthquakes with 25 m slip could be driven by a 50 km-wide downdip region of interseismic strain. Some suggestion that a 10^{-4} compressive failure strain may be too low is suggested by the strain changes accompanying the 2015 Gorkha earthquake. The displacement gradient emplaced north of Kathmandu in 2015 was 5–7 m reducing to zero in a distance of 10–15 km, corresponding to an elastic strain in rocks immediately above the décollement of *c.* 5×10^{-4} strain. The displacement gradient north of the rupture (corresponding to coseismic extension) was only half this amount, corresponding to an interseismic stored strain of 2.5×10^{-4}.

Rupture propagation and subsequent nucleation

For a handful of historical earthquakes, it has been possible to infer rupture propagation directions during the earthquake. For 1505, 1803, 1905 and 1934, this could only be achieved with certain assumptions, but for 2005 and 2015 there is no ambiguity. Each of these major earthquakes has nucleated from an epicentre and ruptured the Main Himalayan Thrust for distances of 50–450 km, and as a result was associated with enhanced directivity of shaking intensity in the rupture propagation direction. This directivity was prominent in the 2005 and 2015 earthquakes, even though the 2005 earthquake was in fact a bilateral rupture, with one-third of the rupture propagating to the NW.

The question can be asked as to why unilateral ruptures occur. One supposition is that a previous earthquake has loaded the epicentre region of a later, contiguous epicentral region, which has then approached critical failure as a result of Indo-Tibetan convergence. If this occurred soon after the earlier earthquake, the initial rupture would presumably propagate away from the region whose strain has recently been released, into the region where it still remains. That is, the earthquake would nucleate near the rupture termination region of a former earthquake, and propagate away from it.

The reverse would appear to be true for the two pairs of earthquakes for which we have relevant information: for 1505/1803 (Fig. 11) and 1947/1950 (Fig. 19). For each pair of earthquakes, the rupture nucleation direction appears to have been from the distal regions of each abutting rupture zone towards the mutual termination region. This suggests that rupture nucleation is not caused by contiguous loading, and lends support to the notion that rupture termination (and nucleation) is associated with geometrical asperities, as has been suggested by some geological studies (Grandin *et al.* 2015; Hubbard *et al.* 2016; Mugnier *et al.* 2013).

One other pair might be considered: the 1833 and 1505 earthquakes. However, we do not know how close these ruptures approached each other's rupture zones (Fig. 12).

Himalayan seismic slip deficit

If we assume that the mean convergence rate in the Himalaya is 15 mm a^{-1} and that the rate has not changed for the past several hundred years, we can address the question of whether observed earthquakes have been sufficient to keep up with India's northwards advance beneath Tibet. A theoretical rate of earthquake productivity is calculated from the length of the Himalaya × its average width × its average slip rate × an assumed shear modulus (Brune 1968). Setting the length of the Himalaya to 2200 km, its average width to 100 km, a modulus of 3.3×10^{11} dyne cm and that the rate of accumulation considerably exceeds the rate of release by earthquakes (Fig. 30), two observed curves are calculated: a low rate taking the lowest estimated magnitude for all earthquakes; and a second for the highest probable magnitude. If we start the clock from 1505, one estimate leads to a slip deficit that can be filled in the present day with one $M_w \approx 8.6$ earthquake; whereas if we include only low estimates for historical magnitudes, the current slip deficit corresponds to two $M_w = 8.6$ earthquakes.

If the Himalaya continues to slip infrequently in earthquakes with magnitudes of less than $M_w = 8.2$, the observed and theoretical curves will necessarily diverge. The total moment accumulation since 1500 corresponds to the energy released by a single $M_w = 9.1$ earthquake. At the current rate of divergence, a $M_w = 9.0$ earthquake would close the slip deficit in a further 500 years. Several theoretical arguments advanced by Stevens & Avouac (2015, 2016) show that $M_w = 9$ earthquakes are needed every 1000–1200 years.

Earthquake timing and the Indian monsoon

It has been known for some years that microseismicity in the Himalaya increases annually during loading by rainfall south of the Himalaya during the monsoon (Bollinger *et al.* 2007; Bettinelli *et al.* 2008). Surface reservoirs are replenished and excess runoff causes rivers to swell, resulting in widespread

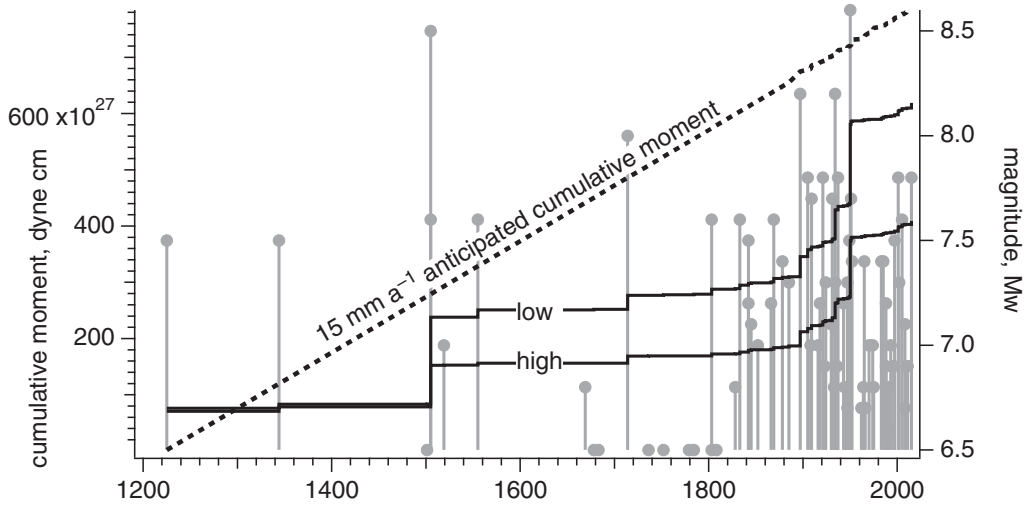

Fig. 30. Seismic slip deficit assuming a mean convergence rate of 15 mm a^{-1} for the Himalaya. The dashed line indicates the theoretical moment release; the solid incremental lines represent the observed rate taking the high and low estimate for historical magnitudes. The divergence of the synthetic and dashed lines imply that one or two $M_w \geq 8.6$ earthquakes, or an equivalent moment release contributed by several $M_w > 8$ earthquakes, are missing and must occur in the future.

surface floods whose delayed runoff acts as a seasonal load in central India and the Ganges Plain. The mass of water has the effect of depressing the Earth's crust beneath the load, and drawing points distant from the load towards it. The resulting stress changes have been quantified by Panda *et al.* (2018) using observed seasonal displacements of Lhasa and Bangalore to verify their calculations. The resulting strain changes are small but sufficient to perturb the tectonic loading and influence the timing of earthquakes in the Himalaya. Figure 31 shows, however, that neither the declustered instrumental record of shallow (≤30 km) $M_w \geq 5.5$ earthquakes 1904–2018 (ISC/GEM v.5) nor the historical record of

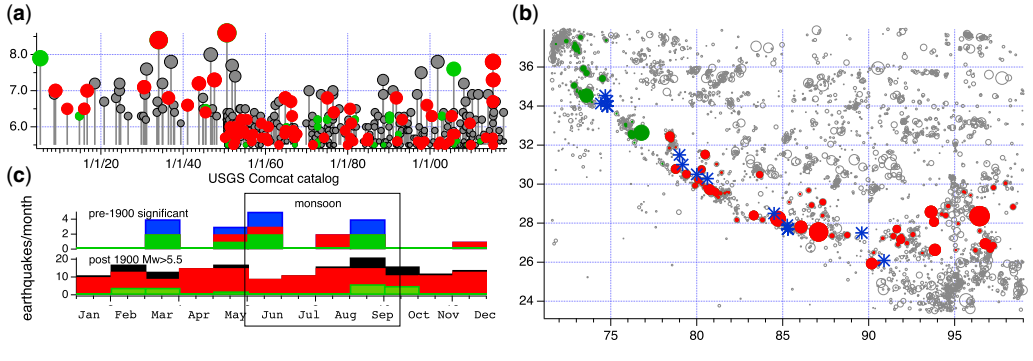

Fig. 31. Seasonal occurrences of historical and recent Himalayan earthquakes. (a) The declustered time history of Himalayan earthquakes 1904–2018 from the ComCat USGS catalog, and is plotted east (https://earthquake.usgs.gov/data/comcat/). Earthquakes east of 78°E are shaded red, and earthquakes to the west are shaded green. (b) map view with same shading. Blue stars depict the approximate locations of historical earthquakes (Table 1). (b) map view indicating locations of Himalayan earthquakes coloured in (a) and (c). (c) Monthly counts of significant pre-1900 earthquakes and post 1900 $M_w \geq 5.5$ earthquakes. Due to the westwards progression of the monsoon, earthquakes in the Western Himalaya should respond later than the Eastern Himalaya; however, this effect and the direct influence of the monsoon on the timing of $M_w \geq 5.5$ earthquakes appears to be insignificant contrary to claims by Panda *et al.* (2018). In each panel in (c), bars indicate cumulative earthquakes per month; east (red) and west (green), and the sum of these two – total counts (blue historical; black 1904–2018).

significant earthquakes show a strong correlation with the monsoon. Thus, while microseismicity is apparently influenced by stress loading during the monsoon, the timing of moderate and major earthquakes is weakly influenced, if at all.

Fatalities from future Himalayan earthquakes

For early earthquakes we have scant information on human losses, but starting in the nineteenth century records become reasonably reliable. The cumulative fatality count since 1800 is approximately 138 000, half of which can be attributed to the 2005 Kashmir earthquake (Fig. 32). The number of fatalities depends not only on the magnitude of the earthquake, and its proximity to human settlements, but on the time of day of the earthquake and the type of construction in the epicentral region. With few exceptions (e.g. Kashmir 1555 midnight, 1803 at 2 am, 1885 at 3–5 am and Kangra 1905 at 6 am), most major Himalayan earthquakes have occurred in daylight hours, when most people are not in their homes. As a result, the death toll from Himalayan earthquakes is almost certainly lower than it would have been had these same earthquakes occurred at night.

The type of construction in the Himalaya has changed considerably in the past 200 years. For example, structures in Assam used to be dominantly made from woven reeds and thatch, and even now some villagers continue to live in reed dwellings. Such structures are rarely damaged by shaking. New construction in Assam favours concrete-frame structures. In parts of the Kangra region and in Kashmir, and other parts of the Himalaya, buildings made of stone were frequently assembled with wooden beams that held structures together during shaking (Rautela & Joshi 2008). Examples of such structures are shown in Figure 33. A scarcity of timber and the need to house population densities in villages and cities that are now 10 times higher than a century ago means that many dwellings in the Kangra region are now based on a concrete skeleton type of construction. Concrete-frame structures can be assembled with earthquake resistance but often the materials needed to ensure structural integrity are omitted or diluted for economic reasons. As a result, we are likely to see many more future fatalities from Himalayan earthquakes (Bilham & Gaur 2013; Bilham 2014).

A number of estimates of future fatalities from Himalayan earthquakes have been published based on anticipated shaking intensity and the vulnerability of mezzo-central structures. Worst-case forecasts estimate that some future earthquakes could result in fatality counts exceeding 200 000 (Wyss 2005, 2017; Wyss *et al.* 2017).

Seismic gaps and the location of future earthquakes

In earlier sections of this chapter, and with variable detail, I have described significant damaging earthquakes that are known to have occurred in the past millennium. A cursory glance at Figure 30 is sufficient to realize that prior to 1800 the record of Himalayan earthquakes is remarkably sparse and that many $M_w \leq 7$ earthquakes must have occurred of which we have no knowledge. Prior to 1500, we may be missing $M_w \geq 8$ earthquakes. However, it is possible to construct maps of where no major earthquake has occurred for a significant time and, hence,

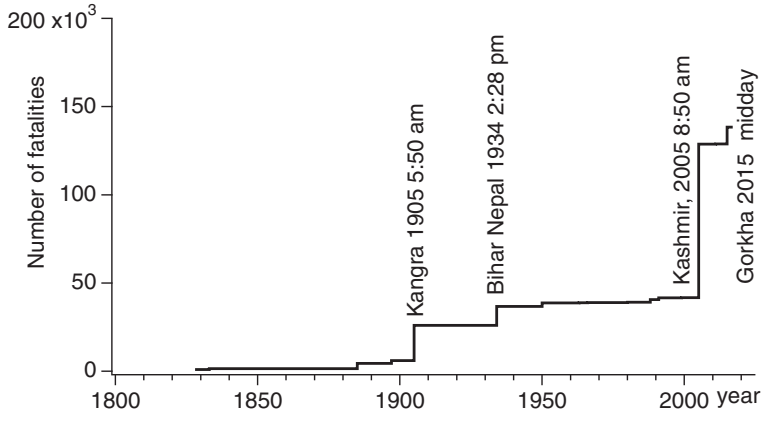

Fig. 32. Cumulative fatalities from Himalayan earthquakes 1800–2018. None of these recent earthquakes have occurred at night, although the Kangra earthquake occurred at 6 am. It is likely that should a nocturnal earthquake occur, especially close to a large population such as Dehra Dun or Kashmir or Kathmandu, the death toll may exceed 100 000. Wyss (2005, 2017) estimated maximum death tolls of twice this for some scenario earthquakes.

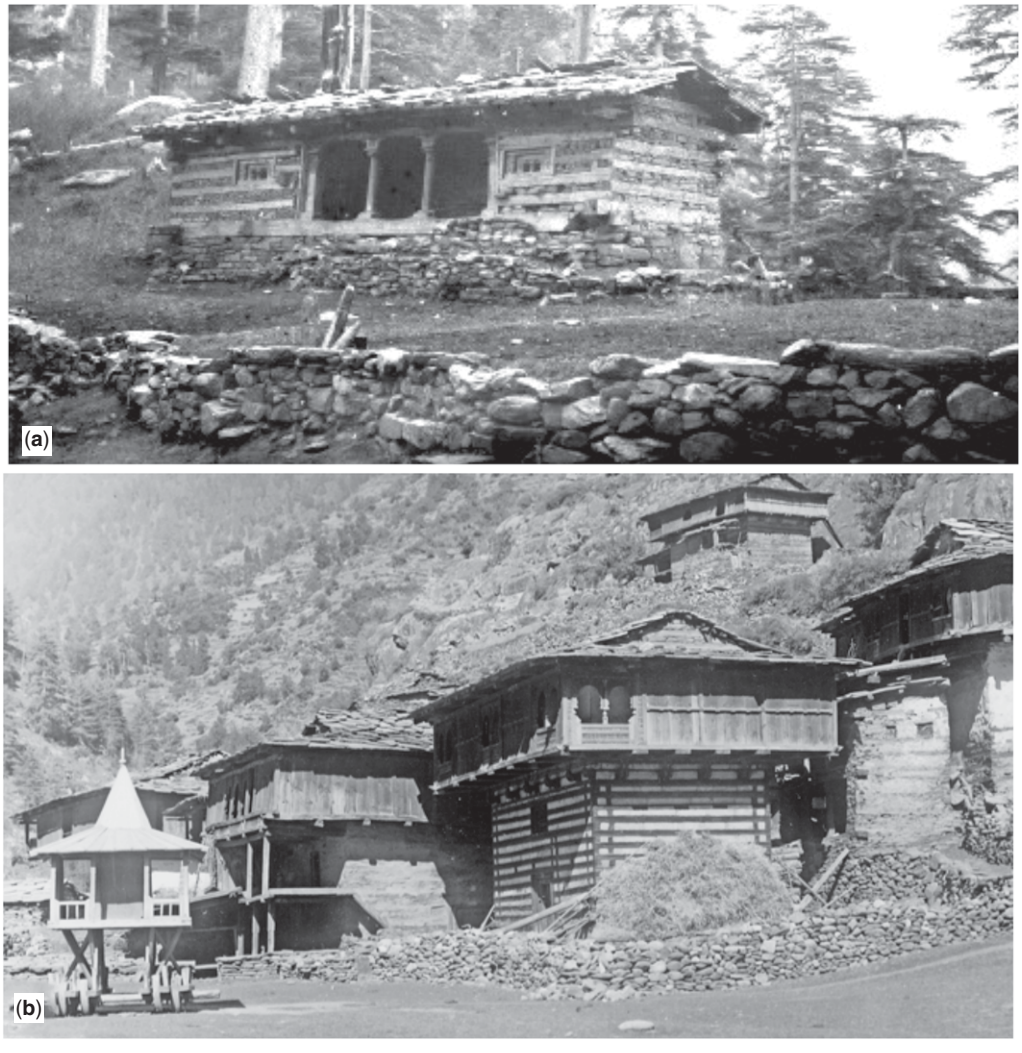

Fig. 33. (**a**) Temple at Saharn, Sutlej Valley with interleaved stone and timber (photographed by Carl Griesbach in 1883). (**b**) A *Koti Banal* dwelling in Manikarn, Kulu that survived the 1905 $M_w = 7.8$ Kangra and earlier earthquakes (photographed by Charles Middlemiss in 1905). Some Koti dwellings succumbed to a 1906 M_w 6.5 aftershock (Szeliga & Bilham 2017). Rautela & Joshi (2008) speculated that this style of architecture was introduced more than 800 years ago as a response to a widespread damaging Himalayan earthquake, and that some of the original structures still remain.

where a future earthquake may be anticipated. Khattri (1987) designated a region between the 1905 Kangra earthquake and the 1934 Bihar Nepal earthquake 'the central Himalayan gap', and pointed out that two great earthquakes could, in principle, occur within it. Its location roughly corresponds to the 1 June 1505 earthquake, knowledge of which was not to become widely known for another quarter of a century (Ambraseys & Jackson 2003; Bilham & Ambraseys 2005). The slip potential along parts of the central gap was evaluated with reasonable certainty from 1800 onwards using early geodetic convergence rates (Bilham *et al.* 2001), and in 2005 this simple estimate of slip potential was refined to include aspects of historical rupture dimensions and to extend the slip potential estimates to 1500 (Bilham & Wallace 2005; Kumar *et al.* 2006). At this time, the possibility of infrequent great Himalayan ruptures attaining $M_w \approx 9.0$ was aired, a notion which resulted in much initial resistance, although it is now considered a necessary component of multi-millennial Himalayan slip (Stevens & Avouac 2016).

The slip-potential method can now be refined further to include a spatially variable convergence rate, improved bounds to historical rupture zones and palaeoseismic information (Fig. 34). Such refinements still offer no estimate of seismic imminence. One promising approach that may permit insight into the location of the next great earthquake may be to focus on the recurrence of $M > 7$ earthquakes that may nucleate future $M_w > 8$ earthquakes. This follows from reasoning that argues that the locking line is inadequate alone to drive M_w 8 earthquakes with less than 10 m of slip, and that such large slip is partly derived from latent strain energy abandoned by former $M_w \approx 7$ earthquakes. Since we do not possess a long history of incomplete $M_w \approx 7$ ruptures, the spatial distribution of latent strain energy is currently unknown. However, the recurrence interval of $M_w \approx 7$ earthquakes, which is of the order of 100 years, may hold clues about the eventual nucleation of such large earthquakes.

A summary of slip in the past five centuries of earthquakes is shown in Figure 34. Seismicity gaps, regions where no earthquake has ruptured the Main Himalayan Thrust in the past 500 years, could be due to incomplete historical reporting or imperfect interpretation of such historical data as are available to us. The Himalaya is divided into 15 segments based on historical ruptures. Segments could fail singly or in multiples, as discussed for Kashmir (Schiffman *et al.* 2013) and for Bhutan (Drukpa *et al.* 2012; Vernant *et al.* 2014). They are briefly discussed from west to east.

The Kashmir segment (Fig. 34) will fail either as a steep reverse fault as part of the Riasi system (Mugnier *et al.* 2013) in a $7.6 < M_w < 7.8$ rupture, or as a deep décollement earthquake with significantly larger magnitude ($M_w \leq 8.2$: Schiffman *et al.* 2013). Should it rupture together with the Kishtwar segment, for which we have no precedence, it will rupture as a $M_w > 8.6$ earthquake; however, should the Kishtwar segment rupture alone, the slip potential is sufficient to drive a $M_w = 8.4$ earthquake.

The Kangra earthquake ruptured in 1905 but it failed to breach the Main Frontal Thrust. Should a replica of the 1905 earthquake occur today with similar rupture area, the current magnitude would again be $M_w = 7.8$, the same as in 1905. However, this represents a minimum magnitude because latent strain now resides near the frontal thrusts that if

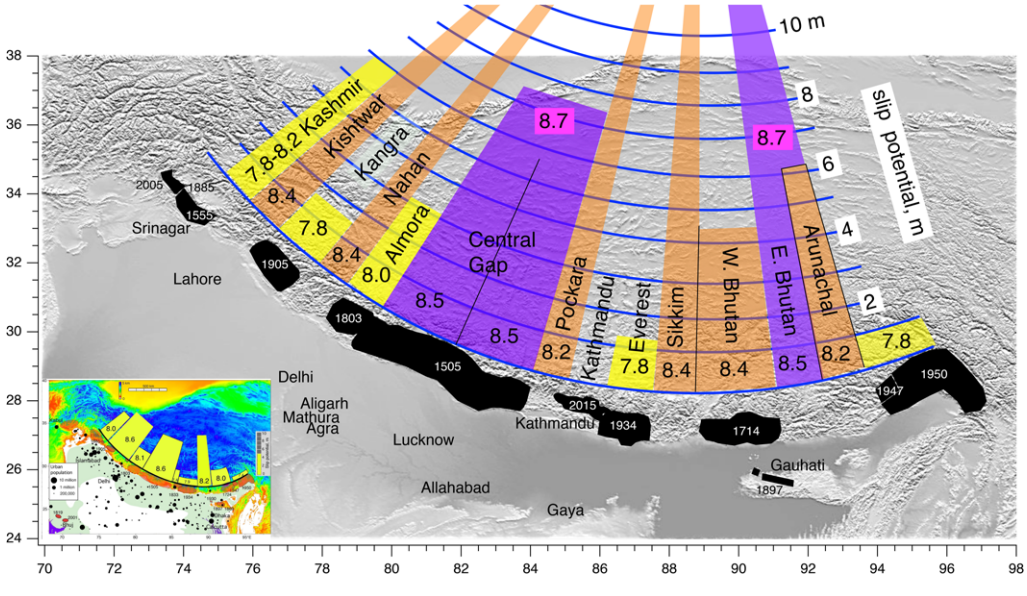

Fig. 34. Five centuries of Himalayan rupture zones (black) and current slip potential (metre scale (right)) since the last rupture in named segments. The colours indicate the maximum magnitude of an earthquake that could occur in the present time should a segment fail in a single event or as partial slip. Two areas with violet shading could host $M_w > 8.7$ earthquakes. Six areas with brown shading could rupture in M_w 8.4 earthquakes. Five areas, shaded yellow, could presently slip in $M_w \geq 7.7$ earthquakes similar to the recent Gorkha earthquake. The Kathmandu region could experience a M_w 7.3 earthquake to its south, but I argue in the text that this is unlikely. The inset shows an earlier version of this plot made before the 2005 and 2015 earthquakes (Bilham & Wallace 2005). The 2005 earthquake occurred to the west of a $M_w = 8.0$ forecast region, and the 2015 earthquake occurred at the junction between $M_w = 7.4$ and $M_w = 7.9$ forecast areas north of Kathmandu. A recurrence of the 1833 earthquake was not anticipated.

cannibalized by a future earthquake would result in a larger earthquake.

The Nahan segment has hosted no earthquake since medieval times Rajendran *et al.* (2018*b*) and could rupture as a unique $M_w \leq 8.4$ earthquake. Should it rupture with the Kangra or Almora segments, the resulting earthquake could exceed $M_w \leq 8.5$. The Almora segment has developed a slip potential of at least 3 m since the 1803 earthquake and could now rupture in a $M_w \leq 8.3$ earthquake.

The central gap of Khattri (1987), should it slip in a single event, will do so now as a $M_w \leq 8.7$ earthquake. It is possible that it will slip in two or more events of appropriately reduced magnitudes.

The Pockara segment lies between the end of the 1505 rupture and the Kathmandu segment that slipped in 2015; however, it is possible that the 1505 rupture slipped in this region. Bollinger *et al.* (2016) proposed that it last slipped in 1344, which implies a *c.* 10 m slip potential and the capability to host a $8 < M_w < 8.2$ earthquake. The Kathmandu region is believed to have little slip potential for a future earthquake since it slipped only 3 years ago; however, the region to its south could accompany rupture of the Pockara segment.

The 1934 rupture is named the Everest segment, and should it slip now could do so in a $M_w = 7.8$ earthquake. Neighbouring Sikkim has not slipped since medieval times and now hosts a ≥10 m slip deficit, approaching that reported in a nearby trench site by Wesnousky *et al.* (2018). The Sikkim segment has not experienced a major earthquake in the past five centuries and therefore hosts a current slip potential equivalent to a $M_w = 8.4$. Should it rupture with contiguous segments, its magnitude would correspondingly increase.

The Bhutan rupture zone of 1714 now hosts a 4.5–5 m slip potential, sufficient to drive a $M_w = 8.4$ earthquake. The East Bhutan region has had no known earthquake since medieval times. Various alternative scenario earthquakes for Bhutan are discussed by Drukpa *et al.* (2012).

The Arunachal region may have had a great earthquake in the seventeenth century. The magnitude of the sixteenth and seventeenth century Assam earthquakes cannot be assessed from currently available historical data. It is the least well constrained of all the segments considered, since the written record here and the density of palaeoseismic trench constraints are also weak. A maximum magnitude of $M_w \leq 8.7$ is provisionally assigned to this segment, although it may rupture in smaller segments.

A version of this earthquake forecast summary was published in 2005 (inset figure lower left in Fig. 34), which provides a measure of the utility of the above interpretations. In 2005, a M_w 7.4–7.9 earthquake was anticipated in the location where the M_w 7.8 Gorkha earthquake occurred in 2015. In contrast, the $M_w = 7.6$ Kashmir earthquake of 2005 occurred to the west of the region designated as sufficiently mature to host a $M_w = 8.2$ earthquake. As with all the potential earthquakes depicted in Figure 34, the timing of neither of these earthquakes was anticipated, merely their location and magnitude.

Palaeoseismic information can be used to supplement and extend Figure 34, which currently shows only the cumulative knowledge of five centuries of earthquakes, during which India has moved roughly 10 m northwards and only one major earthquake is known to have repeated: the Nepal 1833/2015 sequence. The 1803 Almora segment may soon repeat. A 1000 year view of Figure 34 will surely include more repeating ruptures, and more definitive information on the local slip deficit.

Conclusions

This article has examined the history of earthquakes in the Himalaya, focusing largely on the past five centuries but including a slowly emerging palaeoseismic record from earlier centuries. Such a study would have been impossible two decades ago, when the historical record was less complete, the geodetic convergence rate poorly constrained and the palaeoseismic record non-existent. Given the enormous advances in these fields in these two decades, it is not difficult to imagine that the next two decades we will see a number of issues resolved that are currently under discussion. In particular, it is probable that a history of great earthquakes along the Himalayan arc will be developed leading back several thousands of years.

For some historical earthquakes it has been possible to estimate rupture propagation directions, and from these to conclude that contiguous ruptures do not appear to influence future nucleation locations of succeeding earthquakes. This conclusion is weak because we do not have a complete record of historical earthquakes preceding those pairs where this conclusion may be deduced (e.g. Fig. 12). In contrast, we find support for much of the Himalaya having ruptured between 1100 and 1600 as a propagating cluster of great earthquakes with a mean westwards propagation rate of 7.5 km a^{-1} (Fig. 28).

Theoretical considerations lead us to suppose that $M_w > 8.2$ earthquakes cannot nucleate and rupture the Main Frontal Thrust without utilizing elastic strain abandoned by former incomplete ruptures (Fig. 29). The corollary of this conclusion is that great earthquakes probably nucleate as $M_w = 7.5$ earthquakes and then cascade into larger ruptures along strike. The locations of future $M_w \geq 7$ ruptures thus may offer important clues about the future great earthquakes.

The ultimate aim in the study of Himalayan earthquakes is to learn where the next damaging earthquake is likely to occur, and with what magnitude. Distressingly, we are no closer to knowing where the next damaging earthquake will occur than two decades ago. Figure 34 indicates the minimum magnitude of potential future earthquakes (should they occur early in the 21st century) within the confines of fifteen delineated segments. Slip of partial segments will necessarily reduce the indicated magnitudes. Synchronous slip of contiguous rupture areas will necessarily increase their magnitudes. Currently two-thirds of the Himalaya is poised to rupture in one or more great earthquakes, although we have no information of the timing of these future earthquakes.

Perhaps the most alarming feature of those potential future earthquakes (Fig. 34) that are needed to close the gap between observed and synthetic moment release (Fig. 30) is that none are smaller than the recent Gorkha earthquake that claimed almost 10 000 lives. Fortunately, most of the major earthquakes in the past two centuries have occurred during daylight hours when populations are least vulnerable. The estimated death toll that may accompany a nocturnal earthquake in a heavily populated segment of the Himalaya, such as the Almora/Dehra Dun segment, is unprecedented (≥200 000: Wyss 2005). That same earthquake during daylight hours may result in fewer than 20 000 deaths.

Acknowledgements I owe a debt of thanks to many people for help in compiling this overview of Himalayan earthquakes, not the least being Steve Wesnousky and Keith Priestley whose critical reviews have much improved the content and its conclusions. Vinod Gaur is responsible for visits to the Kangra region and for stimulating my interest in Himalayan earthquakes. Sujit Dasgupta kindly helped identify Oldham's photograph of the transient lake near Jhira formed in the 1897 earthquake, and was instrumental in identifying other photographs in the archives of the Geological Survey of India. I thank Ismael Bhat and Bikram Bali for their assistance in research in Kashmir.

Funding This research reports on findings made possible by funding from the National Science Foundation Earth Science Division in the past three decades.

References

Ader, T., Avouac, J.-P. *et al.* 2012. Convergence rate across the Nepal Himalaya and interseismic coupling on the Main Himalayan Thrust: implications for seismic hazard. *Journal of Geophysical Research*, **117**, B04403, https://doi.org/10.1029/2011JB009071

Adhikari, L.B., Gautam, U.P. *et al.* 2015. The aftershock sequence of the 2015 April 25 Gorkha–Nepal earthquake. *Geophysical Journal International*, **203**, 2119–2124, https://doi.org/10.1093/gji/ggv412

Adhikari, S.R., Baysal, G., Dixit, A., Martin, S.S., Landes, M., Bossu, R. & Hough, S.E. 2017. Toward a unified near-field intensity map of the 2015 M_w 7.8 Gorkha, Nepal, earthquake. *Earthquake Spectra*, **33**, S21–S34.

Ahmad, B., Bhat, I.M. & Bali, B.S. 2009. Historical record of earthquakes in the Kashmir Valley. *Himalayan Geology*, **30**, 75–84.

Ahmad, B., Sana, H. & Alam, A. 2014. Macroseismic intensity assessment of 1885 Baramulla Earthquake of northwestern Kashmir Himalaya, using the Environmental Seismic Intensity scale (ESI 2007). *Quaternary International*, **321**, 59–64.

Alam, A., Ahmad, S., Bhat, M.S. & Ahmad, B. 2015. Tectonic evolution of Kashmir basin in northwest Himalayas. *Geomorphology*, **239**, 114–126.

Almeida, V., Hubbard, J., Liberty, L., Foster, A. & Sapkota, S.N. 2018. Seismic imaging of the Main Frontal Thrust in Nepal reveals a shallow décollement and blind thrusting. *Earth and Planetary Science Letters*, **494**, 216–225.

Ambraseys, N. 1971. Value of historical records of earthquakes. *Nature*, **232**, 375–379.

Ambraseys, N. & Bilham, R. 2000. A note on the Kangra Ms=7.8 earthquake of 4 April 1905. *Current Science*, **79**, 101–106.

Ambraseys, N. & Jackson, D. 2003. A note on early earthquakes in northern India and southern Tibet. *Current Science*, **84**, 570–582.

Ambraseys, N. & Bilham, R. 2003*a*. Earthquakes and crustal deformation in northern Baluchistan. *Bulletin of the Seismological Society of America*, **93**, 1573–1605.

Ambraseys, N. & Bilham, R. 2003*b*. Earthquakes in Afghanistan. *Seismological Research Letters*, **74**, 107–123.

Ambraseys, N.N. & Douglas, J. 2004. Magnitude calibration of north Indian earthquakes. *Geophysical Journal International*, **158**, 1e42, https://doi.org/10.1111/j.1365-246X.2004.02323.x

Archer, M. 1980. *Early Views of India – Picturesque Journeys of the Daniell Brothers: 1786-1794*. Thames and Hudson, London, p. 240.

Arora, S. & Malik, J.N. 2017. Overestimation of the earthquake hazard along the Himalaya: constraints in bracketing of medieval earthquakes from paleoseismic studies. *Geoscience Letters*, **4**, 19, https://doi.org/10.1186/s40562-017-0083-6

Auden, J.B. 1935. Traverses in the Himalaya. *Records of the Geological Survey of India*, **69**, 123–167.

Avouac, J.-P. 2003. Mountain building, erosion, and the seismic cycle in the Nepal Himalaya. *Advances in Geophysics*, **46**, 1–80.

Avouac, J.-P. 2015*a*. Mountain building: from earthquakes to geologic deformation *In*: Schubert, G. (ed.) *Treatise on Geophysics. Volume 6: Crustal and Lithosphere Dynamics*. 2nd edn. Elsevier, Oxford, 381–432.

Avouac, J.-P. 2015*b*. From geodetic imaging of seismic and aseismic slip to dynamic modeling of the seismic cycle. *Annual Review of Earth and Planetary Sciences*, **43**, 8.1–8.39.

Avouac, J.P., Ayoub, F., Leprince, S., Konca, O. & Helmberger, D.V. 2006. The 2005, M_w 7.6 Kashimir earthquake: Sub-pixel correlation of ASTER images and seismic waveforms analysis. *Earth and Planetary Science Letters*, **249**, 514–528.

Avouac, J.-P., Meng, L., Wei, S., Wang, T., Ampuero, J.P. 2015. Lower edge of locked Main Himalayan Thrust unzipped by the 2015 Gorkha earthquake. *Nature Geoscience*, **8**, 708–711.

Baduwi, M. 1905. *Earthquakes of India: In which the Events of the 4 April 1905 Earthquake in North India and all of India and other countries are described*. Army Press, Simla (in Urdu).

Banerjee, P., Bürgmann, R., Nagarajan, B. & Apel, E. 2008. Intraplate deformation of the Indian subcontinent. *Geophysical Research Letters*, **35**, L18301, https://doi.org/10.1029/2008GL035468

Bashir, A., Bhat, M.I. & Bali, B.S. 2009. Historical Record of Earthquakes in the Kashmir Valley. *Journal of Himalayan Geology*, **30**, 75–84.

Bashyal, R.P. 1998. Petroleum exploration in Nepal. *Journal of the Nepal Geological Society*, **18**, 19–24.

Bendick, R. & Bilham, R. 2001. How perfect is the Himalayan Arc? *Geology*, **29**, 791–794.

Ben-Menahem, A., Aboodi, E. & Schild, R. 1974. The source of the great Assam earthquake – An interplate wedge motion. *Physics of the Earth and Planetary Interiors*, **9**, 265–289.

Bettinelli, P., Avouac, J.-P., Flouzat, M., Bollinger, L., Ramillien, G., Rajaure, S. & Sapkota, S. 2008. Seasonal variations of seismicity and geodetic strain in the Himalaya induced by surface hydrology. *Earth and Planetary Science Letters*, **266**, 332–344.

Bilham, R. 1995. Location and magnitude of the 1833 Nepal earthquake and its relation to the rupture zones of contiguous great Himalayan earthquakes. *Current Science*, **69**, 101–128.

Bilham, R. 2001. Slow tilt reversal of the Lesser Himalaya between 1862 and 1992 at 78° E, and bounds to the southeast rupture of the 1905 Kangra earthquake. *Geophys. J. Int*, **144**, 713–728, https://doi.org/10.1046/j.1365-246x.2001.01365.x

Bilham, R. 2004. Earthquakes in India and the Himalaya: tectonics, geodesy and history. *Annals of Geophysics*, **47**, 839–858.

Bilham, R. 2006. Comment on 'Interpreting the style of faulting and paleoseismicity associated with the 1897 Shillong, northeast India, earthquake' by C. P. Rajendran *Tectonics*, **25**, TC2001, https://doi.org/10.1029/2005TC001893

Bilham, R. 2008. Tom LaTouche and the Great Assam Earthquake of 12 June 1897; letters from the epicenter. *Seism. Res. Lett.*, **79**, 426–437.

Bilham, R. 2014. Aggravated earthquake risk in South Asia: engineering v. human nature. *In*: Wyss, M. (ed.) *Earthquake Hazard, Risk and Disasters*. Elsevier, Amsterdam, 103–141.

Bilham, R. 2015. Raising Kathmandu. *Nature Geoscience* , **8**, 582–584.

Bilham, R. 2016. The Gorkha earthquake and the Tehri dam, Nepal Engineers Association. *Tech. Journal*, **43**, 39–48.

Bilham, R. & Ambraseys, N. 2005. Apparent Himalayan slip deficit from the summation of seismic moments for Himalayan earthquakes, 1500–2000. *Current Science*, **88**, 1658–1663.

Bilham, R. & Bali, B.S. 2013. A ninth century earthquake-induced landslide and flood in the Kashmir Valley, and earthquake damage to Kashmir's medieval temples. *Bulletin of Earthquake Engineering*, **12**, 79–109, https://doi.org/10.1007/s10518-013-9504-x

Bilham, R. & England, P. 2001. Plateau 'pop-up' in the great 1897 Assam earthquake. *Nature*, **410**, 806–809.

Bilham, R. & Gaur, V. 2013. Buildings as weapons of mass destruction: earthquake risk in South Asia. *Science*, **341**, 618–619.

Bilham, R. & Wallace, K. 2005. Future $M_w > 8$ earthquakes in the Himalaya: implications from the 26 Dec 2004 $M_w = 9.0$ earthquake on India's eastern plate margin. *Geological Survey of India, Special Publications*, **85**, 1–14.

Bilham, R. & Yu, T.T. 2000. The morphology of thrust faulting in the 21 September 1999, Chichi, Taiwan earthquake. *Journal of Asian Earth Sciences*, **18**, 351–367.

Bilham, R., Bodin, P. & Jackson, M. 1995. Entertaining a great earthquake in western Nepal: historic inactivity and geodetic tests for the development of strain. *Journal of the Nepal Geological Society*, **11**, 1–25.

Bilham, R., Larson, K. & Freymueller, J. 1997. GPS measurements of present-day convergence across the Nepal Himalaya. *Nature*, **386**, 61–63.

Bilham, R., Gaur, V.K. & Molnar, P. 2001. Himalayan seismic hazard. *Science*, **293**, 1442–1444.

Bilham, R., Singh, B., Bhat, I. & Hough, S. 2010. Historical earthquakes in Srinagar, Kashmir: Clues from the Shiva Temple at Pandrethan. *In*: Sintubin, M., Stewart, I.S., Niemi, T.M. & Altunel, E. (eds) *Ancient Earthquakes*. Geological Society of America, Special Papers, **471**, 110–117.

Bilham, R., Bali, B.S., Ahmad, S. & Schiffman, C. 2013. Oldham's lost fault. *Seismological Reearch Letters*, **84**, 1–8, https://doi.org/10.1785/0220130036

Bilham, R., Mencin, D., Bendick, R. & Bürgmann, R. 2017. Implications for elastic energy storage in the Himalaya from the Gorkha 2015 earthquake and other incomplete ruptures of the Main Himalayan Thrust. *Quaternary International*, **462**, 3–21, https://doi.org/10.1016/j.quaint.2016.09.055

Blakiston, J.F. 1922. *Kahrauli Zail: List of Muhammadan and Hindi Monuments, Volume 3*. Delhi Province, Government Printing Office, Calcutta, India.

Blunt, J.T. 1794. A description of the Cuttub Minar. *Asiatic Researches*, **4**, 305–311.

Bollinger, L., Perrier, F., Avouac, J.-P., Sapkota, S., Gautam, U. & Tiwari, D.R. 2007. Seasonal modulation of seismicity in the Himalaya of Nepal. *Geophysical Research Letters*, **34**, L08304, https://doi.org/10.1029/2006GL029192

Bollinger, L., Sapkota, S.N. *et al.* 2014. Estimating the return times of great Himalayan earthquakes in eastern Nepal: evidence from the Patu and Bardibas strands of 128 the Main Frontal Thrust. *Journal of Geophysical Research*, **119**, 7123–7163.

Bollinger, L., Tapponnier, P., Sapkota, S.N. & Klinger, Y. 2016. Slip deficit in central Nepal: omen for a repeat of the 1344 CE earthquake? *Earth, Planets and Space*, **68**, 1–12. https://doi.org/10.1186/s40623-016-0389-1

Bomford, G. 1937. Leveling in Bengal and Bihar, 93–97. *In*: Couchman, H.J. (ed.) *Survey of India Geodetic Report, 1936*. Geodetic Branch Survey of India, Dehra Dun, p. 97.

Boncio, P., Liberi, F., Caldarella, M. & Nurminen, F.-C. 2018. Width of surface rupture zone for thrust earthquakes: implications for earthquake fault zoning. *Natural Hazards and Earth Systems Sciences*, **18**, 241–256.

Brett, W.B. 1935. *A Report on the Bihar Earthquake and on the Measures Taken in Consequence Thereof up to the 31st December 1934*. Superintendent Governent Printing Bihar and Orissa, Patna.

Brune, J.N. 1968. Seismic moment, seismicity and rate of slip along major fault zones. *Journal of Geophysical Research*, **73**, 777–784.

Brune, J.N. & Thatcher, W. 2002. Strength and energetics of active fault zones. *International Handbook of Earthquake and Engineering Seismology, Part A*, **81**, 569–588.

Brune, J.N., Brown, S. & Johnson, P.A. 1993. Rupture mechanism and interface separation in foam rubber models of earthquakes: a possible solution to the heat flow paradox and the paradox of large overthrusts. *Tectonophysics*, **219**, 59–67.

Burgess, W.P., Yin, A., Dubey, C.S., Shen, Z-K. & Kelty, T.K. 2012. Holocene shortening across the Main Frontal Thrust zone in the eastern Himalaya. *Earth and Planetary Science Letters*, **357–358**, 152–167.

Burke, J. 1868. Temple of Meruvarddhanaswami at Pandrethan near Srinagar. British Library Shelfmark: Photo 981/1(40).

Burrard, S. 1934. Ground levels in Bihar in relation to the earthquake of January 15 1934. *Nature (London)*, 582–583.

Chander, R. 1988. Interpretation of observed ground level changes due to the Kangra earthquake, northwest Himalaya. *Tectonoophysics*, **149**, 289–298.

Chen, J., Crompton, T., Walton, J. & Bilham, R. 1984. The survey work of the International Karakorum Project, 1980. *In*: Miller, K.J. (ed.) *International Karakorum Project, Volume 2*. Cambridge University Press, Cambridge, 124–139.

Chen, W.-P. & Molnar, P. 1977. Seismic moments of major earthquakes and the average rate of slip in central Asia. *Journal of Geophysical Research*, **82**, 2945–2969.

Chen, W.P. & Molnar, P. 1983. Focal depths of intracontinental and intraplate earthquakes and their implications for the thermal and mechanical properties of the lithosphere. *Journal of Geophysical Research Solid Earth*, **88**, 4183–4214.

Choudhury, R.D. 1985. *Archaeology of the Brahmaputra Valley of Assam: Pre-Ahom period*. Agim-Kala Prakashanm, Delhi, India.

Ciurtin, E. 2009. The Buddha's earthquakes (1) on water: earthquakes and seaquakes in Buddhist cosmology and meditation, with an appendix on Buddhist art. *Studia Asiatica*, **9**, 59–127.

Clark, M. & Bilham, R. 2008. Miocene rise of the Shillong Plateau and the beginning of the end for the Eastern Himalaya. *Earth and Planetary Science Letters*, **269**, 337–351.

Collet, L. 1898. *Guide for Visitors to Kashmir*. Newman and Company, Calcutta, India.

Collins, B.D. & Jibson, R.W. 2015. *Assessment of Existing and Potential Landslide Hazards Resulting from the April 25, 2015 Gorkha. Nepal Earthquake Sequence (ver. 1.1, August 2015)*. United States Geological Survey, Open-File Report, **2015-1142**, https://doi.org/10.3133/ofr20151142

Coningham, R.A.E., Acharya, K.P. *et al.* 2013. The earliest Buddhist shrine: excavating the birthplace of the Buddha, Lumbini (Nepal). *Antiquity*, **87**, 1104–1123.

Coudurier-Curveur, A., Kali, E. *et al.* 2016. Surface rupture of the 1950 Assam earthquake: active faults and recurrence interval along the Eastern Himalayan Syntaxis. Abstract EPSC2016-15794 presented at the EGU General Assembly 2016, 17–22 April 2016, Vienna, Austria.

Coudurier-Curveur, A., Van der Woerd, J., Kali, E., Tapponier, P., Okal, E., Vaideswaran, S. & Baruah, S. 2018. Composite seismic source of the great 1950 Assam earthquake, Eastern Himalayan Syntaxis. *General Assembly Conference Abstracts*, **20**, 14173.

Cunningham, A. 1865. Report of the Proceedings of the Archaeological Surveyor to the Government of India for the Season 1862–63. *Journal of the Asiatic Society of Bengal*, **33**, lix.

Dasgupta, S. & Mukhopadhyay, B. 2014. 1803 Earthquake in Gharwal Himalaya – archival materials with commentary. *Indian Journal of History of Science*, **49.1**, 21–33.

Dasgupta, S. & Mukhopadhyay, B. 2015. Historiography and commentary from archives on the Kathmandu (Nepal)–India earthquake of 26 August 1833. *Indian Journal of History of Science (INSA)*, **50**, 491–513.

Dasgupta, S., Mukhopadhyay, B. & Nandy, D.R. 1987. Active transverse features of the central portion of the Himalaya. *Tectonophysics*, **136**, 255–264.

Davis, D.M. & Engelder, T. 1987. Thin-skinned deformation over salt. *In*: Lerche, I. & O'Brien, J.J. (eds) *Dynamical Geology of Salt and Related Structures*. Academic Press, Orlando, FL, 301–337.

De Bremaecker, J.Cl. 1987. Thrust sheet motion and earthquake mechanisms. *Earth and Planetary Science Letters*, **83**, 159–166.

De Graaff-Hunter, J. 1934. The Indian earthquake (1934). *Nature (London)*, 236–237.

Drukpa, D., Pelgay, P., Bhattacharya, A., Vernant, P., Szeliga, W., Bilham, R. 2012. GPS constraints on Indo-Asian convergence in the Bhutan Himalaya: Segmentation and potential for a $8.2 < M_w < 8.8$ earthquake. HKT meeting, Kathmandu, Nepal Dec 2012. *Journal of the Nepal Geological Society*, **45**, Special Issue, 43–44.

Duke, J. 1888. *Ince's Kashmir Handbook: a Guide for Visitors Re-Written and Much Enlarged*. Thacker, Spink & Co., Calcutta, India.

Dunn, J.A., Auden, J.B., Ghosh, A.M.N. & Wadia, D.N. 1939. *The Bihar–Nepal Earthquake of 1934*. Memoirs of the India Geological Survey, **73**.

Elliott, J.R., Jolivet, R., Gonzalez, P., Avouac, J.-P., Hollingsworth, J., Searle, M. & Stevens, V. 2016. Himalayan megathrust geometry and relation to topography revealed by the Gorkha earthquake. *Nature Geoscience*, **9**, 174–180, https://doi.org/10.1038/NGEO2623

England, P. & Bilham, R. 2015. The Shillong Plateau and the great 1897 Assam earth-quake. *Tectonics*, **34**, 1792–1812, https://doi.org/10.1002/2015TC003902

Esper, J., Cook, E.R. & Schweingruber, F.H. 2002. Low frequency signals in long tree-ring chronologies for reconstructing past temperature variability. *Science*, **295**, 5563.

Fan, W. & Shearer, P.M. 2015. Detailed rupture imaging of the 25 April 2015 Nepal earthquake using teleseismic P waves. *Geophysical Research Letters*, **42**, 5744–5752.

Feldl, N. & Bilham, R. 2006. Great Himalayan earthquakes and the Tibetan Plateau. *Nature*, **444**, 165–170, https://doi.org/10.1038/nature05199

Fraser, J.B. 1820. *Journal of a Tour Through Part of the Snowy Range of the Himálá Mountains*. Dowell, London.

Gait, E.A. 1906. *A History of Assam*. Thacker, Spink & Co., Calcutta, India.

Galetzka, J., Melgar, D. *et al.* 2015. Slip pulse and resonance of Kathmandu basin during the 2015 M_w 7.8 Gorkha earthquake, Nepal imaged with geodesy. *Science*, **349**, 1091–1095, https://doi.org/10.1126/science.aac6383

Gee, E.R. 1934. *The Dhubri Earthquake of the 3rd July 1930*. Memoirs of the India Geological Survey, **65**.

Ghazoui, Z., Bertrand, S., Vanneste, K., Yokoyama, Y., Nomade, J., Gajurel, A.P. & van der Beek, P.A. 2018. Large post-1505 AD earthquakes in western Nepal revealed by a new lake sediment record. *Nature Communications*, in press.

Ghulam Hassan, P. 1954. *Tarikh-i-Hassan, Volume 2*. Kashmir Series of Texts and Studies, **82**. Research and Publication Department, Jammu and Kashmir Government, Srinagar, India (in Urdu, originally published in 1896).

Grandin, G., Doin, M-P., Bollinger, L., Pinel-Puyssegur, B., Ducret, G., Jolivet, R. & Sapkota, S.N. 2012. Long-term growth of the Himalaya inferred from interseismic InSAR measurement. *Geology (Boulder)*, **40**, 1059–1062.

Grandin, R., Vallée, M., Satriano, C., Lacassin, R., Klinger, Y., Simoes, M. & Bollinger, L. 2015. Rupture process of the M_w = 7.9 2015 Gorkha earthquake (Nepal): insights into Himalayan megathrust segmentation. *Geophysical Research Letters*, **42**, 8373–8382, https://doi.org/10.1002/2015GL066044

Grünthal, G. (ed.). 1998. *The European Macroseismic Scale EMS-98*. Conseil de l' Europe Cahiers du Centre Européen de Géodynamique et de Séismologie, **15**. Conseil de l' Europe, Luxembourg.

Gualandi, A., Avouac, J.-P. *et al.* 2017. Pre- and post-seismic deformation related to the 2015, M_w7:8 Gorkha earthquake, Nepal. *Tectonophysics*, **714–715**, 90–109, https://doi.org/10.1016/j.tecto.2016.06.014

Gupta, H.K. & Gahalaut, V.K. 2015. Can an earthquake of Mw ~9 occur in the Himalayan region? *In*: Mukherjee, S., Carosi, R., van der Beek, P.A., Mukherjee, B.K. & Robinson, D.M. (eds) *Tectonics of the Himalaya*. Geological Society, London, Special Publications, **412**, 43–53, https://doi.org/10.1144/SP412.10

Gutenberg, B. & Richter, C.F. 1954. *Seismicity of the Earth and Associated Phenomena*. Hafner, New York.

Hetényi, G., Le Roux-Mallouf, R., Berthet, T., Cattin, R., Cauzzi, C., Phuntsho, K. & Grolimund, R. 2016. Joint approach combining damage and paleoseismology observations constrains the 1714 AD Bhutan earthquake at magnitude 8 ± 0.5. *Geophysical Research Letters*, **43**, 10 695–10 702, https://doi.org/10.1002/2016GL071033

Hossler, T., Bollinger, L., Sapkota, S.N., Lavé, J., Gupta, R.M. & Kandel, T.P. 2016. Surface ruptures of large Himalayan earthquakes in Western Nepal: evidence along a reactivated strand of the Main Boundary Thrust. *Earth and Planetary Science Letters*, **434**, 187–196 https://doi.org/10.1016/j.epsl.2015.11.042

Hough, S.E. & Bilham, R. 2008. Site response of the Ganges basin inferred from re-evaluated macroseismic observations from the 1897 Shillong, 1905 Kangra & 1934 Nepal earthquakes. *Journal of Earth System Science*, **117**, 773–782.

Hough, S.E., Bilham, R., Ambraseys, N. & Feldl, N. 2005*a*. The 1905 Kangra and Dehra Dun earthquakes. *In*: *Contributions to Kangra Earthquake Centenary Seminar 2005*. Geological Survey of India, Special Publications, **85**, 15–22.

Hough, S.E., Bilham, R., Ambraseys, N. & Feldl, N. 2005*b*. Revisiting the 1897 Shillong and 1905 Kangra earthquakes in northern India: site Response, Moho reflections and a Triggered Earthquake. *Current Science*, **88**, 1632–1638.

Hubbard, J., Almeida, R., Foster, A., Sapkota, S.N., Bürgi, P. & Tapponnier, P. 2016. Structural segmentation controlled the 2015 M_w 7.8 Gorkha earthquake rupture in Nepal. *Geology*, **44**, 639–642. https://doi.org/10.1130/G38077.1

Hunt, J. 1953. *The Ascent of Everest Mountaineers' Books*. ISBN 0-89886-361-9.

Iyengar, R.N. 2000. Seismic status of Delhi megacity. *Current Science*, **78**, 568–574.

Iyengar, R.N. & Sharma, D. 1996. Some earthquakes of Kashmir from historical sources. *Current Science*, **71**, 300–331.

Iyengar, R.N. & Sharma, D. 1998. *Earthquake History of India in Medieval Times*. Central Building Research Institute, Roorkee, India.

Iyengar, R.N., Sharma, D. & Siddiqui, J.M. 1999. Earthquake history of India in medieval times. *Indian Journal of the History of Science*, **34**, 181–237.

Jackson, D. 2000. The great Himalayan earthquake of 1505: Rupture of the Central Himalayan Gap? *In*: Blezer, H. (ed.) *Tibet, Past and Present: Tibetan Studies 1. PIATS 2000: Tibetan Studies : Proceedings of the Ninth Seminar of the International Association for Tibetan Studies, Leiden 2000*. Brill, Boston, MA, 147–153.

Jackson, M. & Bilham, R. 1994. Constraints on Himalayan Deformation inferred from Vertical Velocity Fields in Nepal and Tibet. *Journal of Geophysical Research*, **99**, 13897–13912.

Jade, S., Shrungeshwara, T.S., Kumar, K., Choudhury, P., Dumka, R.K. & Bhu, H. 2017. India plate angular velocity and contemporary deformation rates from continuous GPS measurements from 1996 to 2015. *Nature Scientific Reports*, **7**, 11439, https://doi.org/10.1038/s41598-017-11697-w

Jagoutz, O., Royden, L., Holt, A.F. & Becker, T.W. 2015. Anomalously fast convergence of India and Eurasia caused by double subduction. *Nature Geoscience*, **8**, 475–478, https://doi.org/10.1038/ngeo2418

Jayangondaperumal, R., Wesnousky, S.G. & Choudhuri, B.K. 2011. Near-surface expression of early to late Holocene displacement along the northeastern Himalayan Frontal Thrust at Marbang Korong creek, Arunachal Pradesh, India. *Bulletin of the Seismological Society of America*, **101**, 3060–3064, https://doi.org/10.1785/0120110051

Jayangondaperumal, R., Mugnier, J.-L. & Dubey, A.K. 2013. Earthquake slip estimation from the scarp geometry of Himalayan Frontal Thrust, western Himalaya: implications for seismic hazard assessment. *International Journal of Earth Sciences*, **102**, 1937–1955, https://doi.org/10.1007/s00531-013-0888-2

Johnson, J.M., Tanioka, Y., Ruff, L.J., Satake, K., Kanimori, H. & Sykes, L.R. 1994. The 1957 Great Aleution earthquake. *Pure and Applied Geophysics*. **142**, 3–28.

Jones, E.J. 1885*a*. Notes on the Kashmir earthquake of 30th May 1885. *Records of the Geological Survey of India*., **18**, 153–156.

Jones, E.J. 1885*b*. Report on the Kashmir earthquake of 30 May 1885. *Records of the Geological Survey of India*, **18**, 221–227.

Jones, L.E. & Molnar, P. 1976. Frequency of foreshocks. *Nature*, **262**, 677–679.

Kanamori, H. & Brodsky, E. 2004. The physics of earthquakes. *Reports on Progress in Physics*, **67**, 1429–1496. ISSN 0034-4885.

Kargel, J.S., Leonard, G.J. *et al.* 2015. *Geomorphic and Geologic Controls of Geohazards Induced by Nepal's 2015 Gorkha Earthquake*. Interdisciplinary Arts and Sciences Publications, Paper 342, https://digitalcommons.tacoma.uw.edu/ias_pub/342

Kayastha, N.B., Shakya, T.R., Bruneton, A. & Gonnard, R. 1998. Western Nepal Paleogene wedge may signal attractive play. *Oil and Gas Journal*, **96**, 1–5.

Khattri, K.N. 1987. Great earthquakes, seismicity gaps and potential for earthquake disaster along the Himalaya plate boundary. *Tectonophysics*, **138**, 79–92.

Kingdom-Ward, J. 1952. *My Hill So Strong*. Jonathan Cape, London.

Kingdom-Ward, F. 1953. The Assam Earthquake of 1950. *Geographical Journal*, **119**, 169–182.

Kingdom-Ward, F. 1955. The aftermath of the Assam Earthquake of 1950. *Geographical Journal*, **121**, 290–303.

Kreemer, C., Blewitt, G. & Klein, E.C. 2014. A geodetic plate motion and Global Strain Rate Model. *Geochemistry Geophysics Geosystems*, **15**, 3849–3889, https://doi.org/10.1002/2014GC005407

Kumahara, Y. & Jayangondaperumal, Y. 2013. Paleoseismic evidence of a surface rupture along the northwestern Himalayan Frontal Thrust (HFT). *Geomorphology*, **180–181**, 45–56. https://doi.org/10.1016/j.geomorph.2012.09.004

Kumar, S., Wesnousky, W.G., Rockwell, T.K., Ragona, D., Thakur, V.C. & Seitz, G.G. 2001. Earthquake recurrence and rupture dynamics of Himalayan Frontal Thrust, India. *Science*, **294**, 2328–2331.

Kumar, S., Wesnousky, S.G., Rockwell, T.K., Briggs, R.W., Thakur, V.C. & Jayangondaperumal, R. 2006. Paleoseismic evidence of great surface rupture earthquakes along the Indian Himalaya. *Journal of Geophysical Research: Solid Earth*, **111**, B03304.

Kumar, S., Wesnousky, S.G., Jayangondaperumal, R., Nakata, T., Kumahara, Y. & Singh, V. 2010. Paleoseismological evidence of surface faulting along the northeastern Himalayan front, India: timing, size, and spatial extent of great earthquakes. *Journal of Geophysical Research*, **115**, B12422, https://doi.org/10.1029/2009JB006789

Kumar, A., Singh, S.K., Mitra, S., Priestley, K.F. & Dayal, S. 2017. The 2015 April 25 Gorkha (Nepal) earthquake and its aftershocks: implications for lateral heterogeneity on the Main Himalayan Thrust, *Geophysical Journal International*, **208**, 992–1008, https://doi.org/10.1093/gji/ggw438

Kundu, B., Yadav, R.K., Bali, B.S., Chowdhury, S. & Gahalaut, V.K. 2014. Oblique convergence and slip partitioning in the NW Himalaya: Implications from GPS measurements. *Tectonics*, **33**, 2013–2024, https://doi.org/10.1002/2014TC003633

Lal, K.S. 1980. *Twilight of the Sultanate*. Munshiram Manoharlal, Delhi, India.

Lave, J., Yule, D., Sapkota, S.N., Basant, K., Madden, C., Attal, M. & Pandey, R. 2005. Evidence for a great medieval earthquake (*c.* 1100 A.D.) in the central Himalayas, Nepal. *Science*, **141**, 1302–1305.

Lawrence, W.R. 1895. *The Valley of Kashmir*. Henry Froude, London, p. 478.

Lay, T., Ye, L., Koper, K.D. & Kanamori, H. 2017. Assessment of teleseismically-determined source parameters for the April 25, 2015 M_W 7.9 Gorkha, Nepal earthquake and the May 12, 2015 M_W 7.2 aftershock. *Tectonophysics*, **714–715**, 4–20.

LaTouche, T.H.D. 1899. *Shillong Earthquake. Seismograph Diagrams of Earthshocks and Tremors ar Shillong, Assam Since the Great Earthquake of 12th June 1897*. British Library Visual Arts, Photo 190/1 Creation Date 1897–1899.

Le Roux-Mallouf, R., Ferry, M., Ritz, J.-F., Berthet, T., Cattin, R. & Drukpa, D. 2016. First paleoseismic evidence for great surface-rupturing earthquakes in the Bhutan Himalayas. *Journal of Geophysical Research: Solid Earth*, **121**, 7271–7283, https://doi.org/10.1002/2015JB012733

Lindsey, E.O., Natsuaki, R., Xu, X., Shimada, M., Hashimoto, M., Melgar, D. & Sandwell, D.T. 2015. Line-of-sight displacement from ALOS-2 interferometry: M_w 7.8 Gorkha Earthquake and M_w 7.3 aftershock. *Geophysical Research Letters*, **42**, 6655–6661, https://doi.org/10.1002/2015GL065385

Madden, C., Trench, D., Meigs, A., Ahmad, S., Bhat, M.I. & Yule, J.D. 2010. Late Quaternary shortening and earthquake chronology of an active fault in the Kashmir basin, northwest Himalaya. *Seismology Research Letters*, **81**, 346.

Malik, J.N. & Nakata, T. 2003. Active faults and related Late Quaternary deformation along the northwestern Himalayan Frontal Zone, India. *Annals of Geophysics*, **46**, 917–936.

Malik, J.N., Nakata, T., Philip, G. & Virdi, N.S. 2003. Preliminary observations from a trench near Chandigarh, NW. Himalaya and their bearing on active faulting. *Current Science*, **85**, 25.

Malik, J.N., Nakata, T., Philip, G., Suresh, N. & Virdi, N.S. 2008. Active fault and paleoseismic investigation: evidence of historic earthquake along Chandigarh Fault in the frontal Himalayan zone, NW India. *Journal of Himalayan Geology*, **29**, 109–117.

Malik, J.N., Sahoo, A.K., Shah, A.A., Shinde, D.P., Juyal, N. & Singhvi, A.K. 2010*a*. Paleoseismic evidence from trench investigation along Hajipur fault, Himalayan Frontal Thrust, NW Himalaya: implications of the faulting pattern on landscape evolution and seismic hazard. *Journal of Structural Geology*, **32**, 350–361.

Malik, J.N., Shah, A.A. *et al.* 2010*b*. Active fault, fault growth and segment linkage along the Janauri anticline (frontal foreland fold), NW Himalaya, India. *Tectonophysics*, **483**, 327–343.

Malik, J.N., Sahoo, S., Satuluri, S. & Okumura, K. 2015. Active fault and paleoseismic studies in Kangra valley: evidence of surface rupture of a great Himalayan 1905 Kangra earthquake (M_w 7.8), northwest Himalaya, India. *Bulletin of the Seismological Society of America*, **105**, 2325–2342.

Malik, J.N., Naik, S.P., Sahoo, S., Okumura, K. & Mohanty, A. 2017. Paleoseismic evidence of the CE 1505 (?) and CE 1803 earthquakes from the foothill zone of the Kumaon Himalaya along the Himalayan Frontal Thrust (HFT), India. *Tectonophysics*, **714–715**, 133–145.

Marr, J.E. 1900. *The Scientific Study of Scenery*. Methuen & Co., London.

Martin, S. & Szeliga, W. 2010. A catalog of felt intensity data for 589 earthquakes in India, 1636–2009. *Bulletin of the Seismological Society of America*, **100**, 536–569.

Martin, S.S., Hough, S.E. & Hung, C. 2015. Ground motions from the 2015 M_w 7.8 Gorkha, Nepal, earthquake constrained by a detailed assessment of macroseismic data. *Seismological Research Letters*, **86**, 1524–1532, https://doi.org/10.1785/0220150138

Mason, K. 1914. *Completion of the Link Connecting the Triangulations of India and Russia 1913*. Records of the Survey of India, **6**. Survey of India, Dehra Dun, India.

Mathur, L.P. 1953. Assam earthquake of 15th August 1950 – a short note on factual observations. *In*: Ramachandra Rao, M.B. (ed.) *A Compilation of Papers on the Assam Earthquake of August 15, 1950*. Central Board of Geophysics Publication, **1**. National Geographical Research Institute, Hyderabad, India, 56–60.

McNamara, D.E., Yeck, W.L. *et al.* 2017. Source modeling of the 2015 M_w 7.8 Nepal (Gorkha) earthquake sequence: implications for geodynamics and earthquake hazards. *Tectonophysics*, **714–715**, 21–30.

Mencin, D., Bendick, R. *et al.* 2016. Himalayan strain reservoir inferred from limited afterslip following the Gorkha earthquake. *Nature Geoscience*, **9**, 533–537. https://doi.org/10.1038/ngeo2734

Middlemiss, C.S. 1905. Preliminary account of the Kangra earthquake of 4th April 1905. *Records of the Geological Survey of India*, **32**, 258–294.

Middlemiss, C.S. 1910. The Kangra earthquake of 4th April 1905. *Memoirs of the Geological Survey of India*, **38**, 409.

Milne, J. 1886. *Earthquakes and other Earth Movements*. Kegan Paul Trench & cco, London, p. 416.

Mishra, R.L., Singh, A., Pandey, A.K., Rao, P.S., Sahoo, H.K. & Jayangondaperumal, R. 2016. Paleoseismic evidence of a giant medieval earthquake in the eastern Himalaya. *Geophysical Research Letters*, **43**, 5707–5715, https://doi.org/10.1002/2016GL068739

Mohadjer, S., Ehlers, T.A., Bendick, R. & Mutz, S.G. 2017. Review of GPS and Quaternary fault slip rates in the Himalaya–Tibet orogen. *Earth-Science Reviews*, **174**, 39–52.

Molnar, P. & Chen, W.-P. 1983. Focal depths and fault plane solutions of earthquakes under the Tibetan Plateau. *J. Geophys. Res.*, **88**, 1180–1196, https://doi.org/10.1029/JB088iB02p01180

Molnar, P. & Deng, Q. 1984. Faulting associated with large earthquakes and the average rate of deformation in Central and Eastern Asia. *Journal of Geophysical Research*, **89**, 6203–6227.

Molnar, P. & Stock, J.M. 2009. Slowing of India's convergence with Eurasia since 20 Ma and its implications for Tibetan mantle dynamics. *Tectonics*, **28**, TC3001.

Montgomerie, T.G. 1858. *Map of Kashmir, with Part of Adjacent Mountains, Surveyed on the Basis of the Great Trigonometrical Survey of India, under the Instruction of Lieut.-Colonel A. S. Waugh, Engineers, Surveyor-General of India; by Capt. T. G. Montgomerie, Engineers, 1st Assistant G. T. Survey of India, and the Assistants under his Orders, during 1855, '56, and '57. Scale, 2 miles to 1 inch. With an Insertion Entitled, Kashmir Route Map; Scale, 32 miles to 1 inch; on 4 sheets; size, 50 inches by 50 inches*. J. & C. Walker for Surveyor General's Field Office, Dehra Dun, India.

Montgomerie, T.G. 1860. *Synoptical Volume VII*. Great Trigonometrical Survey of India, Dehra Dun, India.

Mugnier, J.-L., Delcaillau, B., Huyghe, P. & Leturmy, P. 1998. The break-back thrust splay of the Main Dun Thrust (Himalayas of western Nepal): evidence of an intermediate displacement scale between earthquake slip and finite geometry of thrust systems. *Journal of Structural Geology*, **20**, 857–864.

Mugnier, J.-L., Gajurel, A., Huyghe, P., Jayangondaperumal, R., Jouanne, F. & Upreti, B. 2013. Structural interpretation of the great earthquakes of the last millennium in the central Himalaya. *Earth-Science Reviews*, **127**, 30–47.

Mugnier, J.-L., Jouanne, F. *et al.* 2017. Segmentation of the Himalayan megathrust around the Gorkha earthquake (25 April) in Nepal *Journal of Asian Earth Sciences*, **141**, Part B, 236–252, https://doi.org/10.1016/j.jseaes.2017.01.015

Murphy, M.A., Taylor, M.H., Gosse, J., Silver, C.R.P., Whipp, D.M. & Beaumont, C. 2013. Limit of strain partitioning in the Himalaya marked by large earthquakes in western Nepal. *Nature Geoscience*, **7**, 38, https://doi.org/10.1038/ngeo2017

Neve, E.F. 1928. *A Crusader in Kashmir*. Seeley, Service & Co., London.

Oldham, R.D. 1899. *Report on the Great Earthquake of 12th June 1897*. Memoirs of the Geological Survey of India, **29**.

Oldham, R.D. 1900. *List of Aftershocks of the Great Earthquake of 12th June 1897*. Memoirs of the Geological Survey of India, **30**.

Oldham, R.D. 1906. The Constitution of the Earth, Quart. *Journal of the Geological Society London*, **62**, 456–475.

Oldham, R.D. 1921. Know your faults. *Journal of the Geological Society, London*, **77**, 7702.

Oldham, T. 1883. *The Cachar Earthquake of 10 January 1869* (edited by Oldham, R.D.). Memoirs of the Geological Survey of India, **19**.

Page, J.A. 1926. *An Historical Memoir on the Qutb: Delhi*. Memoirs of the Archaeological Survey of India, **22**.

Pande, B.M. 2006. *Qutb Minar and its monuments*. Oxford University Press, p. 95.

Pandey, M.R. & Molnar, P. 1988. The distribution of intensity of the Bihar–Nepal earthquake of 15 January 1934 and bounds on the extent of the rupture zone. *Journal of the Geological Society of Nepal*, **5**, 4.

Pant, M.R. 2002. A step toward a historical seismicity of Nepal. *Adarsa*, **2**, 29–60.

Panda, D., Kundu, B. *et al.* 2018. Seasonal modulation of deep slow-slip and earthquakes on the Main Himalayan Thrust. *Nature Communications*, https://doi.org/10.1038/s41467-018-0637

Panza, G.F., Peresan, A. & Zuccolo, E. 2010. Climatic modulation of seismicity in the Alpine–Himalayan mountain ranges. *Terra Nova*, **23**, 19–25.

Pathier, E., Fielding, E.J., Wright, T.J., Walker, R., Parsons, B.E. & Hensley, S. 2006. Displacement field and slip distribution of the 2005 Kashmir earthquake from SAR imagery. *Geophysical Research Letters*, **33**, L20310, https://doi.org/10.1029/2006 GL027193

Paul, J., Blume, F. *et al.* 1995. Microstrain stability of Peninsula India 1864–1994. *Proceedings of the Indian Academy of Sciences – Earth and Planetary Sciences*, **104**, 131–146.

Paul, J., Bürgmann, R. *et al.* 2001. The motion and active deformation of India. *Geophysical Research Letters*, **28**, 647–651.

Pierce, I. & Wesnousky, S.G. 2016. On a flawed conclusion that the 1255 A.D. earthquake ruptured 800 km of the Himalayan Frontal Thrust east of Kathmandu. *Geophysical Research Letters*, **43**, 9026–9029, https://doi.org/10.1002/2016GL070426

Playfair, A. 1909. *The Garos*. David Nutt, London (1975 reprint, Spectrum, Guwahati).

Poddar, M.C. 1950. The Assam earthquake of 15th August 1950. *Indian Minerals*, **4**, 167–176.

Prinsep, J. 1858. *Essays on Indian Antiquities, Historic, Numismatic, and Palæographic, of the Late James Prinsep: to which are added His useful tables, illustrative of Indian History, Chronology, Modern Coinages, Weights, Measures, etc, Volume 2*. John Murray, London.

Priyanka, R.S., Jayangondaperumal, R. *et al.* 2017. Primary surface rupture of the 1950 Tibet–Assam great earthquake along the eastern Himalayan front, India. *Scientific Reports*, **7**, 5433, https://doi.org/10.1038/s41598-017-05644-y

Rajendran, C.P. & Rajendran, K. 2005. The status of central seismic gap: a perspective based on the spatial and temporal aspects of the large Himalayan earthquakes. *Tectonophysics*, **395**, 19–39.

Rajendran, C.P., Rajendran, K., Duarah, B.P., Baruah, S. & Earnest, A. 2004. Interpreting the style of faulting and paleoseismicity associated with the 1897 Shillong, northeast India, earthquake: implications for regional tectonism. *Tectonics*, **23**, TC4009, https://doi.org/10.1029/2003TC001605

Rajendran, C.P., Rajendran, K., Sanwal, J. & Sandiford, M. 2013. Archeological and historical database on the medieval earthquakes of the central Himalaya: ambiguities and inferences. *Seismological Research Letters*, **84**, 1098–1108.

Rajendran, C.P., John, B. & Rajendran, K. 2015. Medieval pulse of great earthquakes in the central Himalaya: viewing past activities on the frontal thrust. *Journal of Geophysical Research: Solid Earth*, **120**, 1623–1641, https://doi.org/10.1002/2014JB011015

Rajendran, K., Parameswaran, R.M. & Rajendran, C.P. 2017. Seismotectonic perspectives on the Himalayan arc and contiguous areas: inferences from past and recent earthquakes. *Earth-Science Reviews*, **173**, 1–30, https://doi.org/10.1016/j.earscirev.2017.08.003

Rajendran, K., Parameswaran, R. & Rajendran, C.P. 2018*a*. Seismotectonics perspectives on the Himalayan arc and contiguous areas: inferences from past and present earthquakes. *Earth-Science Reviews*, **173**, 1–30, https://doi.org/10.1016/j.earscirev.2017.08.003

Rajendran, C.P., Sanwal, J. *et al.* 2018*b*. Footprints of an elusive mid-14th century earthquake in the central Himalaya: Consilience of evidence from Nepal and India. *Geological Journal*, 1–18. https://doi.org/10.1002/gj.3385

Ramos, L.F., Casarin, F., Algeri, C. & Lourenço, P.B. 2006. Investigation techniques carried out on the Qutb Minar, New Delhi, India, *In*: Lourenço, P.B., Roca, P., Modena, C. & Agrawal, S. (eds) *Proceedings of the 5th International Conference on Structural Analysis of Historical Constructions, New Delhi, 2006*. Macmillan, New Delhi, India, 633–640.

Rana, B.S. 1935. *Nepal Ko Maha Bhukampa (The Great Earthquake of Nepal)*. Jorganesh Press, Kathmandu (in nepali), 1–250.

Raper, F.V. 1810. Narratives of a survey for the purpose of discovering the resources of the Ganges. *Asiatic Research*, **11**, 446–563.

Rautela, P. & Joshi, G.C. 2008. Earthquake-safe Koti Banal architecture of Uttarakhand, India. *Current Science*, **95**, 475.

Rice, J.R. 2006. Heating and weakening of faults during earthquake slip. *Journal of Geophysical Research*, **111**, B05311, https://doi.org/10.1029/2005JB004006

Sapkota, S.N., Bollinger, L., Klinger, Y., Tapponnier, P., Gaudemer, Y. & Tiwari, D. 2013. Primary surface ruptures of the great Himalayan earthquakes in 1934 and 1255. *Nature Geoscience*, **6**, 71–76.

Sarkar, J. 1978. *The A'in-i Akbari by Abu'l-Fazl Allami, Translated from the Original Persian by Col. H. S. Jarrett, Corrected and Further Annotated by Jadunnath Sarkar*. 2nd ed. Oriental Books Reprint Corp., New Delhi, 1978.

Sarker, M.H. & Thorne, C.R. 2006. Morphological response of the Brahmaputra–Padma–Lower Meghna River system to the Assam earthquake of 1950. *In*: Smith, G.H.S., Best, J.L., Bristow, C.S. & Petts, G.E. (eds) *Braided Rivers: Process, Deposits, Ecology and Management*. International Association of Sedimentologists (IAS), Special Publications, **36**, 289–310.

Satyabala, S.P. & Bilham, R. 2006. Surface deformation and subsurface slip of the 28 March 1999 $M_w = 6.4$ west Himalayan Chamoli earthquake from InSAR analysis. *Geophysical Research Letters*, **33**, L23305, https://doi.org/10.1029/2006GL027422

Schiffman, C., Bali, B.S., Szeliga, W. & Bilham, R. 2013. Seismic slip deficit in the Kashmir Himalaya from GPS observations. *Geophysical Research Letters*, **40**, 5642–5645, doi: https://doi.org/10.1002/2013GL057700

Seeber, L. & Armbruster, J. 1981. Great detachment earthquakes along the Himalayan arc and long-term forecasts. *In*: Simpson, D. & Richards, M. (eds) *Earthquake Prediction: An International Review*. American Geophysical Union, Maurice Ewing Series, **4**, 259–277.

Sengupta, A. 2010. Estimation of permanent displacements of the Tehri Dam in the Himalayas due to future strong earthquakes. *Sadhana*, **35**, 373–392.

Shah, A.A. 2013. Earthquake geology of Kashmir Basin and its implications for future large earthquakes. *International Journal of Earth Sciences*, **102**, 1957–1966.

Shah, A.A. 2015. Kashmir Basin Fault and its tectonic significance in NW Himalaya, Jammu and Kashmir, India. *International Journal of Earth Sciences*, **104**, 1901–1906.

Shah, A.A. 2016. Pull-apart basin tectonic model is structurally impossible for Kashmir basin, NW Himalaya. *Solid Earth Discussions*, https://doi.org/10.5194/se-2016-4

Sibson, R.H. 1973. Interactions between temperature and pore-fluid pressure during earthquake faulting and a mechanism for partial or total stress relief. *Nature*, **243**, 66–68.

Singh, D.D. & Gupta, H.K. 1980. Source dynamics of two great earthquakes of the Indian subcontinent; the Bihar–Nepal earthquake of January 15, 1934 and the Quetta earthquake of May 30, 1935. *Bulletin of the Seismological Society of America*, **70**, 757–773.

Srivastava, H.N., Bansal, B.K. & Verma, M. 2013. Largest earthquake in Himalaya: an appraisal. *Journal of the Geological Society of India*, **82**, 15–22.

Stein, A. 1892. *Kalhana's Rajatarangini, or Chronicle of the Kings of Kashmir, Sanskrit Text with Critical Notes*. Education Society's Press, Bombay, p. 296.

Stein, A. 1898. *Kalhana's Rajatarangini: A Chronicle of the Kings of Kashmir*. Constable and Co, Calcutta, **2**, 555.

Stein, R.S., Barka, A.A. & Dieterich, J.H. 1997. Progressive failure on the North Anatolian Fault since 1939 by earthquake stress triggering. *Geophysical Journal International*, **128**, 594–604.

Stevens, V.L. & Avouac, J.-P. 2015. Interseismic coupling on the main Himalayan thrust. *Geophysical Research Letters*, **42**, 5828–5837, https://doi.org/10.1002/2015GL064845

Stevens, V.L. & Avouac, J.-P. 2016. Millenary M_w>9.0 earthquakes required by geodetic strain in the Himalaya. *Geophysical Research Letters*, **43**, 1118–1123, https://doi.org/10.1002/2015GL067336, 201

Stirling, M., Goded, T., Berryman, K. & Litchfield, N. 2013. Selection of Earthquake Scaling Relationships for Seismic-Hazard Analysis. *Bulletin of the Seismological Society of America*, **103**, 2993–3011, https://doi.org/10.1785/0120130052

Stolle, A., Bernhardt, A., Schwanghart, W. & Hoelzmann, P. 2017.Catastrophic valley fills record large Himalayan earthquakes, Pokhara, Nepal. *Quaternary Science Reviews*, **177**, 88–103.

Sukhija, B.S., Rao, M.N., Reddy, D.V., Nagabshanam, P., Hussain, S., Chadha, R.K. & Gupta, H.K. 1999. Timing and return of major paleoseismic events in the Shillong Plateau, India. *Tectonophysics*, **308**, 53–65.

Szeliga, W. & Bilham, R. 2017. New constraints on the mechanism and rupture area for the M7.8 Kangra 1905 earthquake, NW Himalaya. *Bulletin of the Seismological Society of America*, **107**, 2467–2479, https://doi.org/10.1785/0120160267

Szeliga, W., Hough, S., Martin, S. & Bilham, R. 2010. Intensity, magnitude, location, and attenuation in India for felt earthquakes since 1762. *Bulletin of the Seismological Society of America*, **100**, 570–584.

Takai, N., Shigefuji, M., Rajaure, S., Bijukchhen, S., Ichiyanagi, M., Dhital, M.R. & Sasatani, T. 2016. Strong ground motion in the Kathmandu Valley during the 2015 Gorkha, Nepal, earthquake. *Earth, Planets and Space*, **68**, 10, https://doi.org/10.1186/s40623-016-0383-7

Tandon, A.N. 1954. Study of the great Assam earthquake of August 1950 and its aftershocks. *Indian Journal of Meteorology and Geophysics*, **5**, 95–137.

Thorn, T. 1818. *Memoir of the War in India Conducted by General Lord Lake, Commander-in-Chief & Major-General Sir Arthur Wellesley, Duke of Wellington; From its Commencement in 1803, to its Termination in 1806*. On The Banks of The Hyphasis, London, p. 527.

Upreti, B.N. *et al.* 2000. The latest active faulting in Southeast Nepal. *Proceedings Active Fault Research for the New Millenium, Hokudan. Int. Symp. and Sch. on Active Faulting*. Awaji Island, Hyogo, Japan.

Upreti, B.N., Kumahara, Y. & Nakata, T. 2007. Paleoseismological study in the Nepal Himalaya – present status. *Proceedings of the Korea-Nepal Joint Symposium on Slope Stability and Landslides*, April 1, 2007, 1–9.

Van der Voo, R., Spakman, W. & Bijwaard, H. 1999. Tethyan subducted slabs under India. *Earth and Planetary Science Letters*, **171**, 7–20.

Vernant, P., Bilham, R. *et al.* 2014. Clockwise rotation of the Brahmaputra Valley: Tectonic convergence in the eastern Himalaya, Naga Hills and Shillong Plateau. *Journal of Geophysical Research*, **119**, 6558–6571, https://doi.org/10.1002/2014JB011196

Vigne, G.T. 1844. *Travels in Kashmir, Ladak and Iskardo, the Countries Adjoining the Mountain Course of the Indus & the Himalaya, North of Panjab, with Map*, 2nd edn, H. Colburn, London, **1**, 406.

Wang, K. & Fialko, Y. 2015. Slip model of the 2015 M_w 7.8 Gorkha (Nepal) earthquake from inversions of ALOS-2 and GPS data. *Geophysical Research Letters*, **42**, 7452–7458, https://doi.org/10.1002/2015GL065201

Wang, Q., Zhang, P.-Z. *et al.* 2001. Present-day crustal deformation in China constrained by global positioning system measurements. *Science*, **294**, 574–577.

Wesnousky, S.G., Kumar, S., Mohindra, R. & Thakur, V.C. 1999. Uplift and convergence along the Himalayan Frontal Thrust of India. *Tectonics*, **18**, 967–997.

Wesnousky, S.G., Kumahara, Y., Chamlagain, D., Pierce, I.K., Karki, A. & Gautam, D. 2017*a*. Geological observations on large earthquakes along the Himalayan frontal fault near Kathmandu, Nepal. *Earth and Planetary Science Letters*, **457**, 366–375, https://doi.org/10.1016/j.epsl.2016.10.006

Wesnousky, S.G., Kumahara, Y., Chamlagain, D., Pierce, I.K., Reedy, T., Angster, S.J. & Giri, B. 2017*b*. Large paleoearthquake timing and displacement near Damak in eastern Nepal on the Himalayan Frontal Thrust. *Geophysical Research Letters*, **44**, 8219–8226, https://doi.org/10.1002/2017GL074270

Wesnousky, S.G., Kumahara, Y., Chamlagain, D. & Neupane, P.C. 2019. Large Himalayan Frontal Thrust paleoearthquake at Khayarmara in Eastern Nepal. *Journal of Asian Earth Sciences*, https://doi.org/10.1016/j.jseaes.2019.01.008

Wesnousky, S.G., Kumahara, Y., Nakata, T., Chamlagain, D. & Neupane, P. 2018. New observations disagree with previous interpretations of surface rupture along the Himalayan Frontal Thrust during the great 1934 Bihar–Nepal earthquake. *Geophysical Research Letters*, **45**, 2652–2658, https://doi.org/10.1002/2018 GL077035

White, J.C. 1909. *Sikkim and Bhutan: Twenty One Years on the North East Frontier, 1887–1908*. Edward Arnold, London.

White, J.C. 2012. Paradoxical pseudotachylyte – Fault melt outside the seismogenic zone. *Journal of Structural Geology*, **38**, 11–20.

Wyss, M. 2005. Human losses expected in Himalayan earthquakes. *Natural Hazards*, **34**, 305–314.

Wyss, M. 2017. Four loss estimates for the Gorkha M 7.8 earthquake, 25 April 2015, before and after it occurred. *Natural Hazards*, **86**, 141–150, https://doi.org/10.1007/s11069-016-2648-7

Wyss, M., Gupta, S. & Rosset, P. 2017. Casualty estimates in two up-dip complementary Himalayan earthquakes. *Seismological Research Letters*, **88**, 1508–1515, https://doi.org/10.1785/0220170091

Xu, W., Burgmann, R. & Li, Z. 2016. An improved geodetic source model for the 1999 Mw 6.3 Chamoli earthquake, India. *Geophysical Journal International*, **205**, 236–242.

Yue, H., Simons, M. *et al.* 2017. Depth varying rupture properties during the 2015 Mw 7.8 Gorkha (Nepal) earthquake. *Tectonophysics*, **714–715**, 44–54.

Yule, D., Dawson, S., Lave, J., Sapkota, S. & Tiwari, D. 2006. Possible evidence for surface rupture of the Main Frontal Thrust during the great 1505 Himalayan earthquake Far-Western Nepal. *Eos, Transactions of the American Geophysical Union*, **87** (52), Fall Meeting Supplement, Abstract S33C-05.

Zheng, G., Wang, H., Wright, T.J., Lou, Y., Zhang, R., Zhang, W. & Wei, N. 2017. Crustal deformation in the India–Eurasia collision zone from 25 years of GPS measurements. *Journal of Geophysical Research: Solid Earth*, **122**, 9290–9312, https://doi.org/10.1002/2017JB014465